ANNUAL·REPORT·92

Central Bureau FOR Nuclear Measurements

JOINT RESEARCH CENTRE

COMMISSION OF THE EUROPEAN COMMUNITIES

EUR 15029 EN

ANNUAL·REPORT·92

Central Bureau FOR Nuclear Measurements

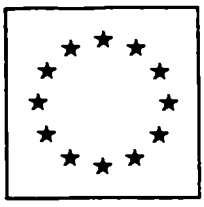

JOINT RESEARCH CENTRE

COMMISSION OF THE EUROPEAN COMMUNITIES

CATALOGUE N° : CD-NA-15029-EN-C

TABLE OF CONTENTS

Page

Note : This Annual Report is the last one being published under the name of the Central Bureau for Nuclear Measurements. In the future reports will appear under the new name

Institute
FOR
Reference Materials and Measurements
(IRMM)

For further information concerning the Research Areas Reference Materials and Reference Measurements within the Programme Measurement and Testing, please contact W. Müller, Programme Manager, IRMM, Retieseweg, B-2440 Geel, Belgium

Editor: H.H. Hansen

REFERENCE MATERIALS AND REFERENCE MEASUREMENTS

Executive Summary

W. Müller

This report covers CBNM's activities during the first year of the multiannual programme 1992-94, based predominantly on the programme "Reference Materials and Reference Measurements" of the 3rd Framework Programme Line "Measurement and Testing".

The structure of the programme was unchanged, the different parts being Specific Programme, Support to Commission Services, Exploratory Research, 3rd Parties Work; the activities are to respect the criterium of subsidiarity, to meet societal needs and to contribute to the improved competitivity of European industry.

Starting with the beginning of the year 1992, the support to the Bureau Communautaire de Référence (BCR) became part of the specific programme; during the reporting period, part of JRC's contribution to Consumer Policy Service (CPS) was taken over from the Environmental Institute (EI) Ispra. The conditions for non-statutory staff were redefined in view of the new Framework Programme Line "Human Capital and Mobility", fostering contracts with post docs, establishing networks and promoting access to large installations.

The work described and the results presented in this annual report 1992 follow a different order than in previous annual reports. This reflects the Institute's reorientation towards emphasis on reference materials and increased contributions to non-nuclear tasks. In addition, at the end of the reporting period, the Commission authorized the change of the previous name of the Geel Institute "Central Bureau for Nuclear Measurements" into "Institute for Reference Materials and Measurements" (IRMM). This renaming of the Institute will, of course, not affect the commitments defined in the Treaty of Rome.

The Specific Programme covers the projects "Reference Materials" and "Nuclear Measurements". The project "Reference Materials" increased its contributions to both, the nuclear and the non-nuclear fields. The project "Nuclear Measurements" furnished nuclear data for standards, fission and fusion technologies and made contributions to nuclear metrology.

The work on nuclear targets and samples was very successful as a large number of items were prepared under the form of thin deposits, special films and bulk samples. Reactor neutron dosimetry reference materials were delivered to customers in various countries.

In the field of non-nuclear reference materials, the support to the BCR was intensified by providing storage and dispatching of a high number of samples. Special reference materials of biological and environmental relevance were prepared, tested or characterized.

The uncertainty of the atomic weight of silicon could be reduced by a factor of 10 which resulted in a more accurate value of the Avogadro Constant. In concordance with EURACHEM, a workshop on "Traceability of Chemical Measurements to the SI Unit Mole" was organized at the Institute attracting more than 60 delegates from all EC and EFTA countries and observers from CIS, Poland, Hungary and USA.

Special efforts went to a measurement series of the standard cross-section ratio of $^{235}U(n,f)/H(n,n)$ using octacosanol layers of different thickness. Apparent discrepancies in the results require additional experiments.

To improve the accuracy of data needed for fission technology, actinide fission cross-sections and structural material neutron interaction data were determined. These studies followed demands collected in the NEA High Priority Request List.

Despite of the delicate condition of the linear electron accelerator (GELINA), the machine could be successfully used in the nuclear data programme as well as in the new radiation physics application. Fortunately, the refurbishment of GELINA could be started by placing the first orders at the end of the year. At the Van de Graaff accelerator the ratio of non-neutron to neutron activities is approaching a value of two.

The construction of the Ultra-Clean Chemical Laboratory has been accomplished, and tests confirmed excellent air quality.

Radiation physics experiments started a couple of years ago as exploratory research. They are concentrating on X-ray and optical transition radiation studies. Trace metal analysis and speciation studies in biological and environmental media are making progress by use of various experimental methods.

Support was given to a couple of other Commission Services. The new support to the Consumer Policy Service departed with the coordination of meetings of the working group "Analytical Methods of Cosmetics".

Work upon requests involved the supply of a large variety of materials and services. Unfortunately, the orders are mostly of very limited significance and the ratio of investment to income is rather unfavourable.

The efficiency of the Institute's work can be demonstrated more clearly by referring to the 42 contributions to conferences, the 65 submissions to scientific/technical journals and books and the 39 special technical reports produced in 1992.

SPECIFIC RESEARCH PROGRAMME

PROJECT 1: REFERENCE MATERIALS

Introduction

W. Müller (a.i.)

In 1992 the activity of the Unit Reference Materials was subdivided into several sub-projects, tackling both nuclear and non-nuclear topics.

The targets and samples preparation activities are on the basis of the nuclear work. The work included the preparation and characterization of ^{10}B and ^{6}LiF reference deposits needed for a redetermination of the life-time of the free neutron in co-operation with NIST, Gaithersburg. More than 100 samples and targets prepared comprised thin deposits, special films and bulk samples of metals, compounds and alloys. During the reporting period 118 reactor neutron dosimetry reference materials were delivered to customers in seven different countries. The detailed analysis of an interlaboratory comparison exercise for the determination of uranium by potentiometric titration is under progress. The application of potentiometry to MOX fuel became operational. Uranium hexafluoride samples were prepared for high precision gamma-ray spectrometry in the frame of a present round of the Regular European Interlaboratory Measurement Evaluation Programme (REIMEP). Actinides (uranium, plutonium) contaminations of soil at the level of 500 Bq/kg were determined after development of adequate separation and measurement procedures.

In the field of non-nuclear reference materials, much effort went into the BCR related activities as storage of various samples, distribution of material for round robins, dispatching of Reference Materials in the different steps of their certification. Biological Reference Materials were prepared, e.g. pig liver, treated by freeze-drying and milling, or characterized, e.g. milk powder.

Environmental Reference Materials (fly-ash, soils, sediments) were prepared for stability and homogeneity testing. The collection of aerosol reference materials continued and reference layers for surface analysis were prepared and characterized by RBS, the scanning nuclear microprobe could be applied for environmental analysis (micro distribution of elements in particles). By adapting a new mass spectrometer, the uncertainty of the atomic weight of silicon was decreased to 3×10^{-7} (1σ), resulting in an improved value of N_A, the Avogadro Constant. Isotope abundance and atomic weight of iron were improved by applying isotope dilution mass spectrometry (IDMS).

The Ultra-Clean Chemical Laboratory has been made operational. Tests performed on the purity of the air in the experimental area below the HEPA filters result in less than 35 particles of a size larger than 0.5 µm per m^3 of air.

For the study of trace metals and speciation in biological and environmental material spectrophotometric electrochemical and chromatographic methods have been applied. The binding of cadmium and zinc by different thioneins was studied. The intracellular distribution of copper, zinc, cadmium and iron in the marine clam Malcoma Baltica collected at the Westerschelde estuary has been determined.

Within the Safeguards activities supporting DG I and DG XVII appropriate uranium/plutonium metal spikes were prepared and characterized. Dried uranium/plutonium spikes were certified and dispatched to IAEA and Euratom Safeguards for use in various reprocessing plants. The Consumer Policy Service of the Commission has been supported by first analyses of lead in hair lotion and creams. Besides this, meetings of the working group "Analytical Methods of Cosmetics" have been coordinated.

In the frame of work requested from outside customers a large number of thin deposits, films and bulk samples have been supplied. Dosimetry materials have been sold successfully. Two reference materials (powder of innards and of tomatoes) were prepared upon request by the BGA (Bundesgesundheitsamt Berlin). The analysis of conditioned and non-conditioned radwaste containers was continued. REIMEP continued with measurement rounds on UF_6, MOX pellets, synthetic input solutions and Pu nitrate solutions. In the International Measurement Evaluation Programme, IMEP, synthetic and natural waters were distributed and measured for trace elements. Finally, boron in low alloys steel samples was certified for NIST by IDMS.

Summarized information on available nuclear and isotopic reference materials is given in Table 1.

Table 1. Nuclear and Isotopic Reference Materials available at CBNM

Code	Material	Application	Certified Quantities and Uncertainties (95 % confidence level)	Certificate	Single Unit Size	Price 1992 ECU/unit
EC-NRM 101	Uranium metal (0.5 - 1g)	element analysis	999.85 ± 0.05 g U·kg^{-1}	EC	1 g	55
EC-NRM 110	Uranium dioxide pellets (1g)		881.34 ± 0.13 g U·kg^{-1}	EC	25 g	220
CBNM-106	Uranium dioxide pellets (10g)		881.43 ± 0.24 g U·kg^{-1}	CBNM	150 g	200
EC-NRM 210	Plutonium dioxide powder (5 g)		880.26 ± 0.44 g Pu·kg^{-1}	EC	5 g	5200
EC-NRM 171	Set of 5 Al cans with U_3O_8 of different ^{235}U/U abundances	^{235}U/U abundance assay by gamma spectrometry	0.3206 ± 0.0002 atom % ^{235}U 0.7209 ± 0.0005 atom % ^{235}U 1.9664 ± 0.0014 atom % ^{235}U 2.9857 ± 0.0021 atom % ^{235}U 4.5168 ± 0.0032 atom % ^{235}U	EC	5 x 200 g	5500
CBNM-271	Set of 3 stainless steel cans with PuO_2 pellets of different Pu isotopic composition and ^{241}Am concentration	Pu isotope abundance/ratio and ^{241}Am concentration assay by gamma spectrometry	84.3985 ± 0.0084 atom % ^{239}Pu 73.4248 ± 0.0098 atom % ^{239}Pu 62.6562 ± 0.028 atom % ^{239}Pu and corresponding values for ^{238}Pu, ^{240}Pu, ^{241}Pu, ^{242}Pu and ^{241}Am	CBNM	3 x 6.65 g	5100
CBNM-011	Boric acid	isotope analysis	19.824 ± 0.020 atom % ^{10}B 80.176 ± 0.020 atom % ^{11}B	CBNM	1 g	160
CBNM-014	Iron cubes 0.5 mm ⌀ wire		See front page		200 mg 50 mg	300 150
CBNM-015	Lithium carbonate		95.610 ± 0.025 atom % ^{6}Li 4.390 ± 0.025 atom % ^{7}Li		50 mg	160
CBNM-016	Lithium carbonate		7.525 ± 0.029 atom % ^{6}Li 92.475 ± 0.029 atom % ^{7}Li		1 g	160
CBNM-017	Silicon		92.233 ± 0.014 atom % ^{28}Si 4.675 ± 0.011 atom % ^{29}Si 3.092 ± 0.008 atom % ^{30}Si		50 mg	150
CBNM-018	Silicon dioxide		92.214 ± 0.014 atom % ^{28}Si 4.688 ± 0.011 atom % ^{29}Si 3.098 ± 0.008 atom % ^{30}Si		5 g	480
CBNM-021			0.43842 ± 0.00022 atom % ^{235}U			
CBNM-022			0.72009 ± 0.00036 atom % ^{235}U			
CBNM-023	Uranium hexafluoride		3.2743 ± 0.0016 atom % ^{235}U		20 g	580
CBNM-024			5.0506 ± 0.0024 atom % ^{235}U			
CBNM-040a	Spike solution; ^{233}U/U: 0.980	element assay by isotope dilution mass spectrometry (IDMS)	0.9382 ± 0.0026 mg^{233}U.g^{-1}	CBNM	10 ml	
CBNM-042a	Spike solution; ^{244}Pu/Pu: 0.979		0.9150 ± 0.0019 µg^{244}Pu ·g^{-1}		10 ml	
CBNM-043	Spike solution; ^{242}Pu/Pu: 0.88		44.25 ± 0.13 ng^{242}Pu ·g^{-1}		10 ml	
CBNM-044	Spike solution; ^{242}Pu/Pu: 0.999		9.213 ± 0.014 µg^{242}Pu ·g^{-1}		10 ml	
CBNM-049	Spike solution; ^{242}Pu/Pu: 0.999		91.23 ± 0.18 µg^{242}Pu ·g^{-1}		10 ml	
CBNM-050	Spike solution; ^{235}U/U: 0.999		0.99996 ± 0.00025 µg^{235}U.g^{-1}		10 ml	290
CBNM-060	Spike solution; ^{230}Th/Th: 0.9985		40.38 ± 0.30 µg^{230}Th ·g^{-1}		10 ml	
CBNM-610	Spike solution; ^{10}B/B: 0.949		36.8778 ± 0.0088 µg ^{10}B.g^{-1}		5 ml	
CBNM-611	Spike solution; ^{11}B/B: 0.802		44.31 ± 0.44 µg ^{11}B.g^{-1}		5 ml	
CBNM-615	Spike solution; ^{6}Li/Li: 0.956		23.18 ± 0.16 µg ^{6}Li.g^{-1}		5 ml	
CBNM-618	Spike solution; ^{87}Rb/Rb: 0.9799		9.743 ± 0.015 µg ^{87}Rb.g^{-1}		5 ml	

Table 1 (continued)

Code	Material	Application	Certified Quantities and Uncertainties (95 % confidence level)	Certificate	Single Unit Size	Price 1992 ECU/unit
CBNM-1027a	Solid spike (dried); $^{235}U/U$: 0.196 $^{239}Pu/Pu$: 0.971	element assay by IDMS	For each individual unit : amount of spike isotope, certified to ≤ 0.1 %	CBNM	50 or 100 mg (U + Pu)	120
CBNM-047a	Dry nitrate; $^{239/244}Pu$ mixture	mass spectrometer linearity or isotopic abundance ratios calibration	$^{239}Pu/^{244}Pu$: 1.2984 ± 0.0025	CBNM	0.15 mg	530
CBNM-072	Set of 15 solutions, different $^{233}U/^{235}U$, equal $^{235}U/^{238}U$ atomic ratios		various $^{233}U/^{235}U$ and $^{235}U/^{238}U$ ratios ±0.03 % of values	CBNM	15 x 1 ml	930
CBNM-199	Uranyl nitrate		$^{233}U/^{238}U$: 1.00001 ± 0.00030 $^{235}U/^{238}U$: 1.00015 ± 0.00020	CBNM EC in preparation	5 ml	570
EC-NRM 501	^{238}Uranium dioxide spheres 0.5 and 1.0 mm diameter,	reactor neutron dosimetry	879.4 ± 2.8 g U · kg^{-1} 10.4 ± 0.5 mg ^{235}U · kg^{-1}U 999.9896 ± 0.0005 g ^{238}U · kg^{-1}U	EC	100 mg (0.5 mm ⌀) 200 mg (1.0 mm ⌀)	170 170
CBNM 502	^{237}Neptunium dioxide spheres 0.5 and 0.8 mm diameter		873 ± 7 g Np ·kg^{-1}	CBNM EC in preparation	100 mg (0.5 mm ⌀) 200 mg (0.8 mm ⌀)	310 310
EC-NRM 521	Nickel 0.1 mm foil 0.5 mm ⌀ wire		< 0.1 mg Co · kg^{-1}	EC	100 cm^2 1 m	250 140
CBNM 522	Copper 0.1 mm foil 1 mm foil 0.5 mm or 1 mm ⌀ wire		< 0.05 mg Co·kg^{-1} 0.95 ± 0.04 mg Ag·kg^{-1}	CBNM EC in preparation	100 cm2 20 cm2 1 m	210 210 110
EC-NRM 523	Aluminium 0.1 mm foil 1 mm foil 1 mm ⌀ wire		< 0.1 mg Na·kg^{-1}	EC	100 cm^2 20 cm^2 1 m	170 170 110
CBNM-524	Iron 0.1 mm foil 0.5 mm ⌀ wire		< 0.05 mg Co·kg^{-1} < 0.1 mg Mn·kg^{-1}	CBNM EC in preparation	100 cm^2 1 m	170 110
EC-NRM 525	Niobium 20 µm foil 0.1 mm foil 0.5 mm ⌀ wire		19.6 ± 1.8 mg Ta·kg^{-1}	EC	20 cm^2 20 cm^2 1 m	210 140 140
EC-NRM 526	Niobium 20 µm or 0.1 mm foil 0.5 mm ⌀ wire		0.30 ± 0.09 mg Ta·kg^{-1}	EC	20 cm^2 1 m	1200 600
CBNM-527	Al - 0.1% Co 0.5 mm ⌀ wire		1.00 ± 0.02 g Co · kg^{-1}	CBNM	1 m	110
CBNM-528	Al - 1% Co 0.5 mm ⌀ wire		10.0 ± 0.2 g Co · kg^{-1}	CBNM	1 m	110
CBNM-529	Rhodium 50 µm foil		Pt < 5 mg·kg^{-1} Ir 25.9 ± 0.6 mg·kg^{-1}	provisional	20 cm^2	660
CBNM-530	Al - 0.1% Au 0.1 mm foil 0.5 mm or 1 mm ⌀ wire		1.00 ± 0.02 g Au·kg^{-1}	CBNM EC in preparation	100 cm^2 1 m	220 150

REFERENCE MATERIALS FOR NUCLEAR APPLICATION

PREPARATION OF SAMPLES AND TARGETS

The reliability of experimental results is very much dependent upon a careful preparation of the material to be studied. Thus, the objective of the work on samples and targets is to provide a well defined basis for the execution of measurements. These measurements cover inside CBNM as outside activities in the nuclear field being data determination or basic research or safety and surveillance duties.

Preparation and Characterisation of ^{10}B and ^{6}LiF Reference Deposits

J. Pauwels, P. Robouch, R.D. Scott*, R. Eykens, J. Van Gestel

In view of an improved redetermination of the lifetime of the free neutron, an agreement for cooperation was signed in 1991 between NIST Gaithersburg and CBNM with the aim to achieve an accuracy close to 0.1 % in neutron counting. In the frame of this agreement an improved vacuum deposition design has been worked out to eliminate border effects and decrease areal density variations in the produced reference deposits. The preparation of improved ^{10}B and ^{6}LiF candidate reference deposits is now completed, and neutron induced particle measurements have been started at BR1 using an upgraded counting facility.

Preparation and Characterization of Samples and Targets

J. Pauwels, C. Ingelbrecht, P. Robouch, R. Eykens, C. Louvrier, F. Peetermans, A. Dean, H. Mast, S. Palmeri, J. Van Gestel

101 Samples and targets covering 40 different requests have been prepared in support to the CBNM specific programme. They comprise thin deposits, special plastic films and various bulk samples of metals, compounds and alloys (Table 2).

---

* Visiting Scientist from SURRC, Glasgow, United Kingdom

Table 2. ***Supply of thin deposits, films and bulk samples in support of the CBNM programme***

Preparation	Number of Requests	Number of Samples	Preparation Methods[1]
Thin deposits			
^{10}B	6	23	VD
Carbon	8	1	FL
Hydrogen	3	5	VD
Nitrogen	1	1	VD
$^{239}PuF_3$	2	2	VD
$^{244+239}PuO_2$	1	1	VD
$^{nat}UF_4$	1	3	VD
$^{238}UO_2$	1	2	SU
Films			
Polyimide	2	5	CE
Bulk samples			
Aluminium	1	1	MA
Al-Ca-Al	1	1	R-MA-VD
Al-Mg-Cu-Ag	1	1	M-R-MA
$^{138}BaCO_3$	2	3	CAN-MA
Calcium	2	4	R-MA
Cadmium	1	10	PR-MA
Cobalt	1	2	MA
Copper	1	2	MA
Iron	1	2	MA
Ga As	1	3	MA
Indium	1	8	R-MA
^{6}Li	1	1	R-MA-CAN
^{6}Li-C_2H_4	1	1	R-MA-CAN
Nickel	1	2	MA
^{58}Ni	2	2	M-R-MA
Silicon	1	3	MA
Tin	1	2	R
Titanium	1	2	MA
^{235}U	1	1	SOL

(1)

CAN	canning	PR	pressing
CE	centrifuging	R	rolling
FL	flotation	SOL	solution
MA	machining	SU	suspension spraying
M	melting	VD	vacuum deposition

New Developments

P. Robouch, J. Pauwels, C. Louvrier

Well-known techniques such as vacuum deposition, electrospraying and spray painting are routinely used at CBNM for the preparation of high quality actinide deposits[1]. The increasing demand for homogeneous deposits of rare and expensive enriched isotopes made it necessary to investigate techniques with a potentially high efficiency, and allowing to make deposits with good resolution for fission fragments and/or charged particles measurements.

(1) J. Pauwels, Nucl. Instr. Meth. B56/57 (1991) 938

A preliminary study was carried out in cooperation with the Target Laboratory of the Technical University of Munich (D), to investigate the use of a laser beam as a source for vacuum deposition. In the experiments the material to be evaporated was placed in an air-cooled copper crucible mounted on an x-y-z moveable table in a vacuum chamber at 10^{-5} Pa. The Nd-YAG CW laser beam (60 - 80 Watt, 3 cm diameter) entered the vacuum system through a plano-convex lens. The focussed beam scanned the crucible surface to melt-evaporate the powder. Tests were performed to study the quantitative evaporation of LiF and UO_2, the homogeneity of deposition and the interaction of the laser beam with polyimide substrate films.
Electrodeposition of uranium and/or plutonium in aqueous and organic ("molecular plating") medium was successfully carried out on stainless steel, aluminium and polyimide substrates. New electrolysis cells allowing deposition of actinides on self-supporting thin metallic foils are under investigation.

Establishment of a Literature Database on Target Preparation
P. Robouch, C. Louvrier

Fifteen Conferences and eighteen years of Newsletters International Nuclear Target Development Society (INTDS) resulted in a collection of more than 530 publications and letters concerning the development, preparation, characterization and/or use of nuclear targets. A computer based database was developed to allow a rapid search of the available information in the field of targetry. Based on Paradox 3.5 (from Borland International), this electronic file is compatible with most of the commercial and public domain spreadsheets and databases; it is available to all INTDS members. This tool has proved to be useful when starting new projects.

REACTOR NEUTRON DOSIMETRY REFERENCE MATERIALS

CBNM in collaboration with the Euratom Working Group on Reactor Dosimetry (EWGRD) is producing a series of reference materials for neutron metrology and reactor surveillance. These are high purity metals certified for interfering trace impurities, alloys of certified composition and fission dosimeters in the form of oxide microspheres. CBNM is responsible for procurement and distribution, reference material preparation and coordination of the certification.

Sale and Certification of Reference Materials

C. Ingelbrecht

Thirteen dosimetry reference materials are currently available and during the last year 118 samples were ordered by customers in seven countries inside and outside the EC (Table 3).

EC certification of the two metal reference materials EC-NRM 522 (copper) and EC-NRM 524 (iron) was approved by the Nuclear Certification Group during 1992. Complementary certification analyses for CBNM-529 (rhodium) were finished. The iridium mass fraction ((26.0 ± 0.6) $mg \cdot kg^{-1}$, at 95 % confidence level) has now been determined by six laboratories and the platinum mass fraction (< 5 $mg \cdot kg^{-1}$) has been determined by three laboratories using four methods. The draft of the certification report has been completed.

Table 3. Sale of reactor neutron dosimetry reference materials

Ref. No.	Material	Number of Units	Country
EC-NRM 501	$^{238}UO_2$	21	SF, USA, F
CBNM-502	$^{237}NpO_2$	18	SF, USA, F
EC-NRM 521	nickel	24	HUN, F, N
CBNM-522	copper	4	HUN, SF, F
CBNM-524	iron	24	HUN, F, N
EC-NRM 526	niobium	12	UK, HUN, F
CBNM-527	Al-0.1 % Co	1	HUN
CBNM-528	Al-1.0 % Co	11	HUN, UK, F
CBNM-530	Al-0.1 % Au	3	D, F

Reference Material Preparation

C. Ingelbrecht, F. Peetermans, S. Palmeri

Titanium metal is useful for measuring fast neutron fluence rates primarily via the $^{46}Ti(n,p)^{46}Sc$ reaction for neutron energies above 4.4 MeV and for irradiations of up to about 250 days. In a thermal neutron environment there may be interference from $^{45}Sc(n,\gamma)^{46}Sc$ and it is important that the scandium impurity content is low. Titanium metal with scandium content of about 0.1 $mg \cdot kg^{-1}$ has been partly transformed into foil of 0.1 or 0.5 mm (1 kg of each) and the preparation of 0.5 mm diameter wire has been started. The certification analyses (for scandium content) have been planned and will start early in 1993.

Three Al-Co (0.01, 0.1 and 1.0 % Co) were prepared by spray deposition of powder (Osprey Metals, UK). Two of these alloys are to replace exhausting stocks of reference materials and the 0.01 % Co composition will be a new reference material for higher neutron fluence rates. The main use of such alloys is thermal neutron metrology using the reaction $^{59}Co(n,\gamma)^{60}Co$. The cobalt homogeneity on a scale of 20 mg is of great importance and metallography of the spraying ingots shows a fine, homogeneous microstructure. The preparation of foil and wire from the three alloys is underway and certifications analyses (for cobalt content) are planned to commence early in 1993.
Another element of interest for thermal neutron metrology is silver via the reaction $^{109}Ag(n,\gamma)^{110m}Ag$. Levitation melted castings of composition Al-0.1 % Ag have been prepared and will be transformed into foil and wire for a candidate reference material.
The preparation of a fission track glass reference material for geological dating is continuing and uranium doped glass powders have been mixed and melted (Institut National du Verre, B) for uranium homogeneity control at the University of Gent.

ACTINIDE REFERENCE MATERIALS

Spike Reference Materials

A. Verbruggen, F. Hendrickx, A. Alonso, K. Mayer

The preparation of Spike Reference Materials is an important task at CBNM. In 1992, a total number of 211 units, corresponding to 14 orders from 12 customers, of Isotopic and Spike Reference Materials, has been delivered to various laboratories within and outside the European Community.
Certification measurements by Isotope Dilution Mass Spectrometry (IDMS) for CBNM IRM-081 and CBNM IRM-082 have been achieved. Both are ^{239}Pu solutions with a certified molar concentration of resp. $(4.820\ 0 \pm 0.002\ 6)\cdot10^{-4}$ mol $^{239}Pu\cdot kg^{-1}$ of solution and $(4.926\ 5 \pm 0.002\ 7)\cdot10^{-5}$ mol $^{239}Pu\cdot kg^{-1}$ of solution. Other plutonium isotopes present are related to the ^{239}Pu concentration through the certified molar abundance ratios:

$^{238}Pu/^{239}Pu$:	0.000 070 63	± 0.000 000 56
$^{240}Pu/^{239}Pu$:	0.047 096	± 0.000 052
$^{241}Pu/^{239}Pu$:	0.000 920 7	± 0.000 007 2
$^{242}Pu/^{239}Pu$:	0.000 075 7	± 0.000 003 4

Analytical Chemistry

M. Bickel, B. Dijckmans, F. Hendrickx, W. Leidert, A. Michiels, W. Nagel, A. Rodriguez, B. Slowikowski

Uranyl Intercomparison: The last results of the second phase of the interlaboratory comparison exercise for the determination of uranium by potentiometric titration, initiated by the ESARDA-LEU Working Group, have arrived. From a preliminary rough data check, they indicate that most of the participating laboratories show satisfying performance in terms of accuracy and precision (Fig. 1). A more detailed analysis is under progress. The raw results have been communicated to the participants in coded form.

MOX Reference Material: The material to be used will be prepared in 1993 by TUI Karlsruhe according to the specifications given by CBNM arising from an inquiry among future users[1]. Production control NDA measurements will be performed by JRC Ispra.

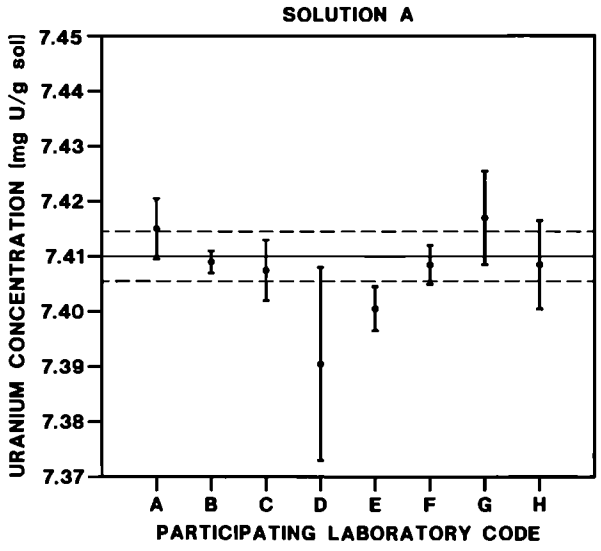

Fig. 1. Part of results of uranyl interlaboratory comparison

The glove box titration device for the determination of uranium in plutonium bearing materials by potentiometric titration, after some warm test runs (uranium only), has gone into operation without any problems. First measurements on MOX materials yielded very satisfactory results, nevertheless, systematic experiments are necessary and will be performed in the near future.

Plutonium determination by constant potential coulometry also has been applied to MOX materials. Results were good but systematic tests are needed.

(1) CBNM Annual Report 91, EUR 14374 EN

Actinides in the Environment: The systematic investigation of precisions achievable in the determination of uranium by ICP-AES has been concluded with the result that at concentrations around 300 ppb the reproducibility is still acceptable (~ 2 % relative), rather independently on the matrix. Taking into account that environmental concentrations are ≧ 3 ppb, possible enrichment factors in the order of 100 are necessary. Systematic studies applying two different enrichment methods, ion exchange and solvent extraction, have been started.

Electrolysis as a tool to prepare alpha activity measurement sources has been further developed. The step from different matrices to the electrolyte matrix (5M NH_4Cl, pH2) has been performed with good results.

As a first "real life" application of the new separation and measurement procedures the uranium and plutonium contents of a contaminated soil sample from an old CBNM waste water transfer container were determined, yielding results of ≧ 500 Bq/kg soil. An alpha spectrum of a source obtained from a soil sample is shown in Fig. 2.

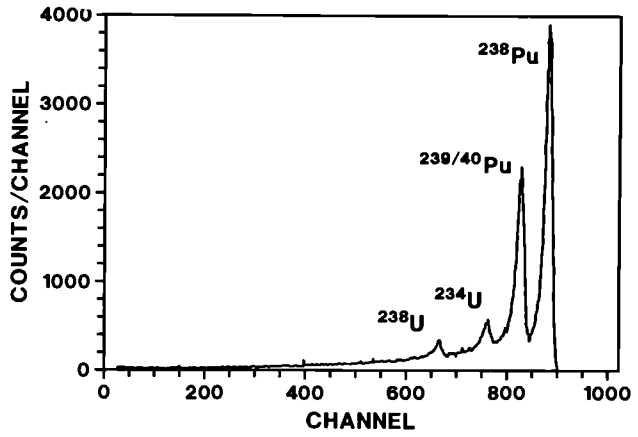

Fig. 2. Alpha Spectrum of a U/Pu source prepared from contaminated soil

Uranium Ores: The evaluation of the γ-ray spectrometry measurement results on EC-NRM 113 and 114 has been finished.

The final certification report containing all verification measurements on EC-NRM 113 and 114 was presented to the Nuclear Certification Group. It was accepted with several changes to be made. Certification will take place by letter after the English translations of the original CEA certification reports have arrived from France.

Iron Determination: The method developed for high precision iron determination by potentiometric titration was further developed and put on a gravimetric basis. The reproducibility improved by a factor of 10 to 0.02 % relative.

Americium Sources: Responding to a request from ILL Grenoble inquiring into possibilities to prepare a 100 kBq ^{241}Am source, several test sources were made applying electrolysis. Chemical yields of ~ 70 % were achieved.

REFERENCE MATERIALS FOR NON-NUCLEAR APPLICATION

BUREAU COMMUNAUTAIRE DE REFERENCE (BCR)

Storage, Sale and Distribution of BCR Samples

E. De Coninck, G.N. Kramer, J. Pauwels

Support to BCR was provided by:

- storage of various samples, materials and documentation;
- distribution of BCR materials for round-robins;
- dispatching of candidate reference materials (RM's) for stability- and homogeneity testing and for certification analysis;
- dispatching of certified reference materials (CRM's) for sale.

In the reporting period, less samples were sold and distributed for analysis than in the previous one (Table 4). This was due on one hand to sales restrictions introduced by BCR, and on the other hand to problems with financing of certification projects. Despite this, the number of dispatches did not decrease considerably, as more smaller orders had to be carried out.

Table 4. Overview of BCR RMs as handled by CBNM

Period	Sale	Samples for analyses	Dispatches
1986/1987	1768	1226	396
1987/1988	2407	1258	475
1988/1989	4775	1126	753
1989/1990	7925	2027	1130
1990/1991	8285	2274	1242
1991/1992	6853	1110	1104

In addition, several new raw materials were received for transformation, as well as > 19 000 new CRM samples (prepared at CBNM or elsewhere) for packing, labelling, bookkeeping and storage under material specific conditions.

Biological Reference Materials

G.N. Kramer, J. Pauwels, K-H. Grobecker, C. Louvrier, P. de Vos, C. Hofmann*

A pig liver candidate reference material for vitamins (BCR CRM-487) was prepared by jaw-crushing under liquid nitrogen cooling, freeze-drying and subsequent stud-milling under liquid nitrogen cooling. The powder was then sieved to < 125 µm, homogenized and bottled in penicillin vials under argon. 1600 Samples of 15 g each were prepared. Stability- and homogeneity testing is carried out at TNO, Zeist (NL).

BCR CRM-63R (spray-dried milk powder) was controlled for its lead and zinc microhomogeneity using solid sampling Zeeman atomic absorption spectrometry (SS-ZAAS). It could be demonstrated that the lead and zinc values certified by BCR are valid for samples of 10 and 87 mg, respectively.

Environmental Reference Materials

G.N. Kramer, J. Pauwels, K-H. Grobecker, C. Louvrier, A. Oostra, P. de Vos

A fly ash candidate reference material for PCDD's and PCDF's (BCR CRM-490) was homogenized by turbula mixing, jet milled to < 125 µm, turbula mixed again and bottled using a sampler-divider. 1100 Bottles of 30 g each were prepared. 50 Samples were sent to VITO, Mol (B) for stability- and homogeneity testing.

Two coking plant soils (A: sandy soil BCR CRM-427; B: marl soil BCR CRM-428) for PAH's, phenols and cyanide were produced according to a similar preparation flow-sheet on soils collected on behalf of BCR by TÜV Essen (D). 1560 bottles of soil A (50 g/bottle) and 1300 bottles of soil B (40 g/bottle) were prepared. Samples of soil A were sent to TÜV Essen (D), for stability- and homogeneity testing.

Moreover, several preparations of soils and sediments with narrowly defined particle size distributions were prepared to study the influence of particle size on the chemical behaviour of environmental CRM's. These studies are carried out on behalf of BCR in cooperation with University of Cordoba (SP), TÜV Essen (D) and the Royal Holloway University, London (UK).

Industrial Reference Materials

C. Ingelbrecht, F. Peetermans, P. de Vos

Fourty zirconium samples doped with trace quantities of boron by quantitative alloying were sent to Max-Planck-Institut für Metallforschung, Dortmund (D)

* EC Fellow from University of Gent, Belgium

in preparation of a candidate reference material (BCR CRM-20).
2000 sharpy test samples were cleaned, greased and packed again on request of BCR.

Freeze-Drying of Isolated Chloroplasts

K.H. Grobecker, G. Zimmermann*, G.N. Kramer, C. Louvrier

The bio-assay of herbicides using chloroplasts from fresh spinach plants was described by Zimmermann et al.[1]. The determination of the oxygen produced by the chloroplasts is used as an indicator for the presence of a group of herbicides inhibiting photosynthesis, and therefore the growth of plants.
To control the observation of legal limits of herbicides in drinking water, the chloroplast bio-assay can be used as a time and cost saving complementary method to the presently used one, i.e. gas chromatography. To perform the test under routine conditions, the testing laboratory has, however, to produce fresh chloroplasts daily.
The present investigation is aimed at producing powdered isolated chloroplasts with an activity (i.e. oxygen production under influence of light) similar to that of freshly isolated chloroplasts and which are stable over a long period of time. First encouraging results were obtained using forced opening of the chloroplasts by osmosis and subsequent freeze-drying. The shelf-life of the powder is expected to be acceptable, but has still to be tested over a longer period of time.

ENVIRONMENTAL AND SURFACE ANALYSIS

Aerosol Reference Material

H. Cavé, M. Kriews**, U. Wätjen

For the elemental analysis of aerosol filter samples by X-ray techniques there is a lack of adequate reference materials (RM's). No genuine aerosol matrix is available, which has been collected on membrane filters from ambient aerosol. It was possible with a special high-volume sampling procedure to collect ambient aerosol samples with a uniformity of 5 % to 15 % in the elemental deposit ranges of 10 ng/cm^2 to µg/cm^2, within probed spots of only 4 mm diameter on suitable filter materials. Fig. 3 shows as an example the mass

---

* Visiting scientist from Fresenius Institut, Taunusstein, Germany
** Universität Hamburg, Germany
(1) G.M. Zimmermann, L. Weil, P. Herzsprung and K.E. Quentin, Z. Wasser u. Abwasser Forsch. 22 (1989) 73-77

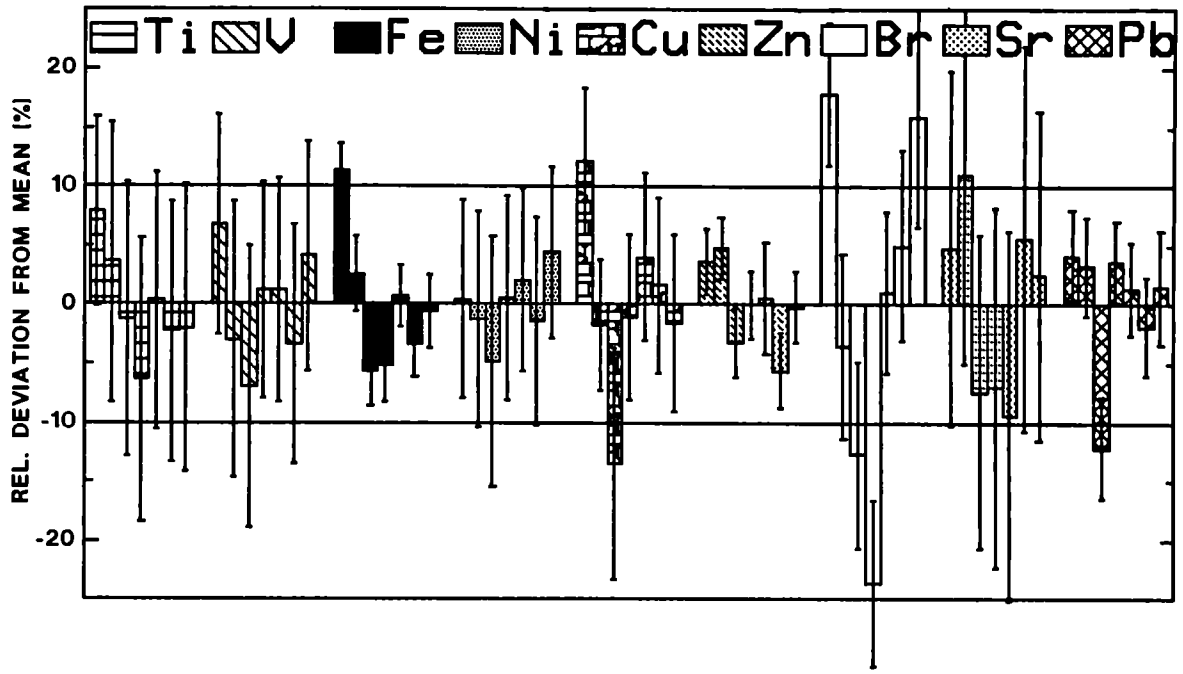

Fig. 3. ***Variation of nine elemental masses in seven individual spots (4 mm Ø) of a cellulose nitrate filter. The relative deviations $d_i = (x_i - \bar{x})/\bar{x}$ of the seven analyses from their mean value are given by the histogramme bars. The error bars indicate the precision Δx_i of the single analysis***

variation of nine elements determined by PIXE analysis in seven individual spots of a particular cellulose nitrate filter. Besides this filter type also polycarbonate (Nucleopore) membranes qualified with the needed uniformity of the dust deposits.

An aerosol collection campaign is now being performed which yielded already filter batches of rural and marine aerosol types, suitable for characterization by different analytical methods and compatible with X-ray fluorescence analysis (XRF). Before entering the characterization phase, the batches of candidate RM's will be completed by an industrially influenced urban aerosol matrix.

Reference Layers and Materials for Surface Analysis

H. Bax, P. Rietveld, U. Wätjen

The computer processing of spectral data is one of the principal limiting factors of accuracy attainable in PIXE and XRF analysis of elements with overlapping peaks. The interference of barium L-shell and titanium K-shell X-ray lines is chosen as a model system for such cases of overlap. In a preliminary study of the influence of varying mass ratios of both elements on the accuracy of their determination with PIXE, inaccuracies of 40 % were found when the Ba/Ti mass ratio was about $3 \cdot 10^{-2}$. A new set of standards has been prepared, consisting

of composite layers of titanium and $BaCl_2$ with different areal densities (Table 5).

Table 5. Approximate areal density ($\mu g/cm^2$) of composite standards evaporated on vitreous carbon

Ti	$BaCl_2$
60	2
60	5
60	20
60	40
25	100
20	100
40	40

The characterization procedure follows the principle of traceability for the absolute values of areal density making use of the CBNM ultrahigh vacuum microbalance. The homogeneity assessment is based on the multi-channel scaling (MCS) of the titanium or barium signal in the RBS spectra of "pure" titanium or $BaCl_2$ samples (Fig. 4), evaporated simultaneously with the composite layers. Up to 19 samples at a time are loaded on a target wheel, which is continuously rotating through the ion beam of 1 mm diameter. Half of the standards set has been investigated so far. Relative inhomogeneities of $< 1\,\%$ have been measured.

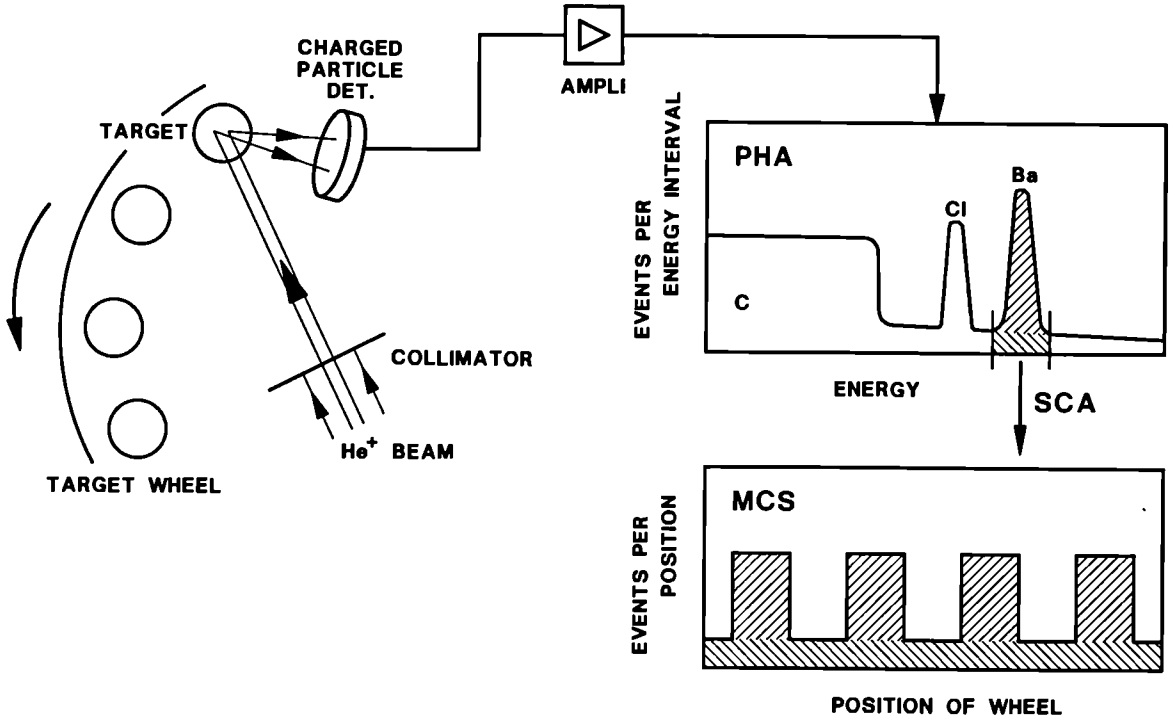

Fig. 4. Scheme of the experimental setup to acquire MCS data of an energy window in an RBS spectrum in dependence of the target wheel position

Demonstrating the Capability of the Scanning Nuclear Microprobe for Environmental Analysis

L. Breitenbach, J. Injuk*, U. Wätjen

During the last two months of the year the scanning nuclear microprobe was available for microdistributional trace analysis. It was applied to two subjects of interest in atmospheric research:

- PIXE microdistribution analysis was done of very large (> 15 µm ∅) deposited dust particles, sampled on passive greasy collection plates according to VDI guideline 2119 part 4 (draft). The following elements could be detected at pg concentrations in some of the dust particles: titanium, chromium, manganese, iron and copper.
- River effluents and direct dumping into the sea have long been known as pollution sources of the North Sea. Recently also wet and dry deposition of atmospheric aerosol have been identified as important contributors to the North Sea heavy metal pollution. In spite of their low concentration in air, large particles (> 3 µm ∅) are of extreme importance for this pathway due to their comparably large individual mass and high deposition velocity. Such particles were collected above the North Sea on the research platform FPN with a cascade impactor. PIXE analysis of more than 100 single aerosol particles (> 5 µm ∅) has been performed with a proton beam of about 3 µm × 3 µm size. In many of these particles the elements titanium, vanadium, chromium, manganese, iron, nickel, copper, zinc and gallium were detected. The quantitative evaluation of the complete data set is under way.

Trace Element Changes and Atherosclerosis

T. Pinheiro**, W. Maenhaut***, H. Cavé, U. Wätjen

Five different brain structures originating from both arteriosclerosis affected and healthy Portuguese individuals were examined for their elemental content. Potassium, calcium, manganese, iron, copper, zinc, selenium and rubidium were determined in all tissues with PIXE. The most prominent differences between the pathological and normal data were found for manganese, iron, copper and zinc in three of the five brain regions. The decrease of the potassium and rubidium content in the five brain structures from the pathological group and the changes for manganese in three of them can be associated with ageing. However, age cannot explain the trace element concentration changes of iron, copper and zinc. Most likely the changes for these elements are due to arteriosclerosis progression.

* Universitaire Instelling Antwerpen, Belgium
** EC Fellow from LNETI, Sacavém, Portugal
*** Rijksuniversiteit Gent, Belgium

Furthermore, the trace element concentration in serum and packed blood cells was investigated in samples originating from patients who had suffered from a myocardial attack and compared to samples from healthy individuals. In blood serum the iron, copper and zinc concentrations were found to be altered from normal, whereas in packed blood cells significant differences were encountered for calcium, manganese, iron, copper, selenium and lead. Factor analysis performed on the data matrices revealed one factor for each sample type which allowed distinguishing between healthy and pathological individuals. The elements related to this discrimination factor were iron and copper for serum and calcium, manganese, iron, copper and zinc for packed blood cells.

ISOTOPE ABUNDANCES AND ATOMIC WEIGHTS

Atomic Weight of Silicon for a better Avogadro Constant

P. De Bièvre, S. Valkiers, F. Schaefer*

The molar mass (atomic weight) M(Si) [g/mol] in a silicon single crystal is an essential parameter of the determination of the Avogadro Constant N_A through the relationship:

$$N_A = \frac{M(Si)}{\rho \cdot a_o^3/8}$$

where ρ[g/cm^3] is the density of the crystal and a_0 [cm] is obtained from lattice constant measurements. Absolute measurements of the molar mass require absolute measurements of isotope abundances f_i of the stable isotopes with atomic mass M_i, i.e. of the abundance ratios R_i. These in turn require calibration by synthetic mixtures of highly enriched silicon isotopes:

$$M(Si) = \frac{\Sigma R_i \cdot M_i}{\Sigma R_i}$$

A long-term project 1980 - 2000 is ongoing at CBNM to reduce the uncertainty on the molar mass of silicon in order to bring back the uncertainty on the Avogadro Constant by a factor of 10 - 100. Later on, the aim will be to reduce the uncertainty contribution of M(Si) such that it becomes insignificant for the uncertainty on N_A.

Anticipating the important need to further reduce the $1 \cdot 10^{-6}$ uncertainty on M(Si) obtained in 1991, CBNM has been planning the construction of a new mass spectrometer of unprecedented capability in gas isotope abundance ratio

* Visiting Scientist from Universität Bremen, Germany

measurements with the mass spectrometer manufacturer Finnigan-MAT, Bremen (D). After construction, assembly and testing of the instrument, appropriate new measurement procedures were designed and incorporated in the software. The characteristics of the new spectrometer are given in Table 6.

Table 6. The characteristics of the new mass spectrometer (MAT 271) compared to the old instrument (MAT CH5)

	MAT - CH5 (up to 1989)	MAT - 271 (1992)
Abundance Sensitivity	$3 \cdot 10^{-5}$	$2 \cdot 10^{-6}$
Maximum Resolution	200	8000
High Ohmic Resistor	Carbon	Fe-oxides
Amplifiers	FET	MOS
Sensitivity	$4 \cdot 10^{-3}$ A/Pa ± 0.1 %	$7 \cdot 10^{-2}$ A/Pa ± 0.1 %
System stability	± $1 \cdot 10^{-4}$/30 min	± $3 \cdot 10^{-5}$/ 30 min
Inlet	Molecular	Molecular + viscous
Detection system	Faraday cup	Faraday cup + ion counting

For the calibration process, a new series of synthetic silicon isotope mixtures was gravimetrically prepared from the same enriched silicon materials that were used in 1989-1991[1,2].

All of these efforts have resulted in a M(Si) = 28.085 446 2 with an uncertainty (1s) of $3 \cdot 10^{-7}$, which will yield an equivalent reduction of the uncertainty of N_A[1].

As a by-product of the measurements[3], it was possible to make well understood mass-dependent corrections as a function of time by extrapolating the observed values to the moment that SiF_4 is first admitted to the spectrometer through the gold-leak. The diffusion of the gas into the ion source is governed by gas kinetic laws. The time constants for diffusion are proportional to $\sqrt{M}$(Si). Noting that the kinetic gas theory relationships are independent of chemical composition, we attempted to apply the calibration by absolute M(Si) values to gases of some other elements[4,5,6]. Concordant results with best current values of their molar masses were obtained (Table 7). The uncertainties displayed in Table 7 are in their own right much superior to previous data and the compatibility of the

(1) P. De Bièvre, S. Valkiers, H.S. Peiser, F. Schäfer, P. Seyfried, CBNM Internal Report GE/R/MS/16/92
(2) F. Schäfer, S. Valkiers, P. De Bièvre, CBNM Internal Report GE/R/MS/17/92
(3) S. Valkiers, G. Lenaers, P. De Bièvre, J. Res. Nat. Bur. Stand. Tech. 96 (1991) 617
(4) S. Valkiers, B. Engelen, CBNM Internal Report GE/R/MS/21/92
(5) S. Valkiers, C. Verwimp, CBNM Internal Report GE/R/MS/27/92
(6) S. Valkiers, L. Wouters, CBNM Internal Report GE/R/MS/34/92

M(E) values in Table 7 within the normal terrestrial ranges of the element E suggest that the error is not large. In the near future an "operational mole" unit for different elements may be defined and "near-absolute" gas isotope mass spectrometry may be performed without calibration since the measurement procedure seems to contain all necessary corrections at a given uncertainty level.

Table 7. ***Some uncalibrated M(E) Measurements with MAT 271 set side by side with IUPAC-designated 'Best Measurements'***

	B (from BF_3)	C (from CF_4)	N (N_2 gas)	Ne	Si (from SiF_4)	S (from SF_6)	Ar	Kr
IUPAC 'Best Measurement' from a single natural source	10.811 825 29	12.011 15 3	14.006 723 14	20.179 96 3	28.085 526 56	32.064 33 14	39.947 68 2	83.796 03 14
MAT 271/CBNM 1992	10.810 588 11	12.010 674 1	14.006 636 9	20.180 24 16	28.085 528 2	32.064 876 2	39.947 74 2	83.798 94 2
IUPAC Evaluation of Extreme Range of *M*(E) between 'normal terrestrial' specimens	0.010	0.002	0.000 14	0.001 2	0.000 6	0.012	0.002	0.02

Traceability of Chemical Measurements to the SI Unit Mole

P. De Bièvre

The insight gained in the Avogadro project has led to specific concepts enabling to organize border crossing comparability of "measurements of amount-of-substance", better known as "chemical measurements". The methods and measurement procedures developed in the Avogadro project, can be used to certify the "certified values" which are offered in CBNM's REIMEP and IMEP programmes thus making them traceable to the SI unit mole. This provides the participating laboratories with a so far closest form of traceability of their measurements to the mole, which is short and practical, pending a more thorough international comparability system. The latter is under discussion in the International Committee on Weights and Measures (CIPM) with CBNM being a member. At the request of EURACHEM, a closed workshop for their Committee Members was organized in Geel in November 1992 on this matter. About 60 delegates attended from all EC and EFTA countries. Observers from Russia, Poland, Hungary and USA were present.

Isotope Abundance and Atomic Weights Measurements of Iron

P. Taylor, R. Maeck*, A. Kynaston**, P. Hansen, D. Vendelbo, P. De Bièvre

At the end of 1991, new absolute isotope abundance ratios as well as a calibrated atomic weight were obtained for the element iron. The new data will be submitted to IUPAC's Commission on Atomic Weights and Isotope Abundances. A special effort has been made to create awareness of the existence of the new Isotopic Reference Material (CBNM IRM 014) in the field of Geochemistry and Cosmochemistry.

Experimental activities were focussed on transforming an existing mass spectrometer (NBS type 90° 12" radius single collector) into an instrument which allows to perform accurate ion counting:

- installation of multiplier and suitable ion counting electronics;
- improving the vacuum (use of ion source housing equipped with gold seals; extensive use of cold traps);
- development of instrument control software for ion counting.

This has been carried out to enable:

- the use of lower ionisation temperatures;
- detection of lower amounts of iron.

The four to five orders of magnitude improvement in detection power (from 10^{-10} to 10^{-15} A) made it necessary to modify existing procedures for loading the sample. A microloading device was constructed, consisting of an XYZ translation stage carrying the filament, a video camera for observing this filament and a micro syringe. The device allows to deposit very small droplets (down to 30 nl) on a very confined area of the sample filament (typical amount loaded: 300 ng of iron), making ion source refocussing superfluous during the measurement.

Preliminary estimates for the reproducibility of the isotope abundance ratios are $3{\cdot}10^{-3}$ for iron and better than 10^{-3} for platinum overplated uranium samples.

The use of lower ionisation temperatures leads to more accurate (reduced isobaric interferences from ^{54}Cr and ^{58}Ni) and more precise results (fractionation in the ion source is reduced and more constant), which lead to improved isotope abundance and atomic weight data. Furthermore, the enhanced detection power combined with suitable chemical and measurement procedures will allow to measure abundance ratios accurately on ng amounts of iron in biological and environmental samples.

For carrying out IDMS in the future, a ^{57}Fe spike is in preparation. The material has been purified using ion exchange procedures and transferred into quartz ampoules.

---

* EC Fellow from Strasbourg University, France
** EC Fellow from Leeds University, United Kingdom

PROJECT 2: NUCLEAR MEASUREMENTS

Introduction

A.J. Deruytter

In 1992, the first year of the multiannual research programme (1992-1994), the Unit Nuclear Physics and Measurements contributed to the specific programme Measurement and Testing in the Project Nuclear Measurements and to Work for Third Parties.

The main objectives of the Project Nuclear Measurements in the subprojects Nuclear Data and Nuclear Metrology are: to improve the neutron standards data set, relative to which partial cross-sections or other quantitites, important for fission and fusion technology, are determined; to improve radionuclide data for standards application; to develop nuclear measurement techniques for nuclear and non-nuclear applications.

The major facilities of CBNM, the Geel linear electron accelerator GELINA and the 7 MV Van de Graaff accelerator were fully operational. They were used for neutron data measurements and in the non-nuclear applications. In 1992 the first phase of a refurbishment plan for GELINA was approved.

The efforts for the improvement of the set of standard neutron cross-sections and for other quantities selected within the INDC/NEANDC Standards File continued. In particular work on the standard cross-section ratio ^{235}U(n,f)/H(n,n) continued with Frisch gridded ionization chambers and using octacosanol samples as hydrogeneous layers.

A double Frisch gridded ionization chamber was used to measure mass-energy- and angular distribution of fission fragments for ^{237}Np(n,f) from 0.5 MeV to 5.5 MeV neutron energy.

Measurements of alpha-particle emission probabilities of ^{239}Pu showed results for the two major emissions to disagree with recent evaluated data.

Requests from the nuclear science community became more and more demanding and follow from deficiencies in available experimental data sets, which are detected by careful evaluation efforts in the framework of the International Evaluation Cooperation (IEC) of the NEA Nuclear Science Committee (NEA-NSC). The requests are summarized in the NEA High Priority Request List.

In the subproject on nuclear data for fission technology a measurement was performed of the normalization of the ^{239}Pu fission cross-section which solved a normalization problem of earlier Weston and Todd data of about 4 %.

Parameters for 384 resonances in ^{58}Ni and 350 resonances in ^{60}Ni have been analyzed upto 1 MeV and 800 KeV, respectively. The data were submitted for inclusion in the JEF and EFF files.

In the field of nuclear data for fusion technology, double differential neutron-emission cross-sections for ^{9}Be(n,2n) for incident neutron energies between 0.6 MeV and 11.1 MeV have been transmitted to the NEA Data Bank. During 1992 an extensive measurement campaign has been performed on neutron emission cross-sections from ^{207}Pb.

New measurements of ^{58}Ni(n,α) relative to the ^{27}Al(n,α) cross-section instead of relative to H(n,n) were performed at 8 MeV neutron-energy under five angles with a ΔE-E telescope. Aim is to resolve the discrepancy of our earlier data with the ENDF/B6 evaluation.

Several more basic measurements linked to our nuclear data programme were performed mainly for PhD research and using GELINA as a high resolution neutron spectrometer unique in Europe. They concern: spin assignments of ^{238}U p-wave resonances as a contribution to parity-non-conservation (PNC) studies at Los Alamos, a search for the shape isomer in ^{239}U and ^{233}Th and the study of γ-ray decay towards the isomeric groundstate in ^{239}U, high resolution ^{138}Ba (n,γ) measurements in view of understanding the s-process nucleosynthesis, the study of radioactive transitions from n-capture in ^{53}Cr resonances, and ^{242}Pu and ^{244}Pu mass and energy distributions and their correlations.

In the radionuclide metrology subproject contributions were made by the preparation of low-energy X-ray standard sources, measurements of K-shell fluorescence yields, standardization of a ^{152}Eu solution, evaluation of the second EUROMET intercomparison of ^{192}Ir brachytherapy sources, and low level measurements on volcanic rock, archeological ceramics, soil and river sediments. Impressive was the background reduction in low-level measurements with a high-purity Ge detector in the underground laboratory HADES (collaboration with SCK/CEN, Mol (B)). The technique of time-differential perturbed angular distributions (TDPAD) of γ-rays with the pulsed beam facility at the Van de Graaff was applied for identification of fluorine residence sites in silicon and germanium, as well as for radiation damage studies in GaAs.

In the area of neutron metrology fast neutron and γ-ray fluences close to the GELINA target were measured in view of damage caused by irradiations with fast neutrons at a fluence level of 10^{15} n/cm^2.

At the 7 MV Van de Graaff accelerator the Nuclear Reaction Analysis (NRA) technique is in operation since the beginning of 1992. It is used currently in the determination of the boron/nitrogen stoichiometry in boron-nitride thin films (superhard coatings) in collaboration with VITO, Mol (B) and in the study of the

oxygen diffusion in aluminium implanted stainless steel samples (oxidation protective layers) in collaboration with the University of Thessaloniki (GR).
Experiments in radiation physics started as exploratory research were continued in 1992. Energy-spectra and angular distributions of X-ray transition radiation emitted by different radiators were obtained; an optical transition radiation system was built that delivers information about the electron energy, beam size and beam divergence, characteristics important for further work in radiation physics. A study of the Smith-Purcell effect to produce intense X-ray beams using ultrarelativistic electrons travelling close to a metallic grating is underway.

NUCLEAR DATA

NUCLEAR DATA FOR STANDARDS

The objective of the work on standard nuclear data is to improve the set of neutron data to be used in measurements consistency checks. Competing reactions, angular and kinetic energy distributions of the reaction products have to be studied to increase the reliability of the given standard cross sections. Appropriate research topics are selected from listings of the INDC/NEANDC Standards File. Complementary work is devoted to radionuclide decay data and associated atomic data requested for calibration and reference purposes.

Neutron Data

Standard Cross Section Ratio $^{235}U(n,f)/H(n,n)$

F.-J. Hambsch, R. Vogt, G. Willems*, P. Robouch, J. Van Gestel, J. Pauwels, A. Rodriguez, R. Besenthal

In continuation of this investigation[1] measurements at incident neutron energies ranging from 0.3 to 2 MeV have been performed for six different octacosanol samples. The thickness of the octacosanol layers under investigation are 136 µg/cm^2, 137 µg/cm^2, 217 µg/cm^2, 280 µg/cm^2, 353 µg/cm^2 and 550 µg/cm^2. The samples were prepared by two different evaporation runs.
Analysis of the proton-recoil spectra carried out for the first measurement series revealed a sharp distribution with an energy resolution of about 14 keV FWHM. This was deduced from the width of a high precision pulse generator peak, which was continuously connected during the experiment. The resolution is demonstrated by a fit with a Gaussian distribution to the measured pulse generator peak in Fig. 5.
Analysis of the second measurement series revealed, however, a much smoother spectral shape of the proton recoils, although the width of the pulse generator peak did not change.
A comparison of the proton recoil spectra measured for samples of 136 µg/cm^2 and 137 µg/cm^2 at about 2 MeV neutron energy at the high energy end of the spectrum is given in Fig. 6. It is obvious that the two spectra are different, which accounts to about 1 % of the total counts. If the aim is to reduce the total measurement error to about 0.5 % such a dissent is not acceptable. This also

---

* Visiting Scientist from KU Leuven, Belgium
(1) CBNM Annual Report 91, EUR 14374 EN

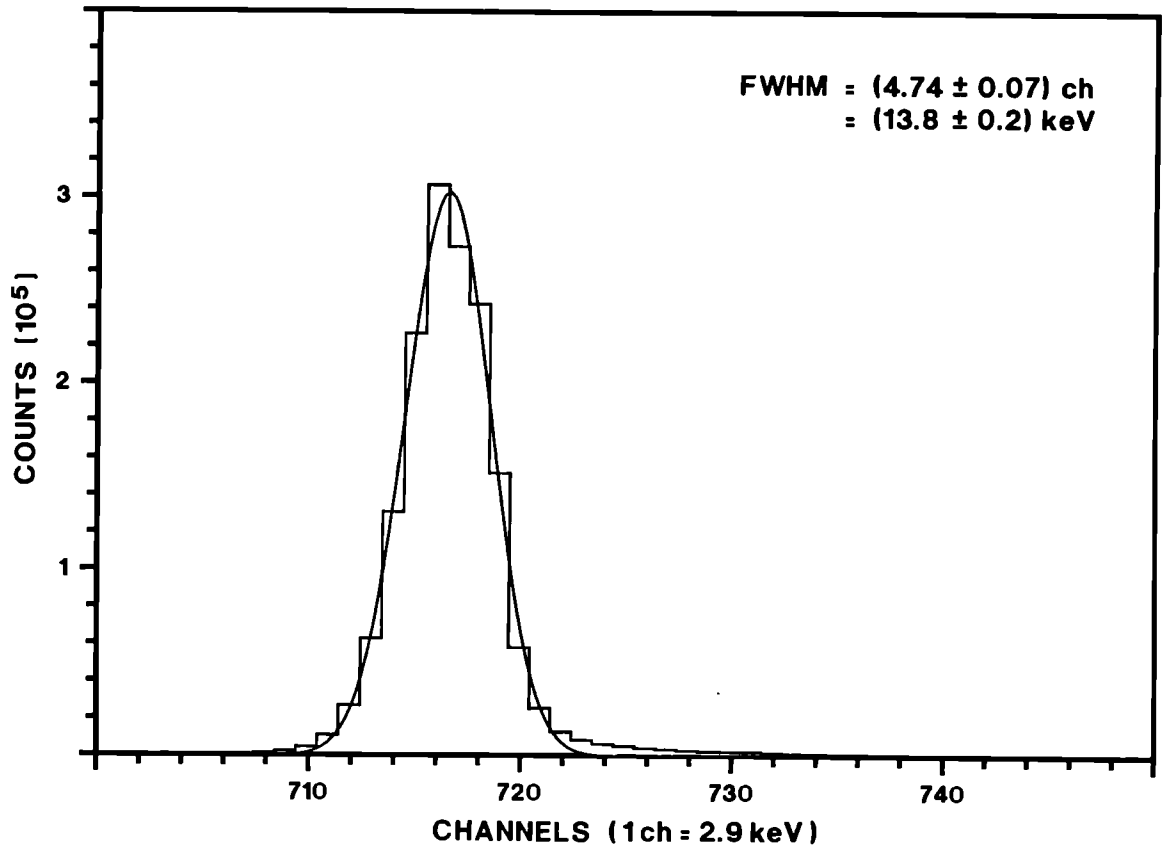

Fig. 5. Precise pulse generator peak and corresponding gaussian fit

because the difference appears at the high energy end of the spectrum, where those events are measured which are emitted close to 0° with respect to the normal on the cathode. There the energy loss in the sample should be a minimum, if a homogeneous surface is present. However, without notice the gas supplier had changed the gas quality. Furthermore also the neutron producing target had been replaced due to a low neutron yield.

Using a certified gas with N50-quality and the former TiT-target for the neutron production resulted in the spectrum shown in Fig. 7 by a dashed line. There is still a visible discrepancy with the first measured spectrum (solid line) at the high energy end. But compared to Fig. 6 the shape has considerably improved. Because of these non reproducible measurements of the proton recoil spectra, we tried to measure and compare also the tristearin samples used in earlier experiments[1]. Up to now only the thinnest tristearin sample of 148 $\mu g/cm^2$ has been investigated. The comparison with the best octacosanol measurement is given in Fig. 8. The two distributions are very much the same. However, the tristearin distribution is obviously more extended to higher channel numbers. This is unexpected because energy loss calculations based on

(1) H.-H. Knitter, C. Budtz-Jørgensen and H. Bax, Proc. Advisory Group Meeting on Nuclear Standard Reference Data, IAEA TECDOC 335 (1985)

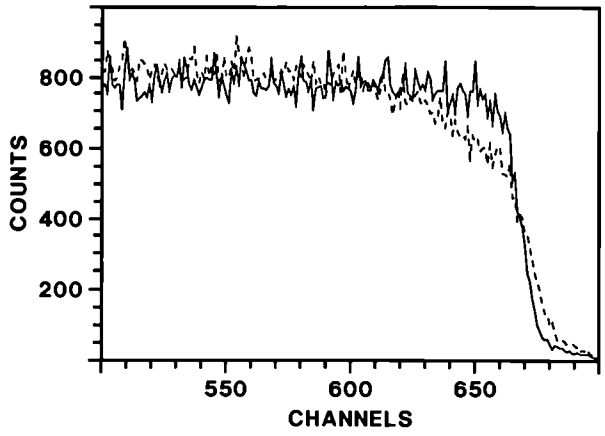

Fig. 6. Comparison of the proton recoil spectra for 2 MeV incident neutron energy and octacosanol sample thicknesses of 137 µg/cm² (solid line) and 136 µg/cm² (dashed line)

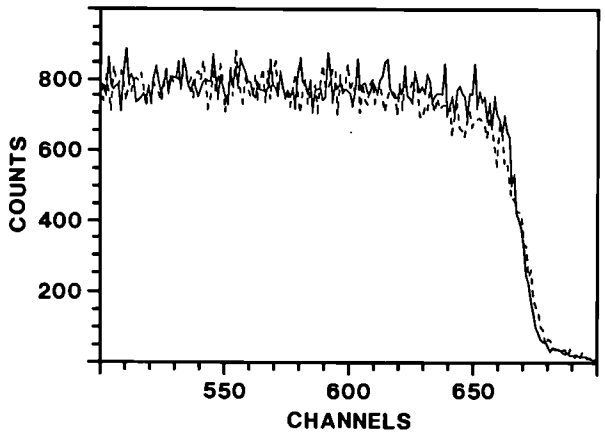

Fig. 7. Comparison of the proton recoil spectra for 2 MeV incident neutron energy and octacosanol sample thicknesses of 137 µg/cm² (solid line) and 136 µg/cm² (dashed line). Certified N50-gas and better TiT-target used

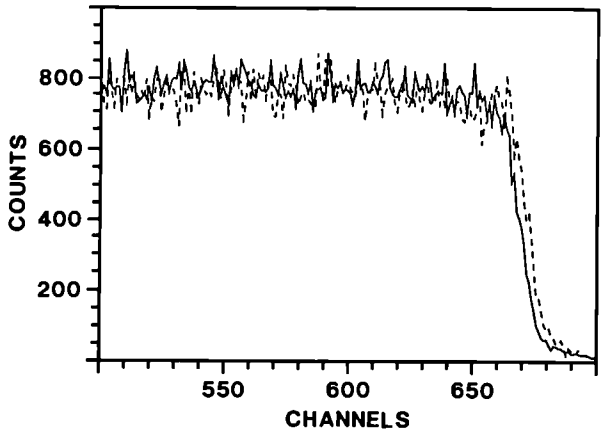

Fig. 8. Comparison of the proton recoil spectra for 2 MeV incident neutron energy and octacosanol sample of 137 µg/cm² (solid line) and tristearin sample of 148 µg/cm² (dashed line)

tables of Ziegler et al.[1] for protons of 2 MeV showed the same value of ~ 25 keV energy loss for both the tristearin sample of 148 µg/cm² and the octacosanol sample of 137 µg/cm². From this it is expected that both distributions end in the same channel. The measured difference of two to three channels, respectively 6 to 9 keV, however, seems to indicate that something might be wrong. For three different octacosanol samples of the first measurement a plot of the energy loss

(1) J. F. Ziegler et al., The stopping and range of ions in solids, Pergamon Press, New York (1985)

versus half height of the proton recoil distribution is given in Fig. 9. A straight line fit to the points gives the stopping power value for octacosanol at 2 MeV proton energy. The resulting value from the fit of 240 keV/mg/cm^2 is in disagreement to the expected value of 179 keV/mg/cm^2 [1].
To solve the existing discrepancies a new measurement series is foreseen including all the different octacosanol and tristearin samples available. To check also the influence of the neutron producing target new TiT-targets have already been ordered.

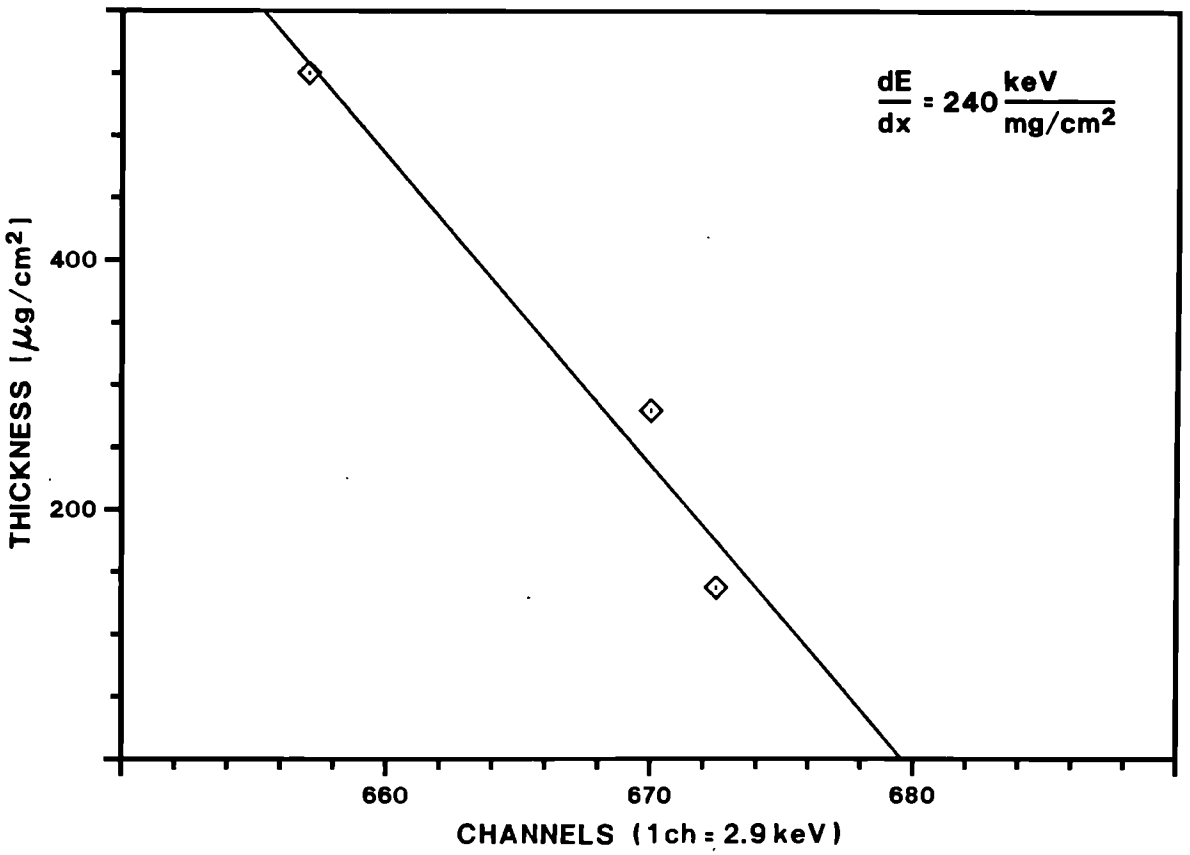

Fig. 9. ***Octacosanol sample thickness versus channel number at half height of the proton recoil distribution. Straight line fit to get the stopping power at 2 MeV incident neutron energy***

The ^{235}U Fission Fragment Anisotropies

F.-J. Hambsch

On request from the NEANDC Standards Subcommittee, which has decided to present the NEANDC/INDC Standards file as an OECD/NEA document, a review on the ^{235}U fission fragment anisotropies has been written. Since the last review in 1983[2] of the status of the measured fission fragment anisotropies as

(1) J. F. Ziegler et al., The stopping and range of ions in solids, Pergamon Press, New York (1985)
(2) S.S. Kapoor , Nuclear Data Standards for Nuclear Measurements, Technical Reports Series Nr. 227, p. 47 (IAEA, Vienna, 1983)

function of incident neutron energy in ^{235}U only a few new measurements have been performed. However, for measurements of fission cross sections which do not cover the whole 2π solid angle or for corrections of self absorption within the target for small emission angles with respect to the plane of the deposit the knowledge of the fragment angular distribution is needed. The main experimental emphasis has been devoted to the neutron energy range from 3 keV to 500 keV[1] and from 0.5 MeV to 6 MeV in steps of 0.5 MeV[2]. The main result was that the measured anisotropies in the energy range from 0.5 MeV to 6 MeV agree with the result already published, but have smaller errors. The negative anisotropies for neutron energies below 0.3 MeV measured already by several other authors have been confirmed.

Investigation of the Correlation Between Prompt Gamma-Ray Emission and Fission Fragments from $^{252}Cf(SF)$

F.-J. Hambsch, R. Vogt

Recently this type of activity has been partly restarted under different aspects. In a first instance the fission fragment signals from the used Frisch gridded ionization chamber served as input to a newly developed four parameter data acquisition system. This system connected to the SUN-SPARC based local area network made it possible to do directly data acquisition and online monitoring with LISA (LIstmode and Spectral data Analysis, see page 83 for details) based on the commercial visualization package PV-WAVE.

The four parametric listmode data were directly acquired via the SCSI-interface onto 4 mm DAT-tapes with 2 GByte capacity. Approximately $2.5 \cdot 10^8$ events have been registered up to now. Different steps of data analysis are ongoing before fission fragment mass- and total kinetic energy distributions can be calculated.

The second aim of this experiment is to check the quality of the ionization chamber, the data reduction and the spontaneous fissioning target by the achieved mass resolution in comparison to recently published data of fission fragment properties in the cold fragmentation region of $^{252}Cf(SF)$.

Furthermore in a recent investigation[3] of the correlation of fission fragments with prompt neutron emission from $^{252}Cf(SF)$ an increased yield at asymmetric fragment masses has been found. This is especially interesting to be verified because the prompt neutron database measured[3] is extremely good ($\sim 10^8$ coincident events) and inconsistencies with older prompt neutron measurements of fission fragments may become visible.

(1) F.-J. Hambsch, H.-H. Knitter, C. Budtz-Jørgensen, Proc. of the Seminar on Fission, ed. C. Wagemans, Habay-la-Neuve, 1986, BLG586
(2) Ch. Straede, C. Budtz-Jørgensen and H.-H. Knitter, Nucl. Phys. A462 (1987) 85
(3) J. van Aarle, W. Westmeier and P. Patselt, Verhandlungen der DPG 1992,p. 165

Neutron Induced Fission of ^{237}Np

P. Siegler*, F.-J. Hambsch, R. Vogt

The already mentioned measurement [1] of the fission fragment properties of the reaction ^{237}Np(n,f) has been started using the 7 MV Van de Graaff accelerator as a neutron source. A double Frisch gridded ionization chamber is used to measure the mass-, energy- and angular distribution of fission fragments as function of the incident neutron energy.

The fact, that ^{237}Np has a fission threshold at about 0.7 MeV neutron energy, makes an investigation in this energy region especially interesting. It has not yet been clearly proven by other experiments[2, 3] whether or not the fission fragment properties exhibit changes with incident neutron energy.

Up to now measurements at 0.5, 0.7, 1, 1.09, 1.3, 1.6, 4, 4.6, 5, 5.5 MeV neutron energy were performed. About $2 \cdot 10^5$ coincident fission events have been measured at all neutron energies except the lowest. The D(d,n) reaction has been used for neutron energies above 4 MeV and the T(p,n) for the lower energies.

In the threshold region, where finer energy steps are needed the spread in neutron energy due to energy loss of protons in the tritium target becomes severe. To reduce this spread several additional runs between 0.3 MeV and 0.7 MeV with thin lithium-fluoride targets using the ^{7}Li(p,n)^{7}Be reaction are planned.

A difficulty for pre-neutron mass calculations is the fact that $\bar{\nu}$, the number of prompt neutrons emitted as function of fragment mass is not known for ^{237}Np(n,f). Therefore the same setup has been used to measure the thermal neutron induced fission of ^{235}U. The results will serve as a reference for the analysis of the ^{237}Np data because for $^{235}U(n_{th},f)$ all the distributions of the different fission fragment parameters are well known. The target dimensions were similar to those of the neptunium target and therefore the necessary corrections to the raw data can be compared and adapted. The large fission cross section for $^{235}U(n_{th},f)$ allowed a short measuring period of two days only with a total number of $2 \cdot 10^6$ events.

Another very important fact which has to be taken into account is the pulse height defect in gases like the used 90 % Ar 10 % CH_4. Calculations for the pulse height defect of fission fragments in the energy and mass range covered, have been started using a computer code based on the energy loss tables of Ziegler et al.[4].

---

* EC Fellow from Technical University Darmstadt, Germany

(1) CBNM Annual Report 91, EUR 14374 EN
(2) B. D. Kuzminov et al., Sov. Jour. Nucl. Phys. 11(1970)166
(3) R. Müller et al., Phys. Rev. C29(1984)885
(4) J. F. Ziegler et al., The stopping and range of ions in solids, Pergamon Press, New York (1985)

The calculations concerning the multi-modal random neck-rupture model of Brosa, Grossmann and Müller[1] have been completed. The existence of the so-called standard channels as well as the superlong channel could be established. Complete data sets for every fission channel with all the shape parameters as well as the binding energies are available. Fig. 10 displays the results of the channel search for the compound nucleus ^{238}Np. The channels are drawn as function of the half length l and the neck radius r of the corresponding shape of the nucleus.

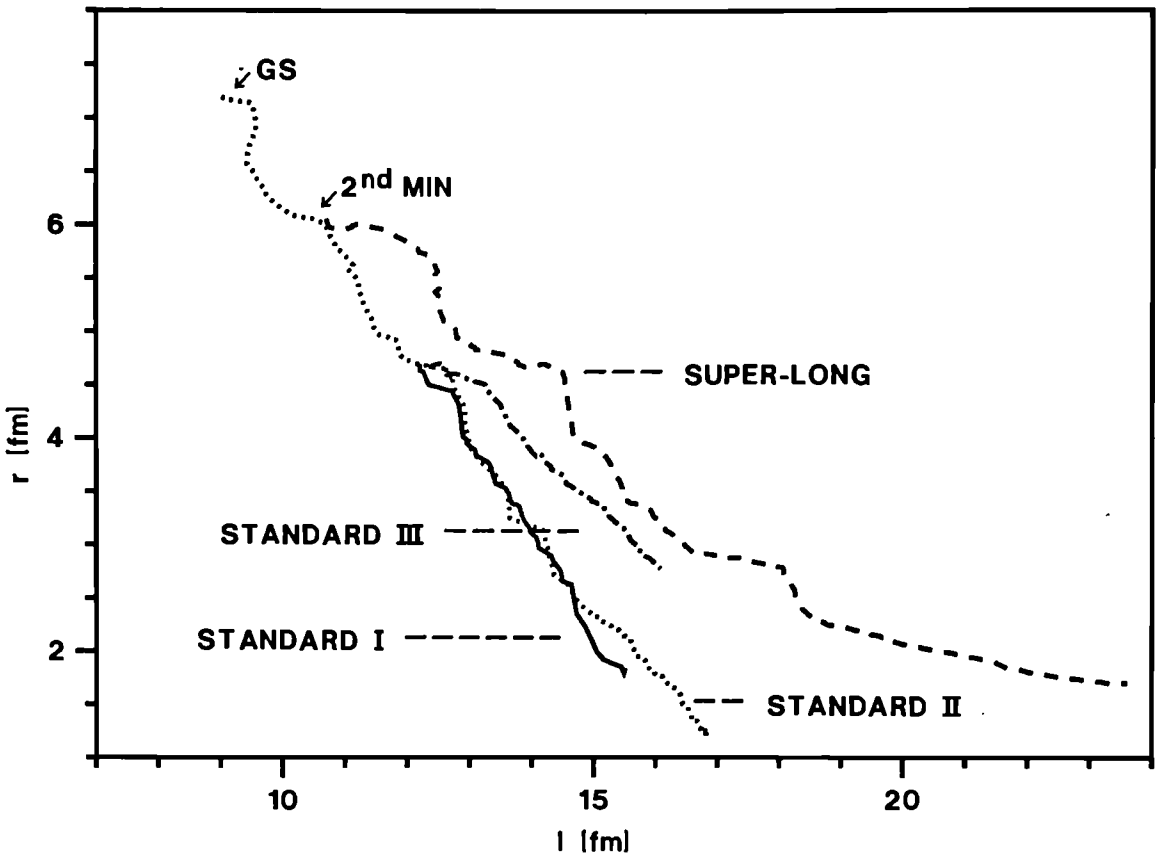

Fig. 10. Projection of the fission channels to the plane represented by the choosen parametrization of the nucleus

In the second minimum the first bifurcation takes place and the superlong channel starts. Following the standard channel after the second barrier another bifurcation exists where the splitting into the three standard channels occurs. The end of each standard channel represents a prescission configuration which is associated within the random neck-rupture model to certain fission properties. The prescission configuration of the superlong channel is deduced from the minimum in Fig. 11 for E_{gs}-E_{def} at l = 21 fm.

(1) U. Brosa et al., Phys. Reports 197(1990)167

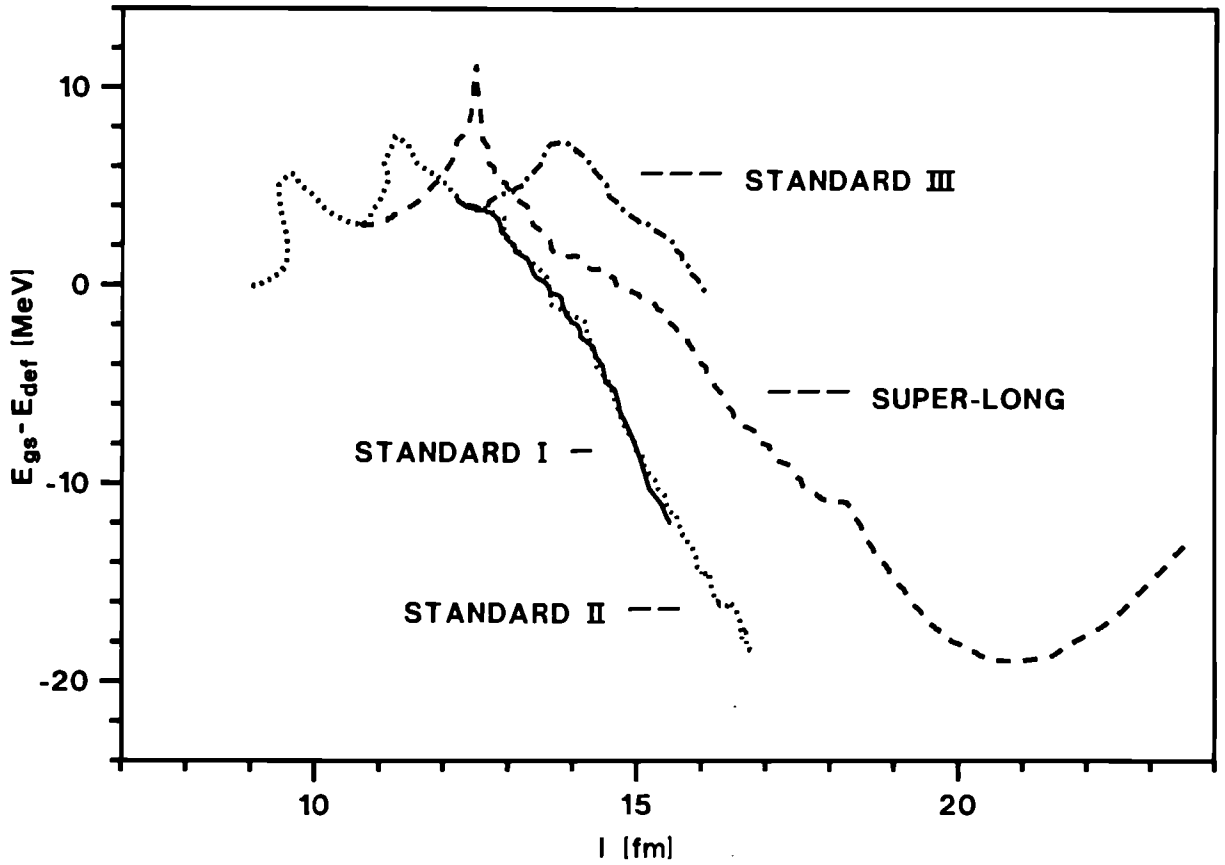

Fig. 11. Potential energy E_{gs}-E_{def} of the deformed nucleus for the different fission channels as function of the elongation parameter l

Table 8. Pre-scission parameters and deduced fission fragment properties for each fission channel

	E^*_S [MeV]	B [MeV]	ΔU [MeV]	V_{cou} [MeV]	$-V_{nuc}$ [MeV]	TKE [MeV]	σ_{TKE} [MeV]	A	σ_A	Z	σ_Z	V_{mul}	l [fm]	Δl [fm]	TOTL [fm]	r [fm]	z [fm]
STANDARD I	6,6	7,5	17,7	223,0	32,9	189,8	9,6	135,4	3,4	52,9	1,3	1,92	15,5	4,2	29,2	1,8	0,3
STANDARD II	9,3	7,5	24,7	207,1	28,1	178,6	9,6	139,1	5,5	54,4	2,1	3,33	16,8	5,5	31,6	1,2	0,7
STANDARD III	2,3	7,4	6,1	196,7	30,3	173,0	6,1	153,7	3,2	60,0	1,3	1,72	16,1	2,3	30,2	2,8	2,2
SUPERLONG	9,3	10,9	24,7	174,8	18,2	155,0	10,0	119,0	13,0	46,5	5,1	7,12	21,0	8,5	39,4	2,0	0,2

From Fig. 10 and Fig. 11 it is obvious that standard I and II are difficult to be separated. However, by comparing the calculated mass splits based on the full set of shape parameters it was possible to assign calculated points to the different channels. Special is also the standard III channel with its third barrier and the early ending. It is interesting to see if this component influences the experimental results.

The predictions of the fission properties of the individual channels equivalent to the components of fission given in Table 8 are now possible.

The $^{10}B(n,\alpha)\ ^{7}Li$ Cross Section

E. Wattecamps

On request of the INDC/NEANDC nuclear standards subcommittee the status of the $^{10}B(n,\alpha)\ ^{7}Li$ standard cross section was collated in a paper submitted for publication as an OECD/NEA document. The report covers the following topics:

- status of the requests;
- status of the recommended reference data;
- status of recent and ongoing measurements.

Non-Neutron Data

Alpha-Particle Emission Probabilities (P_α) of ^{239}Pu

E. García-Toraño*, M. Aceña*, G. Bortels, D. Mouchel

The P_α of 16 transitions were measured and analysed at CBNM and CIEMAT. A solution of 99.994 % enriched ^{239}Pu (by activity) was provided for this purpose by NIST, USA. Both laboratories measured and analyzed the spectra using their own computer code. The results for the two major emissions disagree with recent evaluated data[1]. Final results for the five most important emissions only are shown in Table 9.

Table 9. ***Selected P_α of ^{239}Pu, measured at CBNM and CIEMAT as compared with evaluated data***

Present Measurements		NDS[1]			
$P_\alpha \cdot 100$		$P_\alpha \cdot 100$		E_α [keV]	
.047	(13)	0.030	(4)	5055.35	(14)
.078	(8)	0.036	(4)	5076.29	(14)
11.94	(7)	11.5	(8)	5105.5	(8)
		< 0.03		5111.2	(2)
17.11	(14)	15.1	(8)	5144.3	(8)
70.77	(14)	73.3	(8)	5156.59	(14)
		0.03		5156.66	(20)

* Centro de Investigaciones Energéticas, Medioambientales y Tecnológicas (CIEMAT), Madrid, Spain

(1) M.R. Schmorak, Nuclear Data Sheets 66 (1992) 839

NUCLEAR DATA FOR FISSION TECHNOLOGY

The objective of the work on nuclear data for fission technology is to reach a more accurate knowledge of data requested in fission research and in fission technology. Measurements cover actinide fission cross section data as well as structural material neutron interaction data. Research topics are taken to fulfil European demands collected in the NEA High Priority Request List.

Neutron Data of Actinides

Fission Cross-Section of ^{239}Pu

C. Wagemans*, P. Van Uffelen**, A. Deruytter, R. Barthélémy, J. Van Gils

A good knowledge of the $^{239}Pu(n,f)$ cross-section is required for various applications in nuclear industry (e.g. fast reactors, MOX-fuel elements). Despite the large number of $\sigma_f(E)$-measurements for ^{239}Pu, the uncertainty on this quantity remains too important. This is mainly due to the fact that the high resolution measurements of Weston and Todd[1] in the neutron energy region from 20 eV to 100 keV are systematically lower (by about 4 %) than all recent evaluations (ENDF-B6, JEF-2, JENDL-3) and almost all other experimental data.

To tackle this problem, a NEACRP/NEANDC International Evaluation Cooperation Subgroup was created. The present work is one of the actions decided by the subgroup. Its aim is not to deliver a new set of $\sigma_f(E)$-data, but to determine a reliable value for

$$I_f = \int_{100\,eV}^{1000\,eV} \sigma_f(E)dE,$$

since Weston and Todd[1] normalized their measurements on $I_f = 8996$ b·eV.

This value was determined from a separate measurement going down to thermal neutron energy, but with fairly poor statistics. As a consequence, the uncertainty on this integral is rather important: 1.9 % normalization uncertainty, about 1 % systematic uncertainty and 0.15 % statistical uncertainty.

In order to verify the suspicion of a too low normalization factor in the Weston and Todd[1] data, two independent experiments were performed at two 8 m flight-paths of GELINA, the accelerator being operated at a 100 Hz repetition frequency with 11 ns burst widths and with an average electron current of 8 μA.

---

* Rijksuniversiteit Gent, Belgium
** Vrije Universiteit Brussel, Belgium

(1) L. Weston and J. Todd, Nucl. Sci. Eng. 88 (1984) 567

In both cases the neutron flux was determined via the detection of the $^{10}B(n,\alpha)^{7}Li$ reaction products emitted after neutron bombardment of thin ^{10}B layers.

The first experiment was performed in a low detection geometry, using two 30 cm^2 large surface barrier detectors placed outside the neutron beam for the detection of the $^{239}Pu(n,f)$ fission fragments and the $^{10}B(n,\alpha)^{7}Li$ reaction products. These detectors were placed in a large evacuated detection chamber, in the centre of which a $^{239}PuF_3$ and a ^{10}B layer were mounted back-to-back. The ^{10}B layer had a thickness of 10.2 $\mu g/cm^2$ and an isotopic enrichment of 94 % ^{10}B. The $^{239}PuF_3$ layer contained 106 μg $^{239}Pu/cm^2$; the isotopic enrichment of the plutonium used was 99.9774 % of ^{239}Pu. It is clear that absorption and self-absorption effects are very small with such layer thicknesses.

For the second measurement, a double gridded ionization chamber was used, operated with a very pure CH_4 flow as counting gas, so here the detection geometry was almost 2π. The ^{239}Pu and ^{10}B layers were mounted back-to-back on the cathode. The $^{239}PuF_3$-layer thickness was 186 $\mu g/cm^2$ (isotopic enrichment: 99.9774 % ^{239}Pu). The ^{10}B-layer thickness was 10.5 $\mu g/cm^2$, with an isotopic enrichment of 94 % ^{10}B.

In both experiments, the background was determined using the black resonances of cadmium, rhodium, tungsten, cobalt and manganese. A separate measurement was performed to check the background due to neutrons from overlapping burst by operating GELINA at a repetition frequency of 50 Hz. In another test, the not-beam-dependent background was measured by operating GELINA at a 100 Hz repetition frequency but with zero power.

Both experiments were performed in parallel. After digitizing the detector signals, bi-dimensional pulse-height versus time-of-flight spectra were stored in two HP 1000 data acquisition systems. In Fig. 12 the $^{10}B(n,\alpha)$ and $^{239}Pu(n_{th},f)$ counting rate spectra as a function of the neutron energy are shown for the measurement with the ionization chamber.

The data reduction was done adopting the ENDF-B6 values for the $^{10}B(n,\alpha)$ and the $^{239}Pu(n_{th},f)$ cross sections, the latter one being used for the normalization of the σ_f data. Combining the results of both measurements, a weighted value I_f = (9250 ± 100) b·eV was obtained, in perfect agreement with the result of an independent experiment recently performed by Weston et al., yielding I_f = (9300 ± 110) b·eV, indicating that the old Weston and Todd data should be renormalized, which will remove the major part of the discrepancy.

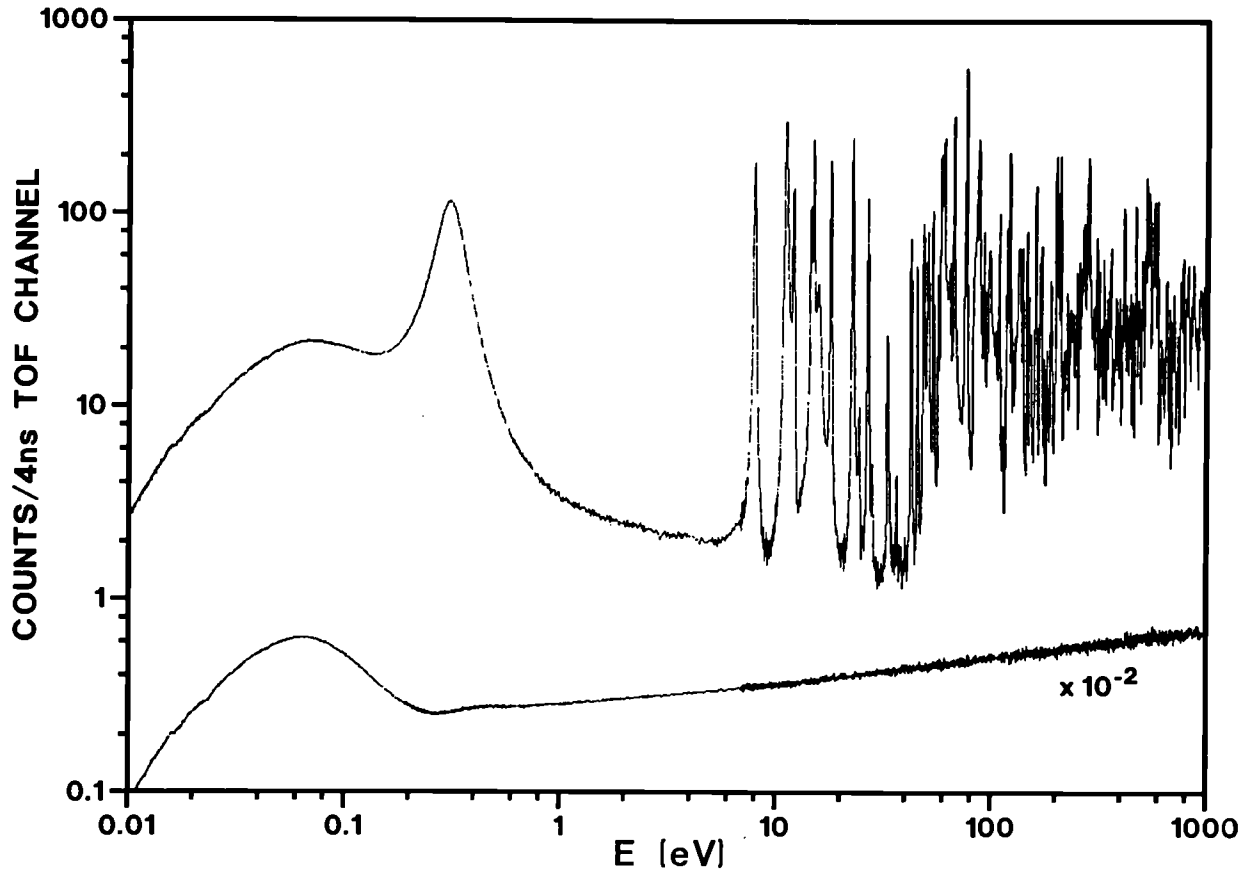

Fig. 12. *^{10}B (n,α) (lower) and ^{239}Pu(n,f) (upper) counting rate spectra as a function of the neutron energy*

Investigation of the Characteristics of the ^{242}Pu and ^{244}Pu(SF)-Fragments Distributions

C. Wagemans*, L. Dematté**, S. Pommé***, A. Deruytter, R. Barthélémy, J. Van Gils

In the frame of a systematic study of the mass and energy distributions (and their correlations) of the spontaneously fissioning plutonium isotopes, more than 30.000 ^{242}Pu(SF) events have been recorded. The measurements were performed relative to the well-known $^{239}Pu(n_{th},f)$ reaction, for which purpose a thermal neutron beam of the BR1 reactor of the SCK/CEN(Mol) was used. These data are being analysed, giving special attention to cold fission events.
In the case of ^{244}Pu about 7.000 spontaneous fission events have been recorded so far. These measurements are being continued.

* Rijksuniversiteit Gent, Belgium
** EC Fellow from University of Bologna, Italy
*** EC Fellow from University of Gent, Belgium

A Multi-Purpose Charged Particle Detection System

C. Wagemans*, S. Druyts**, R. Barthélémy, J. Van Gils

A multi-purpose charged particle detection system consisting of two gridded gas-flow ionization chambers and two 2000 mm^2 large, 1000 µm thick surface barrier detectors and the corresponding data acquisition system have been further developed and optimized.

In its simpliest configuration (using only one gridded ionization chamber), the $^{35}Cl(n,p)^{35}S$ and $^{36}Cl(n,p)^{36}S$ reactions have been studied from thermal up to 10 keV neutron energy. The $^{35}Cl(n,p)$ results obtained at 8 and 30 m flight-path lengths are shown in Fig. 13 and compared with the data of Koehler[(1)]. The resolution in our experiments is definitely better; the resonance strengths however agree within the uncertainties quoted.

By combining each ionization chamber with the corresponding surface barrier detector, a double ΔE-E telescope is formed, enabling the identification of light charged particles. In this configuration, the detector is suited for ternary fission studies.

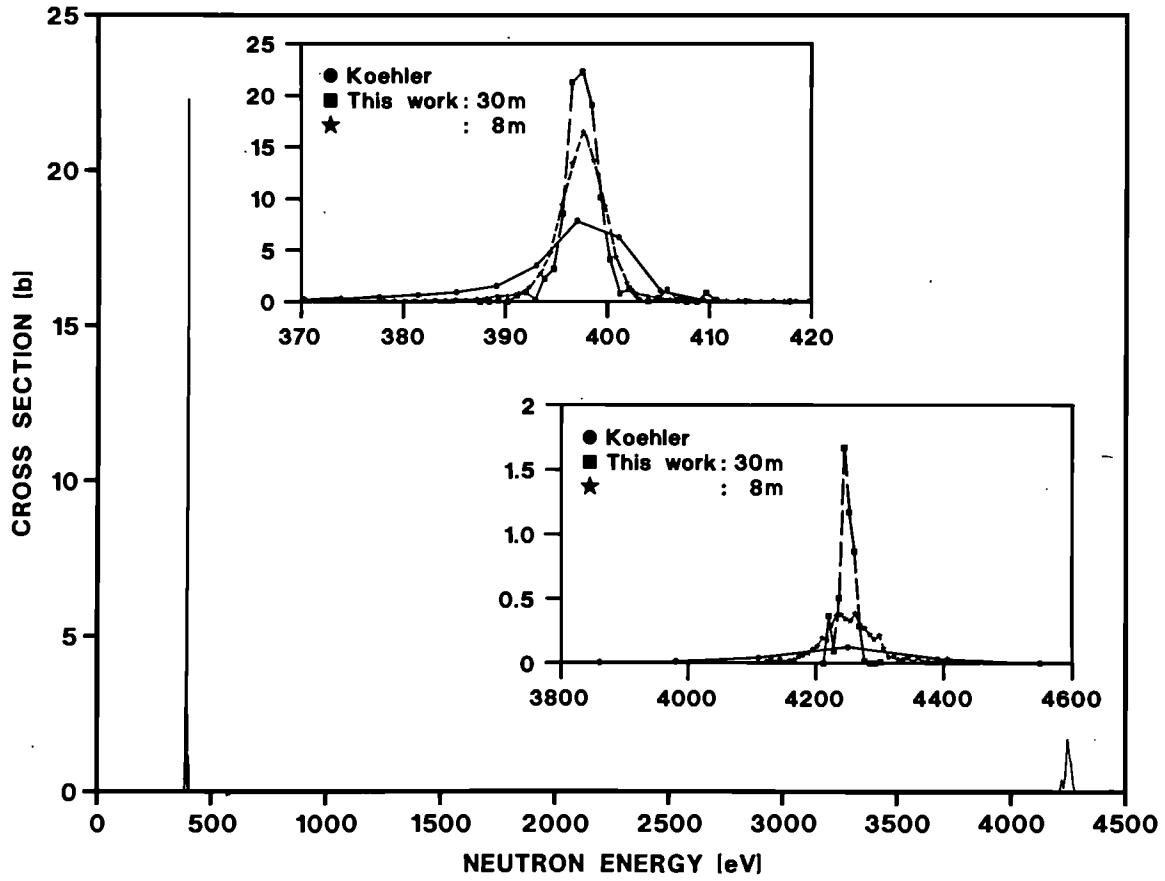

Fig. 13. ***$^{35}Cl(n,p)$ cross section versus neutron energy. The magnified inserted drawings show the results obtained for the 398 eV and 4250 eV resonances***

* Rijksuniversiteit Gent, Belgium
** EC Fellow from KU Leuven, Belgium

(1) P.E. Koehler, Phys. Rev. C44 (1991) 1675

Spin Assignment of ^{238}U p-Wave Resonances

F. Gunsing*, F. Corvi, H. Postma**, K. Athanasopoulos, A. Mauri***

The aim of this experiment is to contribute to parity-non-conservation (PNC) studies, performed at Los Alamos in the frame of the TRIPLE collaboration. In fact, polarized neutron measurements carried out at the LANSCE facility allowed the investigation of sixteen ^{238}U p-wave resonances and the discovery of parity mixing in a number of them[1]. For the interpretation of these data, the spin of the relevant resonances is needed.

The employed method exploits the fact that the population of the low-lying levels of the compound nucleus ^{239}U formed in neutron capture depends significantly on the initial spin. These relative populations of the levels are determined by looking at the intensities of gamma transitions de-exciting them. The spin effect is then enhanced by measuring the intensity ratio of two transitions de-exciting levels of different spins. The most promising combination is the ratio of the intensity of the ground state transition de-exciting the $J^\pi = 5/2^-$ state at 539.3 keV and the intensity of the unresolved doublet consisting of the 552.1 and 554.1 transitions de-exciting states with $J^\pi = 3/2^-$ and $1/2^+$, respectively.

A measurement carried out in 1991 suffered from an important background due to the presence of 2000 ppm ^{235}U impurity. The measurement was repeated in 1992 using a uranium disc of 11.1 cm diameter and 694 g mass on loan from ORNL, containing only 9 ppm of ^{235}U. The time-of-flight capture spectra of the two runs are compared in Fig. 14 for the neutron energy range 8 - 88 eV. The structure present in the first run (upper part) due to ^{235}U resonances disappears in the second run.

From the 1992 measurements values of the ratio r = I(539)/(I(552) + I(554)) were calculated and plotted vs neutron energy as shown in Fig. 15. In spite of the large errors, a split into two groups whose average values are shown by dotted lines can be deduced. The higher group is associated with $J^\pi = 3/2^-$ in view of the larger relative population of the $5/2^+$ level at 539 keV.

In the high energy part of the γ-ray spectrum the primary transitions to the ground state and/or to the 194 keV level (both having $J^\pi = 5/2^+$) for five p-waves could be observed: clearly these resonances have $J^\pi = 3/2^-$. The preliminary spin assignments obtained with the low-level population method and with the primary transitions are summarized in Table 10. The results of the two methods are in good agreement. The longitudinal asymmetry values P of the Los Alamos group are listed in the last column of Table 10. With the exception of the 10.2 eV resonance, these data are consistent with the present spin assignment.

---

* EC Fellow from Technical University of Delft, The Netherlands
** Visiting scientist from Technical University of Delft, The Netherlands
*** National expert from ENEA, Bologna, Italy

(1) X. Zhu e.al., Phys. Rev. V 46 (2), 1992, p. 768

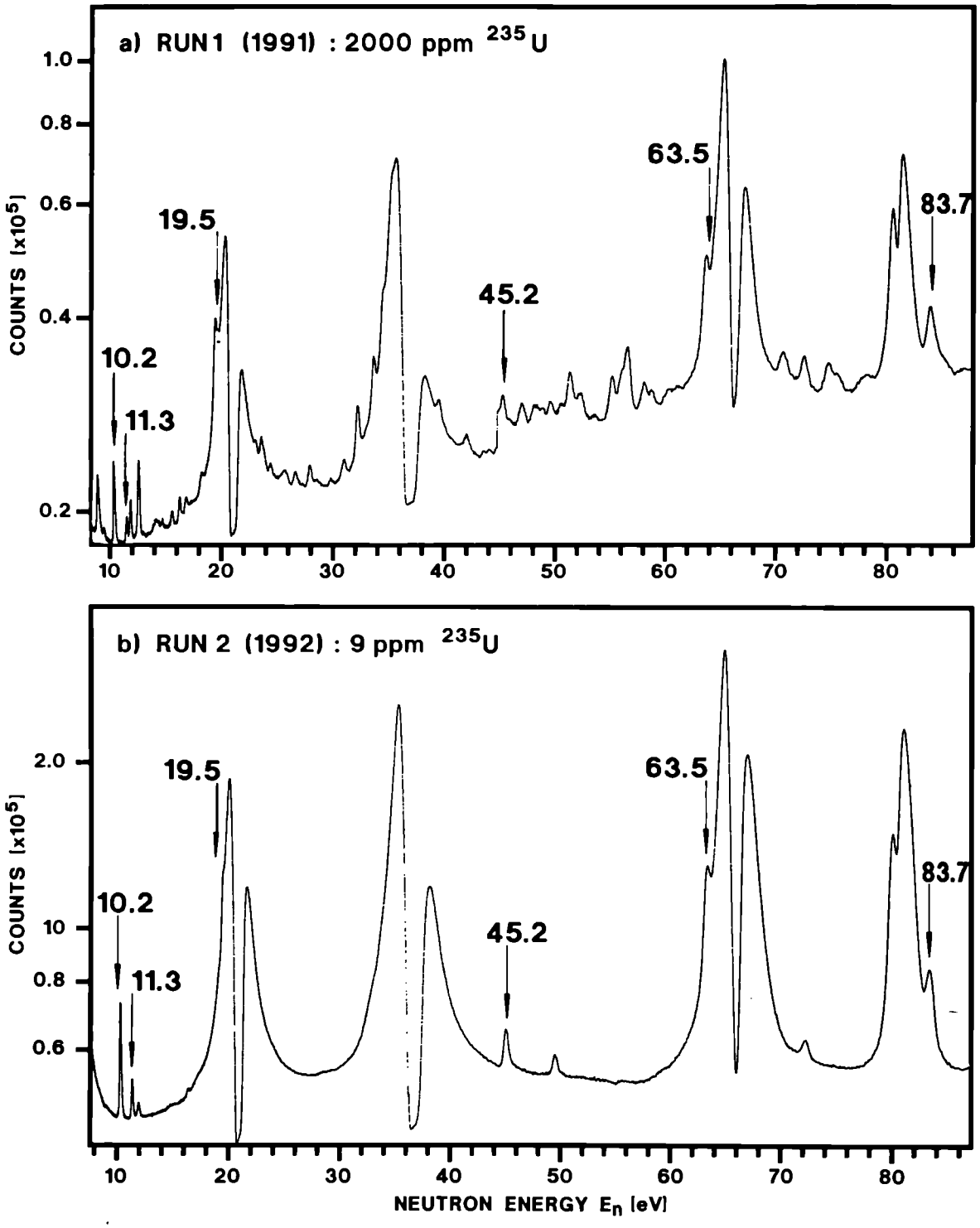

Fig. 14. Time-of-flight capture spectra as a function of the neutron energy: a) RUN 1 (1991), b) RUN 2 (1992)

The measurement is continuing in order to reduce the statistical errors and to extend the assignment to weaker resonances.

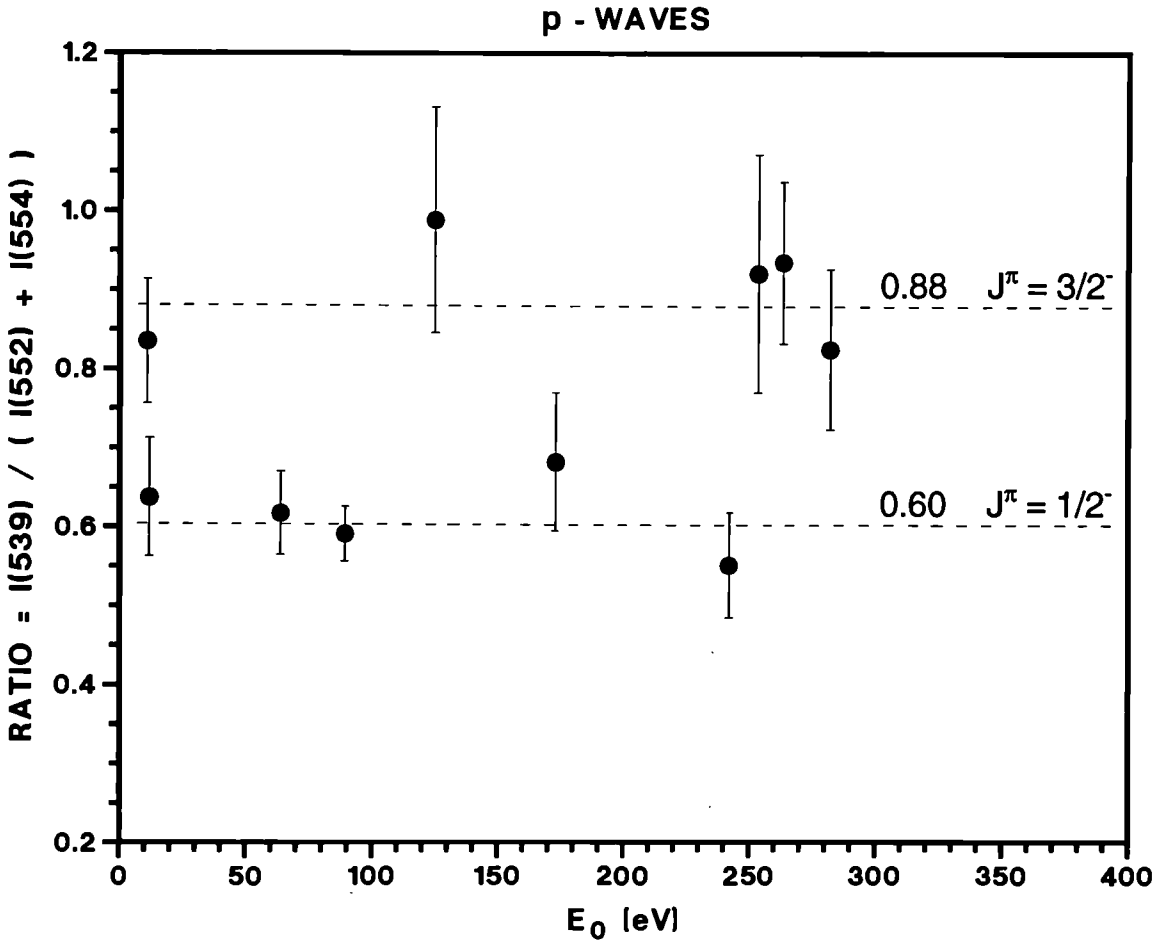

Fig. 15. Spin ratio as a function of resonance energy

Table 10. Results of the present spin assignment and values of the longitudinal asymmetry P for eleven ^{238}U p-waves

E_0 [eV]	Level spin J^{π}		$P = (\sigma_+ - \sigma_-)/(\sigma_+ + \sigma_-)$ [10^3]
	low-level popul.	primary trans.	
10.2	3/2	3/2	− 1.7 ± 0.9
11.3	1/2		7.2 ± 4.0
63.5	1/2		25 ± 4
89.2	1/2		− 2.4 ± 1.1
125.0	3/2		11 ± 9
173.2	1/2		11 ± 8
242.7	1/2		− 6.1 ± 6.2
253.9	3/2	3/2	− 1.6 ± 6.4
263.9	3/2	3/2	− 0.1 ± 4.1
282.5	3/2	3/2	3.8 ± 13
351.9		3/2	

Search for the Shape Isomer in ^{239}U and ^{233}Th

S. Oberstedt*, H. Weigmann, H. Wartena, C. Bürkholz, J.P. Theobald**

In the past a series of shape isomers in actinide nuclei with $Z \geq 94$ were found all decaying via the fission channel. For the lighter actinides ($Z < 94$) only a few examples exist, where the shape isomer could be detected. However, in this mass region the cross sections show intermediate structure phenomena in subthreshold fission. The interpretation in terms of the double humped fission barrier leads to discrepancies with the results from calculations on fast-fission data, especially in uranium. Therefore it has been proposed to interprete intermediate structure in $^{238}U(n, f)$ as delayed fission through a shape isomeric state with a half-life of a few ns[1]. In order to search for this reaction path, the 721.6 eV-neutron resonance in ^{239}U was investigated in a γ-γ coincidence experiment performed at the time of-flight spectrometer GELINA.

In ^{233}Th a weak indication exists for a shape isomeric state with a half-life $T_{1/2}$ of about 10 ns[2, 3], but no measurable subthreshold fission cross-section exists below $E_n < 50$ keV. Therefore, with the same experimental set-up the neutron resonances in ^{233}Th for $E_n < 4.2$ keV were investigated in order to search for intermediate structure in the relative delayed γ-ray yield.

The data-taking has now been completed. In the next two paragraphs the new experimental findings will be compared with existing systematics on isomeric half-lives and barrier parameters.

a) Is there isomeric fission in ^{239}U?

The analysis of the coincidence spectrum of the 721.6 eV-resonance (Fig. 16 left part) does not show any significant contribution of delayed coincidences stemming from isomeric fission. Testing the line-fitting procedure by simulating the coincidence spectrum with a Monte Carlo technique on the basis of theoretical assumptions on the resonance parameters shows that a shape isomer with a half-life between 1 and 10 ns must be excluded.

To be more sensitive to longer half-lives, additionally the relative delayed γ-ray yield R, i.e. the ratio between the resonances areas for delayed and prompt coincidences, was investigated. As shown in the right part of Fig. 16 the 721.6 eV resonance behaves significantly different compared to its neighbour s-wave resonances, which show apparent delayed γ-ray yield due to accidental coincidences. However, the observed difference is primarily due to the detection of fission neutrons by the detector. True delayed γ-rays from a shape isomer with a half-life $T_{1/2} < 250$ ns should show a clearly larger effect and can be excluded. This result does not depend on the assumption of either the case of

---

* EC Fellow from Technische Hochschule Darmstadt, Germany
** Technische Hochschule Darmstadt, Germany

(1) J.E. Lynn, Proc. Int. Conf. 50 years with Nuclear Fission, Vol. I, p. 148 (1990)
(2) J. Schirmer et al., Jahresbericht des MPI für Kernphysik Heidelberg, 1988, p. 67
(3) P. Reiter et al., GSI Scient. Report, 1990, p. 25

delayed fission or prompt fission and isomeric γ-ray decay back to the first potential minimum.

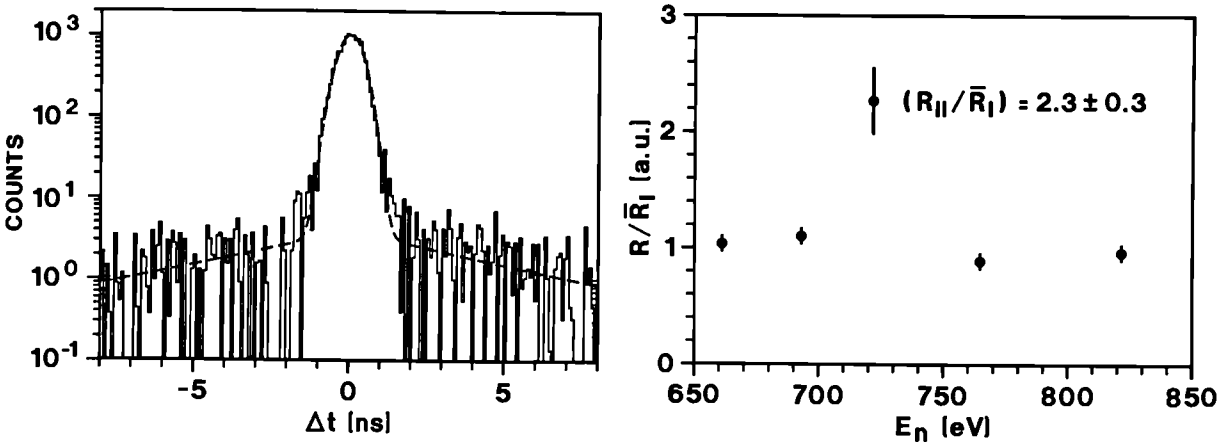

Fig. 16. ***In the left part the coincidence spectrum of the 721.6 eV-resonance in ^{239}U is shown. The dashed line indicates the result of fitting the data with a Gauss+exponential function. The right part gives the relative delayed γ-ray yield R in units of the average value R_I***

On the basis of the experimental results the assumption that intermediate structure in the subthreshold fission cross-section of ^{238}U is caused by isomeric fission cannot be sustained. Moreover, this result may be seen as an indication that the usual parametrization of the fission barrier in terms of parabolic segments is not valid generally.

b) Intermediate structure and the shape isomer of ^{233}Th.

In Fig. 17 the distribution of the relative delayed γ-ray yield R as a function of neutron energy E_n for resonances in $^{232}Th + n$ is displayed. The left part shows the data including all γ-ray energies. The data in the right part were obtained by setting different conditions on both the first and the second γ-ray energy. The visible structures produced by larger R-values at 1 keV and 2 keV in both distributions were statistically tested against the hypothesis of a normal distribution. Including the non-statistically distributed positions for the increased R-values, a probability of less than 10^{-4} (right part of Fig. 17) was found for the hypothesis of no structure, thus indicating the existence of two class-II states in ^{233}Th in this energy range. From the shape of these structures the class-II level spacing D_{II}, the isomeric ground state energy E_{II}, the coupling width $\Gamma\downarrow$ and, in the framework of the picket-fence model, the maximum class-II fraction c_{II} could be estimated (Table 11). A further analysis of the data using the parameters from Table 11 shows that the isomeric half-life $T_{1/2}$ should lie between 1 ns and 100 ns. From the experimental values on $\Gamma\downarrow$ and $T_{1/2}$ the parameters of the inner barrier (E_A, $\hbar\omega_A$) could be estimated (Table 12). These parameters seem to fit into the global trend as it might be seen in Table 12.

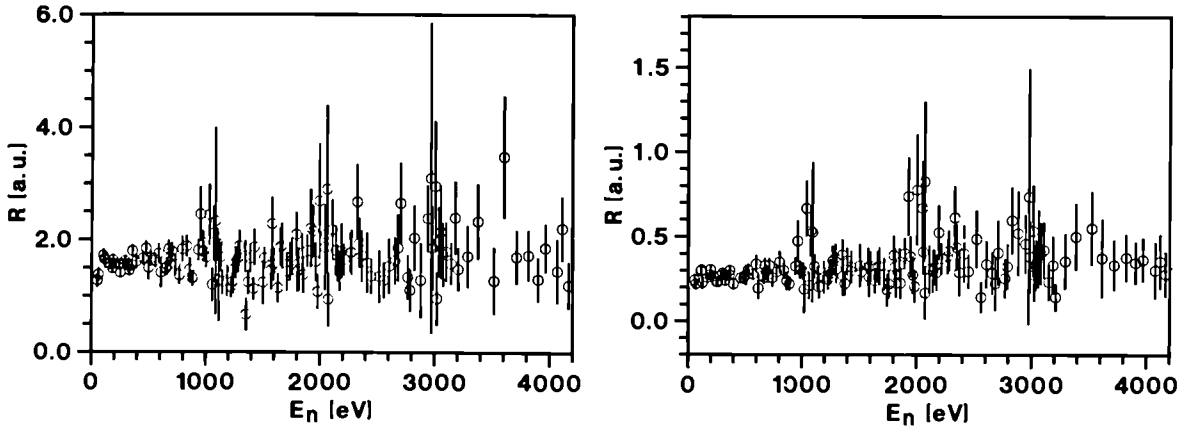

Fig. 17. Relative delayed γ-ray yield as a function of incident neutron energy E_n. The left part shows the data without γ-ray energy conditions. For the data in the right part the following γ-ray energy regions were selected: $E_{\gamma 1}$ ε (2.0,3.5) MeV and $E_{\gamma 2}$ ε (0.4, 2.9) MeV

Table 11. Experimentally obtained intervals for the class-II level spacing D_{II}, the isomeric groundstate energy E_{II}, the coupling width $\Gamma\downarrow$ and the maximum class-II admixture c_{II}

D_{II}	[keV]	0.6	2.1
E_{II}	[MeV]	1.6	2.1
$\Gamma\downarrow$	[meV]	60	200
c_{II}		0.16	0.05

Table 12. Estimate of the inner barrier parameters E_A, $\hbar\omega_A$ of ^{233}Th. For comparison the value of $\hbar\omega_A$ for two additional nuclei were calculated

Comp. Nucl.	E_{II} [MeV]	E_A [MeV]	$T_{1/2}$ [ns]	$\hbar\omega_A$ [MeV]
^{233}Th	1.85 ± 0.25	$4.7^{+0.8}_{-0.1}$	1 ... 100	$1.2^{+0.2}_{-0.1}$
^{236}U	2.35[a)] 2.56[a)]	5.6[b)] 5.7[b)]	115[a)] 240[a)]	1.26 1.16

a) p. 45 and b) p. 30 of C. Wagemans (Editor), The Nuclear Fission Process, CRC Press (1991)

Non-Statistical Effects Observed in s-Wave Neutron Resonances of ^{238}U

G. Rohr, R. Shelley

A very interesting non-statistical effect of the level spacings is observed in the s-wave neutron resonances of ^{238}U. This effect can be deduced from the sixteen spacings up to 380 eV as a function of the spacing sequence (number) observed with increasing neutron energy. The first two spacings are equal, the third is double and the fourth is once more the same spacing as for the first two. The first seven spacings are part of a regular spectrum with three different average spacings different by a multiple of 7.3 eV. The uncertainty of all average spacings is (7.3 × 0.15) eV. With increasing energy, distortions in the resonance spectrum can be observed for the spacing numbers 8, 9, 10 and 13. However, the sum of spacings 8 and 9 as well as 10 and 13 have a multiple of 7.3 eV and may give a hint to the reaction process.

The statistical relevance of the regular spacings can be discussed using a Wigner distribution with an average spacing of 20.2 eV calculated from the sixteen spacings. The probability to observe regular spacings at the energies of (M × 7.3) eV in the energy window (7.3 × 0.15) eV for randomly distributed values can be estimated. The results for M = 2, 3 and 4 are PM = 0.082, 0.073 and 0.048, respectively. According to this the detection of two consecutive spacings with M = 2 for a random sample is $0.67 \cdot 10^{-2}$. The probability for the first seven spacings being regular is less than $2 \cdot 10^{-8}$, and is statistically excluded. Therefore the observation of only three successive regular spacings in the energy windows of ± 15 % are relevant for a non-statistical effect.

The nearest level spacing distribution for resonances below 380 eV contains four peaks. In contrast the level distribution of simple resonances for nuclides A < 100 (^{40}Ca, ^{54}Fe, ^{58}Fe and ^{96}Zr) has less structure and could be called a Gaussian-like distribution. With the inclusion of ^{238}U resonances up to 2000 eV the level distribution approaches a Wigner function. Therefore the nearest level spacing distribution for simple resonances and medium light nuclides changes from a Gaussian-like function to a distribution containing several peaks for medium heavy and heavy nuclides. When resonances of higher energy are included the distribution approaches a Wigner function.

γ-Ray Decay Towards the Isomeric Groundstate in ^{239}U

S. Oberstedt*, F. Gunsing**, F. Corvi

The 721.6 eV-resonance in $^{238}U + n$ is assumed to be a nearly pure class-II state. Therefore its capture γ-ray spectrum should show lines corresponding to the

* EC Fellow from Technische Hochschule Darmstadt, Germany
** EC Fellow from Technische Universiteit Delft, The Netherlands

decay within the second potential well. In a high resolution measurement of γ-rays from neutron capture in ^{238}U four hitherto unknown γ-ray transitions could be found in the 721.6 eV-resonance as indicated in the upper part of Fig. 18. They are not observed in any other ^{238}U resonance. For comparison the γ-ray spectrum of the 661.14 eV resonance, which is a pure class-I state, is shown in the lower part of Fig. 18. This first indication for γ-ray transitions towards the isomeric state has to be validated by a more quantitative analysis.

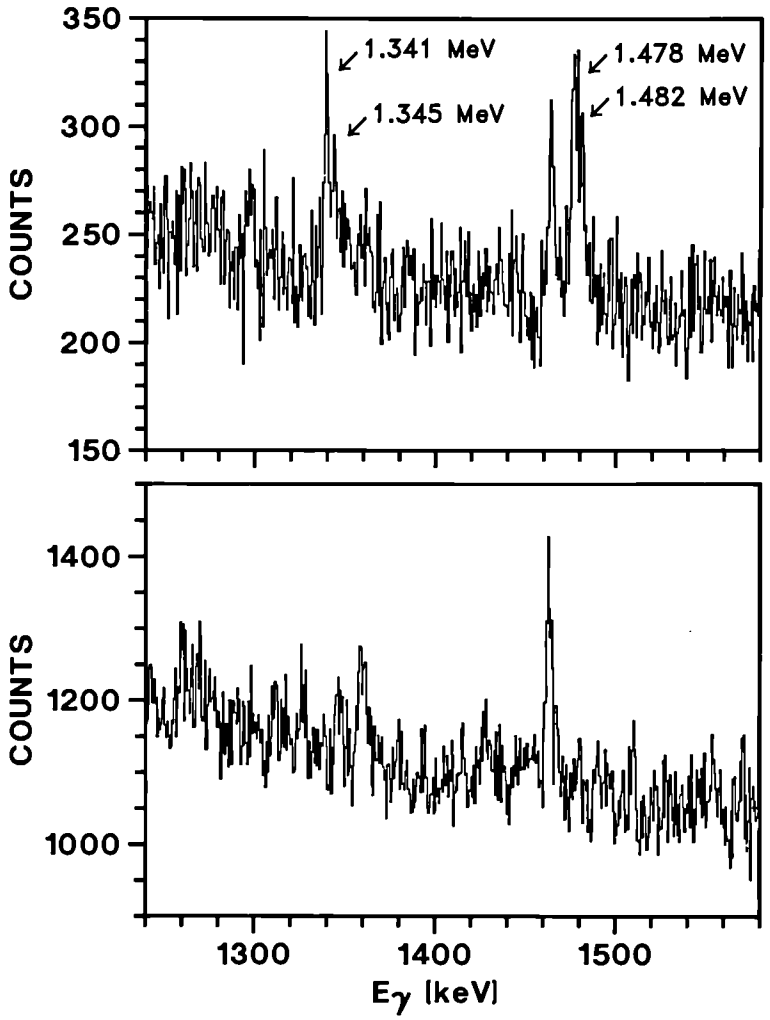

Fig. 18. *γ-ray energy spectrum of the 721.6 eV-resonance (upper part) with the four transitions indicated. The lower part shows the γ-ray spectrum of the 661.14 eV-resonance for comparison*

Resolution Function of Neutron Time-of-flight Measurements

C. Coceva*, M. Magnani**

In neutron cross-section measurements performed at the time-of-flight GELINA facility, a precise knowledge of the resolution function is of essential importance for the deduction of reliable values of resonance parameters, as required in various nuclear applications.

This resolution function results from the convolution of three independent components:

1) Time distribution of fast neutrons generated within the Linac target.
2) Delay time distribution, from the generation of neutrons to their escape from the target-moderator assembly.
3) Delay time distribution, from neutron entrance into the detector material to the corresponding detection time signal.

Part 1) follows closely the time distribution of the accelerated electrons as they impinge on the target.

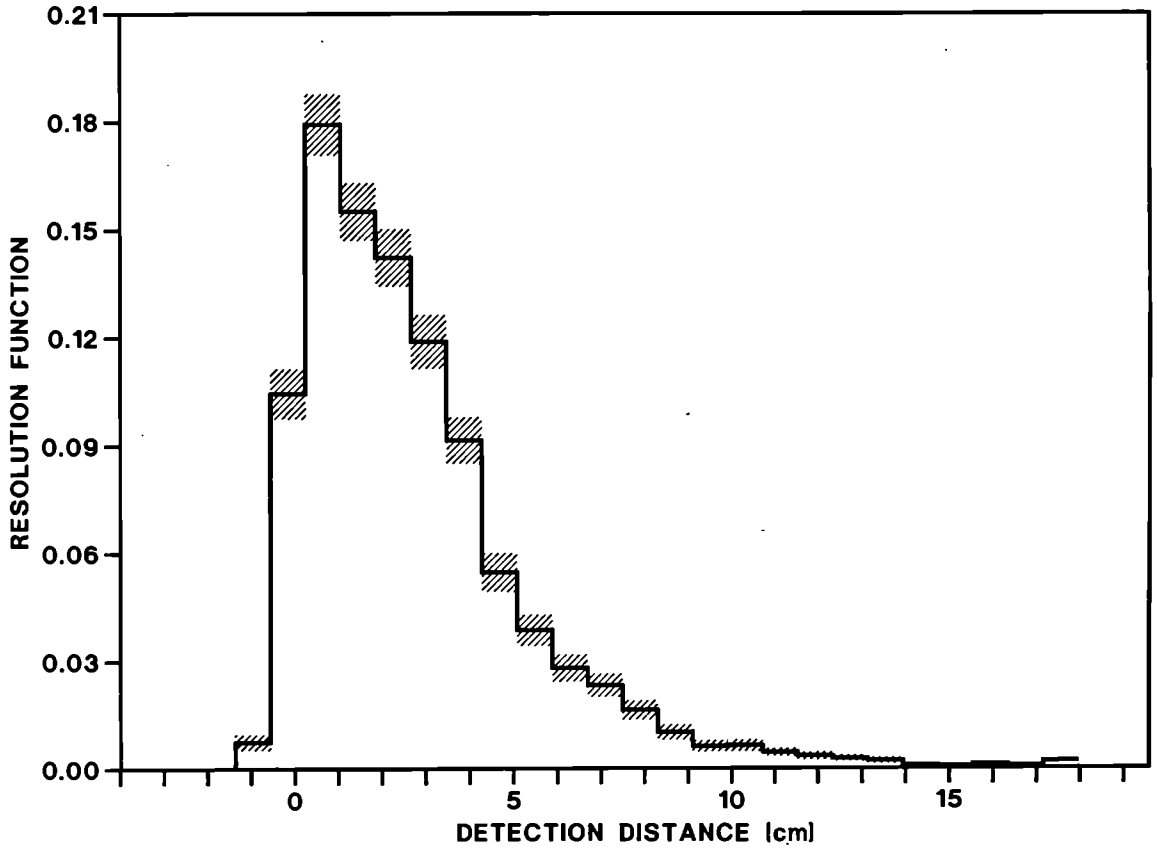

Fig. 19. ***Calculated resolution function for neutrons escaping from the moderator at 0° and with final energies in the range from 50 up to 250 keV***

* Visiting Scientist from ENEA, Bologna, Italy
** ENEA, Bologna, Italy

For the contribution 2) a Monte Carlo simulation was performed considering the spacial distribution of the neutron source, the rotating uranium target, the cooling system, and the water-beryllium moderator tanks[1,2]. Neutron distributions were obtained for energies from 4 eV to 6 MeV and for each flight-path direction.
It was found that the large amount of material necessarily introduced by the geometry of the rotating target, produces long tails in the time distribution of the emitted neutrons, spoiling the resolution.
Fig. 19 shows a calculated resolution function for neutrons escaping from the actual rotary target-moderator assembly of GELINA.
Contribution 3) was obtained for two different detectors:

a) A ^{6}Li-loaded glass scintillator, in the neutron energy range of 30 eV - 300 keV;
b) A ^{10}B plug, in the neutron energy range of 100 eV - 200 keV.

The above calculations were performed by means of a Monte Carlo simulation too[3]. In all cases, JEF cross-section data files were employed.

Neutron Data of Structural Materials

Total Cross Section Measurements of Natural Iron

K. Berthold*, G. Rohr, C. Nazareth

A series of high resolution neutron total cross section measurements through several thicknesses of natural iron have been started. Two first transmission measurements with a running time of 10 days each for the sample thickness of 16 mm and 48 mm have been performed. These measurements result in a much better resolution than previous transmission data.
To measure the complete spectrum of neutron energy originated by the 1 ns burst of electrons impinging on a uranium target, a plastic scintillator detector (2.5 cm thick) is linked to the Nuclear Data 9900 data acquisition system to record events in two 64 k channels energy spectra of 1 ns/channel. At a 400 m distance of the detector from the neutron target the neutron energy range is recorded from 175 keV to 25 MeV.
Another measurement with a rather thick sample of 140 mm is ongoing and will be used to check whether the total cross section is responsible for the

---

* EC Fellow from Technische Hochschule Darmstadt, Germany
(1) A. Bignami, C. Coceva and R. Simonini, EUR 5151e (1974)
(2) C. Coceva, R. Simonini and D.K. Olsen, Nucl. Instr. Meth. 211 (1983) 459
(3) C. Coceva, P. Giacobbe and M. Magnani, Nucl. Sci. Eng. 91 (1985) 209

underestimation of fast neutron transmission through steel structures such as reactor pressure vessels.
It is planned to analyse the resonance structure up to 1 MeV. The resulting resonance parameter data will enable a systematic investigation of the statistical description of the cross section in the higher MeV region. In addition the underlying statistical properties of resonance parameters will be studied with respect to intermediate structure and/or non-statistical effects of the level density.

Neutron Resonance Parameters of ^{58}Ni+n and ^{60}Ni+n From Very High Resolution Transmission Measurements

A. Brusegan, R. Shelley, G. Rohr, E. Macavero, C. Van der Vorst

This work is part of the investigation of neutron cross sections of structural materials. Descriptions of the several measurements performed and initial analyses can be found in the two previous annual reports.
In order to supplement the 50, 100, 200 and 400 m flight-path data previously obtained with the 1 ns burst width of GELINA a new measurement of the neutron transmission through a 1.5 mm thick enriched sample of ^{58}Ni was done at 100 m with a 6 mm thick lithium glass detector.
The complete data sets have now been re-analysed and extended up to neutron energies of 1.01 MeV for ^{58}Ni and 800 keV for ^{60}Ni, taking into account the improved description of the resolution function of the present GELINA neutron source configuration.
For the resonance parameter analysis the codes REFIT[1] and MULTI[2] have been used, the latter being recently extensively modified to accomodate the new resolution function distributions for the neutron source, with and without moderator, and for the detectors (boron slab and lithium glass). Parameters for 384 resonances in ^{58}Ni and 350 resonances in ^{60}Ni have been sent to KFK, where the collection of data required for the joint European and fusion files, JEF/EFF is coordinated.
Fig. 20 shows a small part of the measured cross section data fitted with our final resonance parameter data sets for typical mid-energy regions. The spectra show the best energy resolution presently available and was recorded at a neutron flight path of 400 m in 1 ns channels. For each isotope total cross section data for 35000 energy points in the range 0.5 - 15 MeV have been sent to the NEA data bank.

(1) M.C. Moxon, AEA-In Tec-0630 and CBNM/ST/90-131/1
(2) G.F. Auchaupaugh, Report CA-5473-MS (1974)

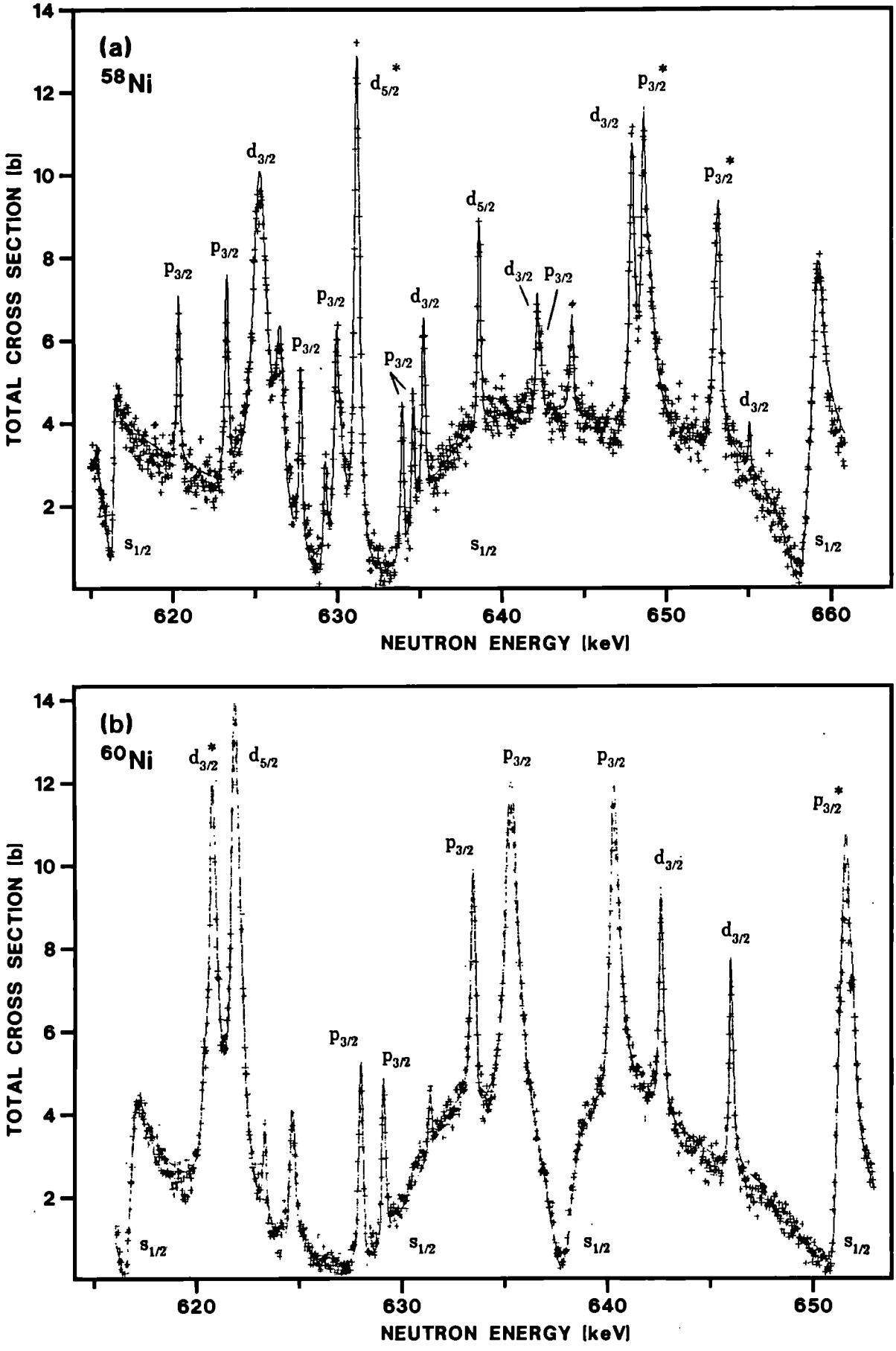

Fig. 20. *^{58}Ni (a) and ^{60}Ni (b) total neutron cross sections measured in the energy range 615 to 660 keV and fitted with our final resonance parameter data set. Spin assignments of the resonances are shown except for small levels which are assumed $p_{1/2}$ (*doublet)*

Neutron Data for Other Materials

High Resolution ^{138}Ba (n,γ) Measurements

F. Corvi, H. Beer*, A. Mauri**, K. Athanasopoulos

The overall structure of s-process nucleosynthesis is determined by a few small capture cross sections of isotopes which form so-called bottle-necks for the s-process flow. One of the most important nuclides is ^{138}Ba , with magic neutron number 82, which is half way between the iron seed (A = 56) and the s-process termination at ^{209}Bi. The necessary strength of neutron exposure to build up the elements beyond mass number 142 is chiefly dependent on the size of the ^{138}Ba capture cross section. For a test of the current stellar double pulse s-process model[1] (where neutrons are produced by the combined burning of the $^{13}C(\alpha,n)$ and $^{22}Ne(\alpha,n)$ reactions at temperatures of kT = 12 and 25 keV, respectively) a precise ^{138}Ba stellar reaction rate as a function of kT is needed. This requires the knowledge of the $^{138}Ba(n,\gamma)$ excitation function from a few eV to about 200 eV.

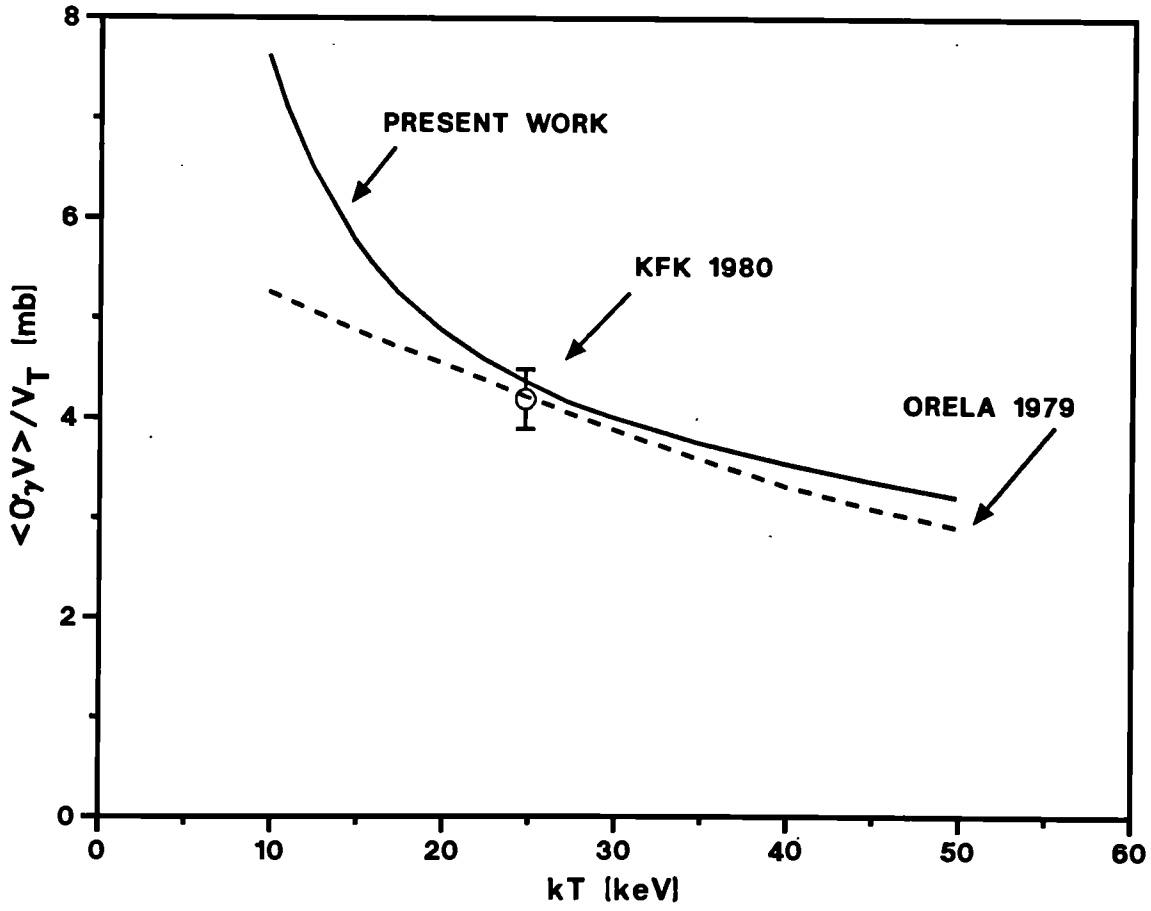

Fig. 21. The Maxwellian-averaged capture cross section vs stellar temperature

* Visiting Scientist from KFK, Karslruhe
** National Expert from ENEA, Bologna

(1) R. Gallino, in Evolution of Peculiar Red Giant Stars, eds. H. R. Johnson, B. Zuckermann, Cambridge University Press, 1989, p. 176

High resolution neutron capture measurements were performed at a 28.4 m flight path using a $BaCO_3$ sample of 43 g, enriched to 99.8 % ^{138}Ba. A total of 54 neutron resonances were resolved and analysed in the energy range 0.2 - 105 keV in order to derive their capture areas. In particular two strong resonances at E_0 = 0.648 and 1.946 keV were observed for the first time. The data were normalized to capture in gold at 4.9 eV employing the saturated resonance method. The Maxwellian-averaged capture cross section $<\sigma_\gamma v>/v_T$ calculated from the present data is given as a function of kT in Table 13 and compared in Fig. 21 to a curve from ORNL and to an activation data point at 25 keV from KFK.

While both curves are compatible with the KFK value, their behaviour vs temperature is quite different. The present data suggest a much steeper rise with decreasing kT. This means that an s-process dominated by the burning of $^{13}C(\alpha, n)$ at kT = 12 keV can drive the synthesis through the bottle-neck ^{138}Ba up to lead and bismuth more efficiently also with a reduced neutron flux (~ 30 %) than according to the previous ORNL data. A much larger capture cross section at kT = 12 keV has also consequences for the ^{138}Ba s-process abundance if formed at this stellar temperature. This may concern the interpretation of the s-process nucleosynthesis in barium stars and s-process related isotopic anomalies of barium in meteorites.

Table 13. ***Maxwellian-averaged (n,γ) cross section of ^{138}Ba for various kT values***

kT [keV]	$<\sigma_\gamma v>/v_T$ [mb]	kT [keV]	$<\sigma_\gamma v>/v_T$ [mb]
10	7.64 ± 0.52	25	4.38 ± 0.34
12.5	6.53 ± 0.46	30	4.02 ± 0.30
15	5.79 ± 0.42	35	3.76 ± 0.35
17.5	5.27 ± 0.39	40	3.55 ± 0.38
20	4.90 ± 0.35	45	3.37 ± 0.40
22.5	4.61 ± 0.34	50	3.20 ± 0.43

Radiative Transitions From Neutron Capture in ^{53}Cr Resonances

C. Coceva*

A measurement was performed of gamma-ray spectra emitted after neutron capture in s- and p-wave resonances of ^{53}Cr in the range 2 - 70 keV. The studied decay scheme concerns 38 levels of ^{54}Cr, with excitation energies from 0 up to 5.6 MeV. New information is obtained on the multiplicity of gamma cascades, on the spin and parity of ^{54}Cr levels, and on the spin of neutron resonances of ^{53}Cr.

* Visiting Scientist from ENEA, Bologna, Italy

Partial E1 and M1 radiative widths are obtained for transition energies from 4.1 to 9.7 MeV. Their frequency distributions follow chi-square functions with $\nu(E1) = 1.6$ and $\nu(M1) = 1.7$ degrees of freedom.
The overall energy behaviour of E1 reduced widths is in rough agreement with a Lorentzian shape, but the average intensity is higher than expected from photo-neutron data. The measured average E1 strength is $\langle S(E1) \rangle = (8.1 \pm 0.8) \cdot 10^{-15}$ MeV^{-5}. Fluctuations around this average are non-random, showing the existence of an intermediate structure. Reduced E1 widths are strongly correlated with the reduced neutron widths in the whole energy interval. Although with less evidence, an indication was found for a correlation between reduced E1 widths and spectroscopic factors of ^{54}Cr levels.
The measured average M1 strength $\langle k(M1) \rangle = (5.7 \pm 0.8) \cdot 10^{-9}$ MeV^{-3} appears to be energy-independent as in the single particle model. Reduced M1 widths exhibit wide random fluctuations. No significant correlation is found between E1 and M1 strengths.

NUCLEAR DATA FOR FUSION TECHNOLOGY

The objective of the work on nuclear data for fusion technology is to contribute to an improved knowledge of data for neutron transport calculation in the blanket and for an estimate of the gas production. Measurements are presently done in three areas: (1) double-differential neutron emission cross sections; (2) double-differential charged particle emission cross sections and (3) total and radiative capture cross sections of structural materials; since the latter are related to fission as well as to fusion technology, they are described in the section on fission technology.

Double-Differential Neutron-Emission Cross-Sections

J.A. Wartena, H. Weigmann, C. Bürkholz

The experimental methods applied as well as the main steps in the data analysis have been described in the preceding annual report.
The analysis of the data on the ^{9}Be(n,2n) cross section has been completed. In this analysis multiple scattering corrections are included which take into account the approximate angular distributions of the emitted neutrons as obtained from the preliminary analysis of the same experimental data. The final double-differential neutron emission cross sections for incident neutron

energies between 1.6 and 11.1 MeV have been transmitted to the NEA data bank.

During 1992 an extensive measurement campaign has been performed on neutron emission cross sections from ^{207}Pb. Apart from the neutrons also γ rays emitted after inelastic scattering have been recorded by the NE-213 detectors using pulse shape discrimination techniques. An example of the raw experimental data is shown in Fig. 22. It shows, for incident neutron energies between 7.7 and 8.4 MeV, the pulse height distributions measured by the detector which is positioned at an angle of 40 degrees with respect to the incident neutron beam; Fig. 22(a) is for emitted secondary neutrons. Fig. 22(b) for γ rays. Analysis of these data is in progress.

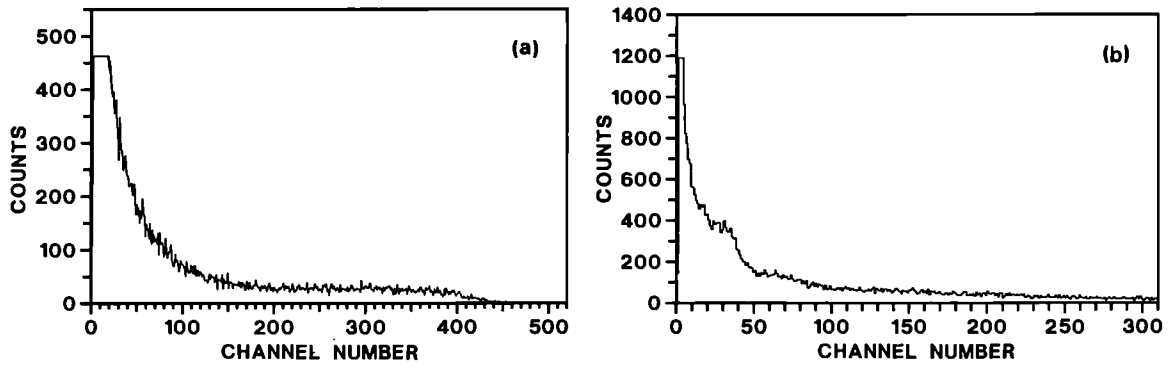

Fig. 22. Pulse height distributions measured by NE-213 detector for (a) neutrons and (b) γ-rays emitted from ^{207}Pb for incident neutrons between 7.7 and 8.4 MeV energy

Correction Programmes for Multi-Parameter Data of the ΔE-E-T Telescope

G. Rollin, E. Wattecamps

A light ion telescope was designed to measure (n,x) cross-section data at the pulsed Van de Graaff accelerator (burst width of 400 ps). To be particle specific and to separate well foreground from background reactions the energy loss, the energy and the time of flight of the particles are determined. To this end six parameters of each event are measured, called E_1, E_2, T, Z, D and Y, which are respectively:

- two pulse height spectra, E_1 and E_2, and one timing pulse T from the photomultipliers viewing the pilot-U scintillator (E detector);
- one time of flight information, Z, from the Multi-Wire-Parallel-Plate-Avalanche-Counter (MWPPAC) to the pilot U scintillator;
- one pulse height spectrum, D, of the MWPPAC (ΔE detector); and
- one time of flight information, Y, from the pick-up electrode in front of the target to the pilot U scintillator.

A sequence of programs was written in C language for use at the SUN computer with the following purposes:

- correction for time dispersion in the pilot-U scintillator: typically time resolution improvement from 1000 ps down to 300 ps;
- correction for pulse height dispersion in pilot-U scintillator due to attenuation of light: typically energy resolution improvement from 37 % down to 28 %;
- transformation of light output scale into particle energy scale for particle energies from 1.5 to 9 MeV. Calibration points together with an analytical fit are shown in Fig. 23;
- correction for energy loss in the telescope from the sample to the pilot-U scintillator (38 cm distance) across three zones of isobutane and across four foils of the MWPPAC;
- correction for time delays in the observed time of flight from the sample to the pilot U scintillator (38 cm) due to the energy losses mentioned before.

The corrections are illustrated in Fig. 24 showing two-dimensional spectra of time of flight versus alpha particle energy for Ni(n,α) at 8 MeV neutron energy. Spectrum "A" is a distribution of observed time of flight, corrected for dispersion in the scintillator, versus light output which is also corrected for dispersion in

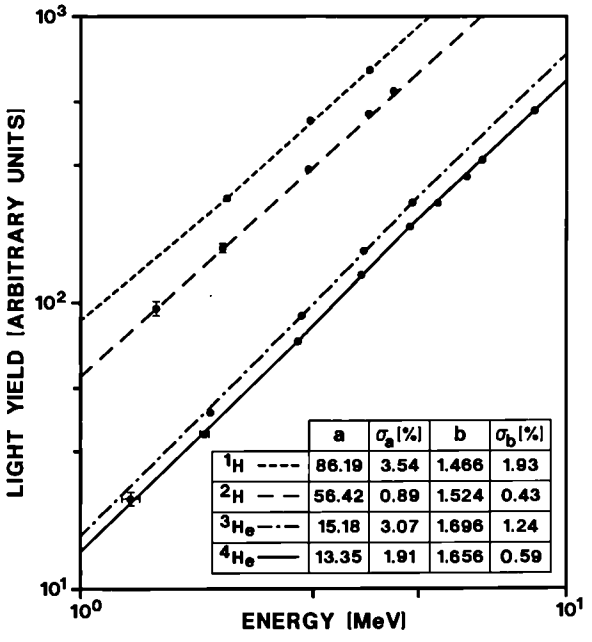

Fig. 23. Light yield produced in pilot U scintillator by various particles. Fitting equation: $Y = a \cdot E^b$

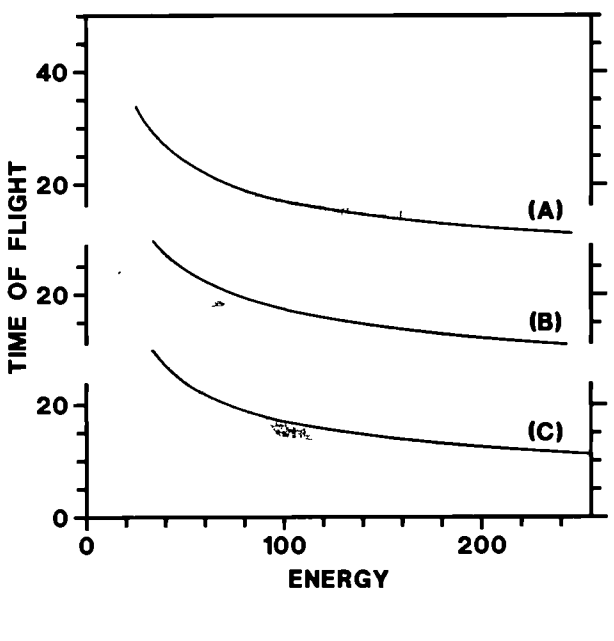

Fig. 24. Measured two-dimensional spectra of time of flight versus energy for Ni(n, α) reaction at 8 MeV neutron energy. (A) Observed time of flight versus light output. (B) Observed time of flight versus energy. (C) Time of flight versus energy, corrected for energy loss in the telescope

the scintillator. This spectrum is quite different from the expected dependence time of flight ~ $1/\sqrt{E}$.
Spectrum "B" shows time of flight versus alpha particle energy.
Spectrum "C" shows time of flight versus alpha particle energy both corrected for the effects of energy loss. It agrees well in shape and in absolute terms with the $1/\sqrt{E}$ dependence of the time of flight.

Test of Prompt Alpha Particle Detection from the $^{27}Al(n,\alpha)$ Reaction

G. Rollin, C. Tsabaris*, E. Wattecamps

Measurements of (n,α) cross-section data were made in the past at the Van de Graaff relative to the well known cross section of H(n,n)H. Results for nickel, copper and their separated isotopes, were presented at the International Conference on Nuclear Data for Science and Technology, Jülich, 1991. Recent Ni(n,α) data are much lower than those of the ENDF-B evaluation. Recent and older experimental data from the CBNM, and data from other laboratories as well, scatter by more than one standard deviation. Therefore, new measurements of ^{58}Ni(n,α) relative to ^{27}Al(n,α) are in progress, using the five angles ΔE-E telescope.
To check whether the well known activation cross section of the ^{27}Al(n,α) reaction can be used as a reference cross section for prompt alpha particle detection, the alpha particle energy spectrum of the ^{27}Al(n,α) reaction with neutrons of 8 MeV has been determined.
The foreground for ^{27}Al(n,α) and the background were observed by the telescope under 51 degrees. The background is the limiting factor especially at the low energy side of the alpha particle spectrum. It could be shown that the spectrum is measurable by the ΔE-E telescope down to the lowest alpha particle energy present (0.5 MeV).
A typical foreground two-dimensional spectrum of energy loss ΔE versus energy E of alpha particles of ^{27}Al at 8 MeV neutron energy is shown in Fig. 25. Three areas can be identified:

- area A: alpha particles from ^{27}Al(n,α), with the typical energy dependence of dE/dX versus energy;
- area B: alpha particles from ^{28}Si, with opposite energy dependence of dE/dX versus energy. It is explained by alpha particles crossing the telescope in the opposite direction (up stream, from surface barrier detector (E) to proportional counter (ΔE)) and not separable from down stream alpha particles by coincidence conditions as broad as 1 μs;
- area C: protons and less ionising radiation.

---

* EC Fellow from the University of Athens, Greece

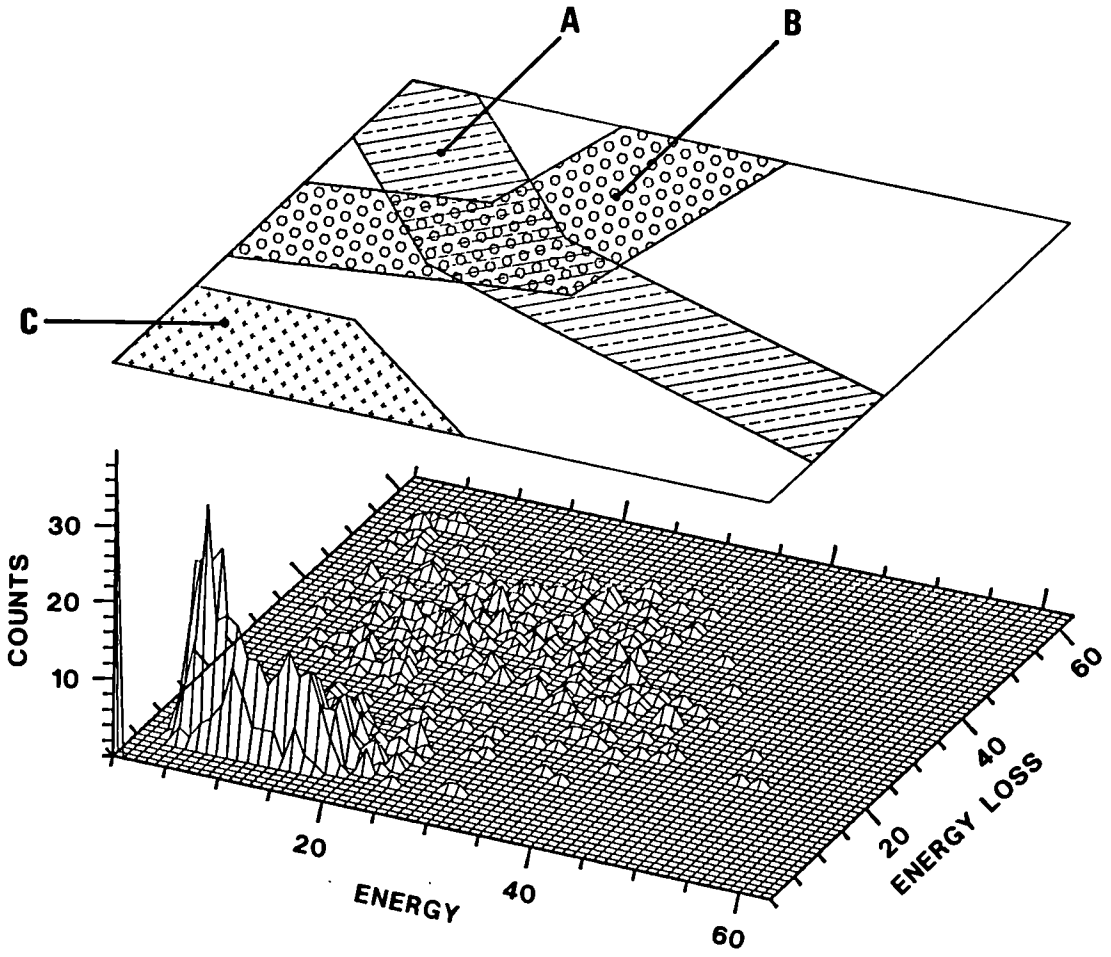

Fig. 25. Two dimensional spectrum of energy and energy loss observed from $^{27}Al(n,\alpha)$ with neutrons of 8 MeV during 3 hours at 2 μA beam current

The background in the common part of areas A and B was measured with a tantalum sample at the site of the aluminium. A typical alpha particle energy spectrum of foreground and background is shown in Fig. 26. The foreground to background ratio is 3 : 1. As net signal the difference between aluminium minus the tantalum data within area A was taken.
A measurement of the reaction rate ratio of $^{58}Ni(n,\alpha)$ versus $^{27}Al(n,\alpha)$ with five telescopes, thus covering the entire angular range, is in preparation.

Total Neutron Cross-Section Measurement of ^{27}Al at High Energy

R. Shelley, G. Rohr, C. Nazareth, M. Moxon*

A study of the neutron cross section of ^{27}Al is relevant to the structural material data required for reactor and fusion studies and recent progress made with the

* Visiting Scientist from AEE, Harwell, United Kingdom

investigation of resonance spacings and their distribution. For this isotope no new data has become available for almost two decades and, with the present very high resolution capabilities of GELINA, the energy resolution compared to earlier measurements has been improved by an order of magnitude.
This has been achieved by measuring, at a distance of 400 m, the transmission of the neutron beam from the linac uranium target using the time-of-flight (TOF) technique. With the 1 ns pulsed linac operating at 800 Hz, the transmission through a 99.5 % pure aluminium sample (0.19293 at/b thick) was detected by a NE110 plastic scintillator viewed by four RCA photomultipliers. The resultant TOF spectra were stored in 64 k channels of 1 ns width and covered a neutron energy range from 175 keV to 25 MeV.

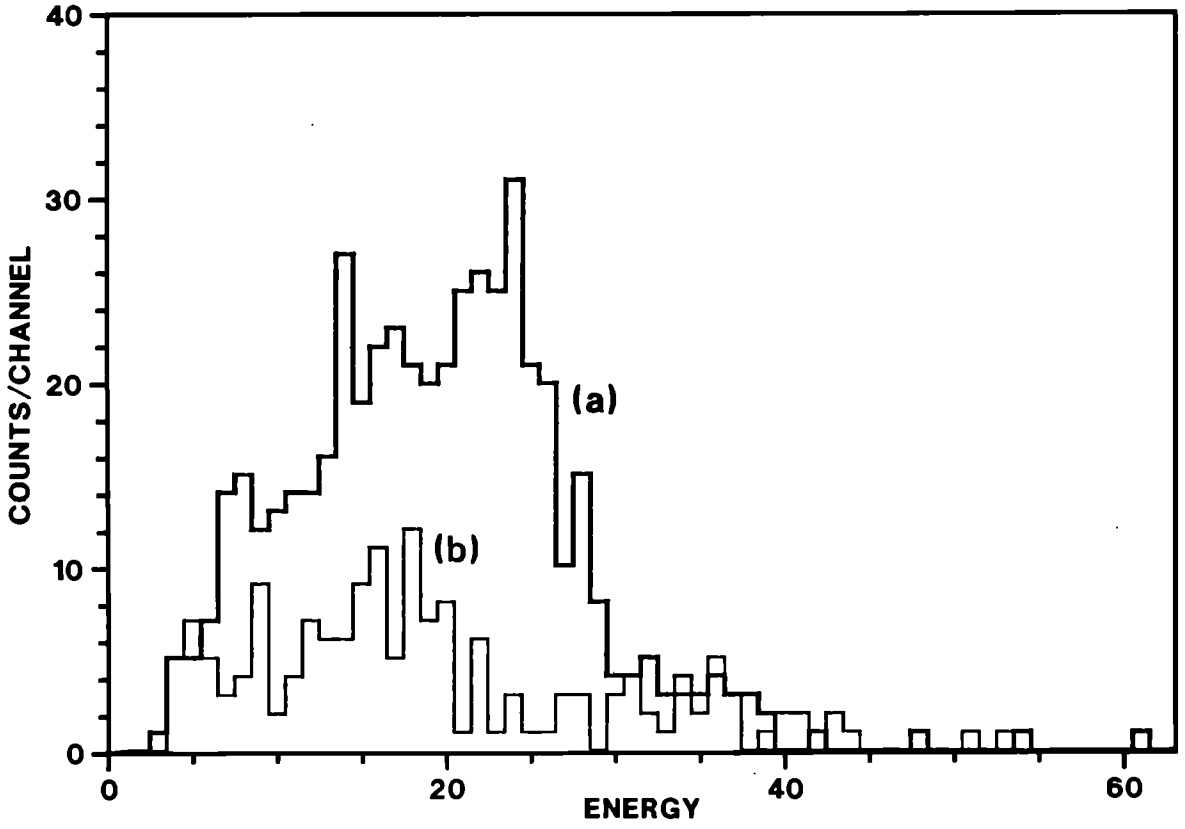

Fig. 26. ***Alpha particle energy spectrum for particles pertaining to area A in the ΔE - E spectrum for a measuring time of 3 hours. (a) for ^{27}Al(n,α) or foreground, (b) for tantalum or background***

The data reduction to correct the transmission data for background and dead time effects has been completed and the cross section spectra are now available. Fig. 27 shows the complexity of the resonance structure in the cross section even when the 1 ns data have been crunched by a factor of eight. At higher energies this complexity increases dramatically, the threshold for inelastic scattering is at 844 keV, and the resonance parameter analysis, which is presently at a very preliminary stage, will therefore be restricted to the energy range below 1 MeV.

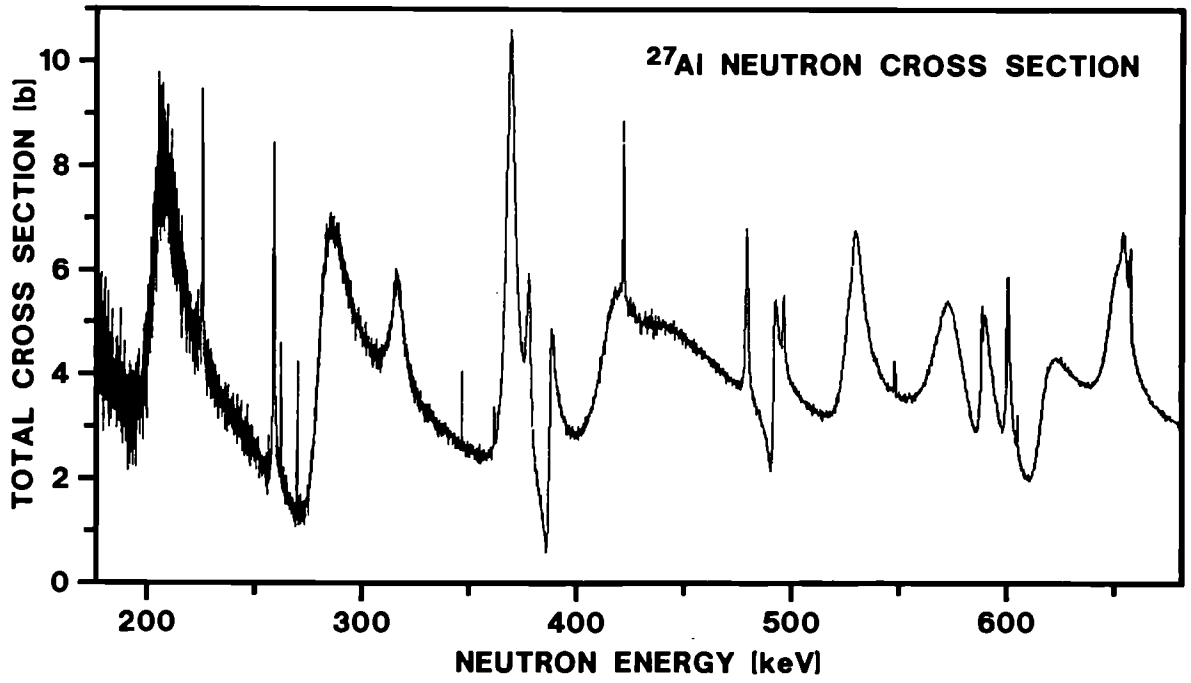

Fig. 27. *^{27}Al total neutron cross section in the energy range 180 to 680 keV. (measured data available with 1 ns/channel but presented with 8 ns/channel for ease of viewing)*

^{4}He Emission in the Interactions of Fast Neutrons with ^{48}Ti and ^{50}Ti

S.M. Qaim*, M. Uhl**, N.I. Molla*, H. Liskien

Excitation functions were measured radiochemically for the ^{48}Ti(n,α)^{45}Ca and ^{50}Ti(n,α)^{47}Ca reactions over the neutron energy range of 12.6 to 19.6 MeV. Use was made of low-level anticoincidence β^-counting in the radioactivity measurement of ^{45}Ca and of high-resolution γ-ray spectroscopy in the case of ^{47}Ca. Statistical model calculations taking into account preequilibrium effects described the proton emission well; the calculated ^{4}He emission results were, however, consistently lower than the experimental data, both as regards emission spectrum and excitation function. Inclusion of a direct three-nucleon pickup component in the ^{4}He emission calculation improved the agreement between theory and experiment.

* Institut für Nuklearchemie, Forschungszentrum Jülich, Germany
** Institut für Radiumforschung und Kernphysik, Universität Wien, Austria

NUCLEAR METROLOGY

RADIONUCLIDE METROLOGY

The objective of the work on radionuclide metrology is to advance the experimental know-how in the field of radioactivity. This is done in four major areas: the determination of decay-scheme data, the improvement and development of measurement techniques, the preparation of particular standard and reference samples and the participation in international comparisons and evaluations.

Low-Energy X-Ray Standard Sources

B. Denecke, G. Grosse

Four sources of 5 MBq ^{55}Fe in the form of stable metallic layers were produced by electrodeposition onto small copper rings. The yield of electrolytic deposition was up to 60 %. A transport container with special tools for safe and precise positioning of the interchangeable fluorescence targets with respect to the excitation source was designed to hold up to ten fluorescence layers and the X-ray excitation source.

Measurement of K-Shell Fluorescence Yields

V.A. Solé*, B. Denecke, G. Grosse, W. Bambynek

There are only few measurements of the K-shell fluorescence yield of calcium reported in the literature. The results show a large scatter and disagree with predicted values. For potassium no measured data are reported. New measurements were made using metallic samples of calcium and potassium. In these layers K-shell vacancies were produced by photo effect using a collimated beam of manganese KX-rays, the emission rate of which was measured with a gas-flow proportional counter. The fluorescent radiation was measured with a windowless Si(Li) spectrometer at a defined low solid angle. Taking advantage of the standardized low energy X-ray sources developed by CBNM, the detector efficiency could be measured with an accuracy of about 1 %. The K-shell fluorescence yields are $\omega_K(Ca) = 0.164 \pm 0.004$ and $\omega_K(K) = 0.144 \pm 0.004$.

---

* EC Fellow from the University of Valencia, Spain

Standardization of α-Particle Emitting Samples

B. Denecke

A cooperation with NIST was started to measure with highest achievable accuracy the emission rate of α-particle emitting samples prepared at CBNM. Three ^{233}U samples have been measured at two different defined low solid angles. They will be measured independently also at NIST. The data evaluation is in progress.

Second EUROMET Intercomparison of ^{192}Ir Brachytherapy Sources

D.F.G. Reher

The evaluation of the results from the second EUROMET intercomparison of ^{192}Ir brachytherapy sources showed that there were problems for the mass determination of the highly radioactive wires, the calibration of ionization chambers in terms of activity, and the interpretation of calorimeter measurements. In most cases the sources of error could be identified and improvement was achieved. The results of this second intercomparison will be published in 1993.

Standardization of a ^{152}Eu Solution

D.F.G. Reher, T. Altzitzoglou, B. Denecke, E. De Roost

For the standardization of a 50 GBq $^{152,154}Eu$ volume source used to determine the linear power dissipation of irradiated fuel pins from material testing reactors, it was necessary to standardize a ^{152}Eu solution. A 2 ml mother-solution with an activity concentration of 100 MBq/g having a ^{154}Eu impurity of 1.32 % was prepared from material obtained from Amersham. From this solution 5 dilutions, 17 quantitative solid sources and 3 solutions in standard ampoules were prepared. For the standardization two independent methods were chosen: the $4\pi\beta$-γ-coincidence method and 4π-CsI spectrometry. The complexity of the ^{152}Eu decay scheme was of advantage for the measurements with the 4π-CsI sandwich spectrometer (redundant radiation cascades), whereas the actual set-up of our $4\pi\beta$-γ-coincidence system produced results which depended strongly on the cut-off energy in the γ-channel. An example of a spectrum obtained with the 4π-CsI spectrometer is shown in Fig. 28. The only significant correction applied was the low energy cut-off correction of about 0.4 %. The solution was standardized with an uncertainty of 0.4 % (one standard deviation).

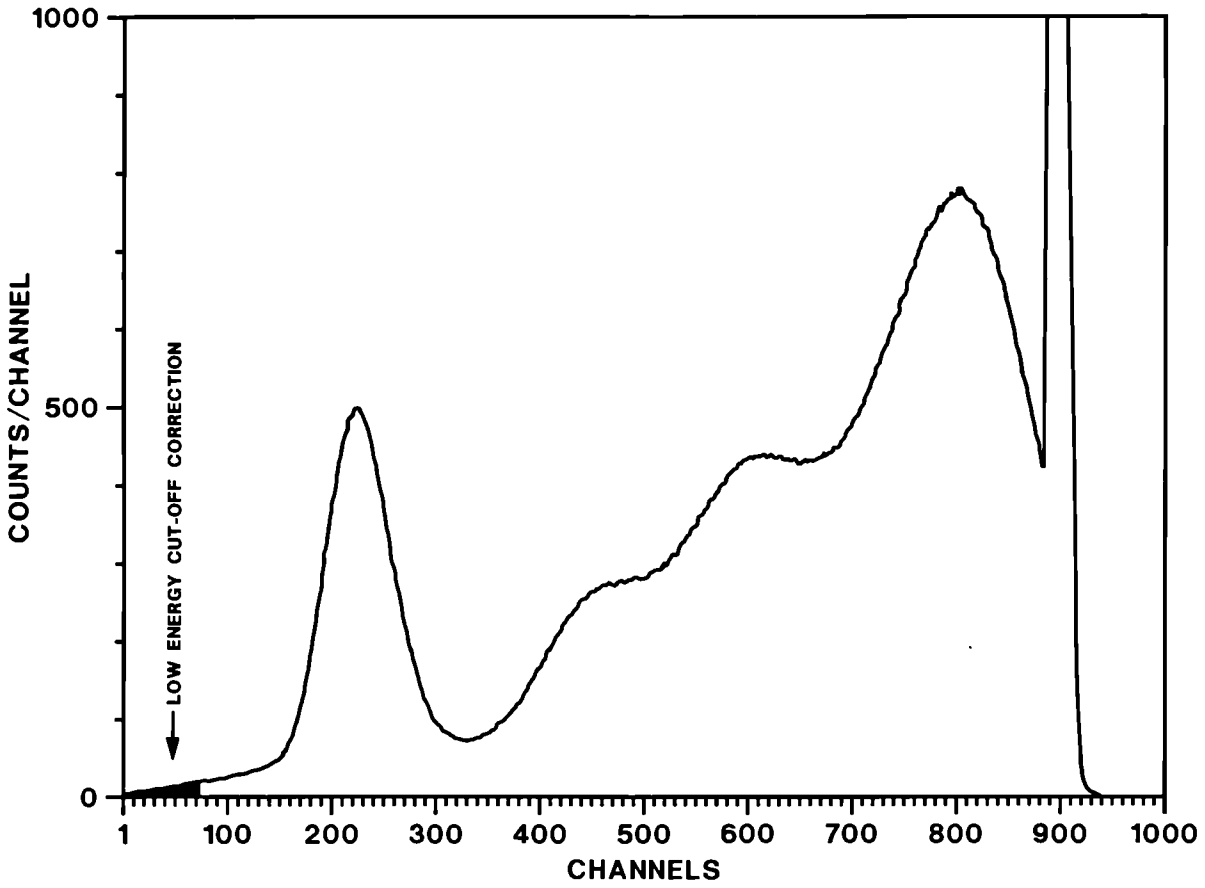

Fig. 28. A typical spectrum of ^{152}Eu obtained with the 4π-CsI spectrometer

Efficiency Curve for the CBNM Radionuclide Calibrator

D.F.G. Reher, G. Sibbens

The CBNM radionuclide calibrator is a well-type ionization chamber (20th Century Electronics, type IG-12) which has been calibrated for various radionuclide solutions in NIST/BIPM standard ampoules. Calibration always requires highly pure standards. However, often secondary standardization of material with significant impurities has to be done. Furthermore, one needs to standardize a radionuclide solution for which no calibration figure is available. In these cases an efficiency curve as a function of energy is needed. Such a curve was established (Fig. 29) using preferably nuclides emitting only a single γ-ray. Additionally, we could use data points measured by Urquhart[1] with the same type of ionization chamber.

(1) D.F. Urquhart, Calibration and Operation of the AAEC Working Standard of Measurement for the Activity of Radionuclides, AAEC Report 1986

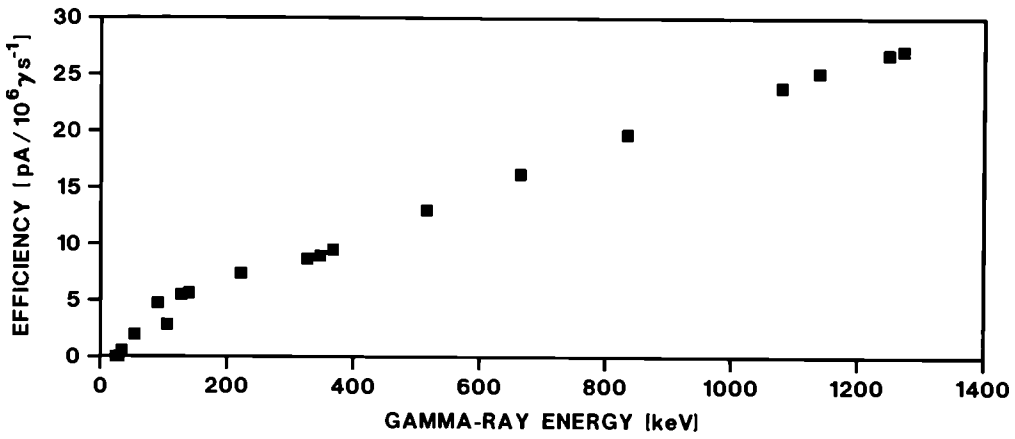

Fig. 29. The CBNM radionuclide calibrator efficiency curve

Investigation of the Natural Radioactivity in Volcanic Rock Samples Using a Low Background γ-Ray Spectrometer

R. Wordel, D. Mouchel, V.A. Solé*

A low-level HP Ge detector system was used to investigate powdered volcanic rock samples of different origin. An efficiency calibration of the detection system was performed with a powdered solid source, spiked with suitable radionuclides and having a chemical composition close to that of the investigated samples. To obtain the full-energy-peak efficiency ε_γ for the different extended samples corrections for geometry, self-absorption and absorption have been applied using a Monte Carlo programme.

The studied samples originate from the Eastern Sunda Volcanic Arc in Eastern Indonesia, where the subduction of the Australian plate under the Asian plate takes place. The samples were taken from volcanoes, at places where the depth of the Australian plate varies from 100 to 300 km. The concentration of radionuclides from the natural decay chains in the samples was compared with that in a well known reference sample. A correlation between some of the radionuclide concentrations and the subducting depth was established.

Measurement of Low-Level Radioactivity in Archaeological Ceramics

R. Wordel, D. Mouchel

On request and in collaboration with the Technical University of Munich (D), measurements of low-level radioactivity in archaeological ceramics of Celtic origin, using a low-level HP Ge γ-ray detection system were done. The place where the samples were excavated is situated close to Manching (D). The aim of the measurements was to characterize the clay on the basis of natural

* EC Fellow from the University of Valencia, Spain

radionuclides and to study a possible disequilibrium in the natural decay series for a geological identification of the clay used to produce the Celtic pottery.

Measurement of Low-Level Radioactivity in soil and river sediment

R. Wordel, D. Mouchel

Determination of radionuclide concentrations in soil, sand and aquatic samples collected close to an industrial site, and also from unpolluted areas has been performed. Field samplings, sample preparation (17 samples) and measurements in Marinelli beaker geometry were done. The data analysis is in progress. Fig. 30 shows two strongly varying spectra of river sediment samples together with a background measurement. Both, the total radioactivity and the ratios between different natural radionuclides are very different.

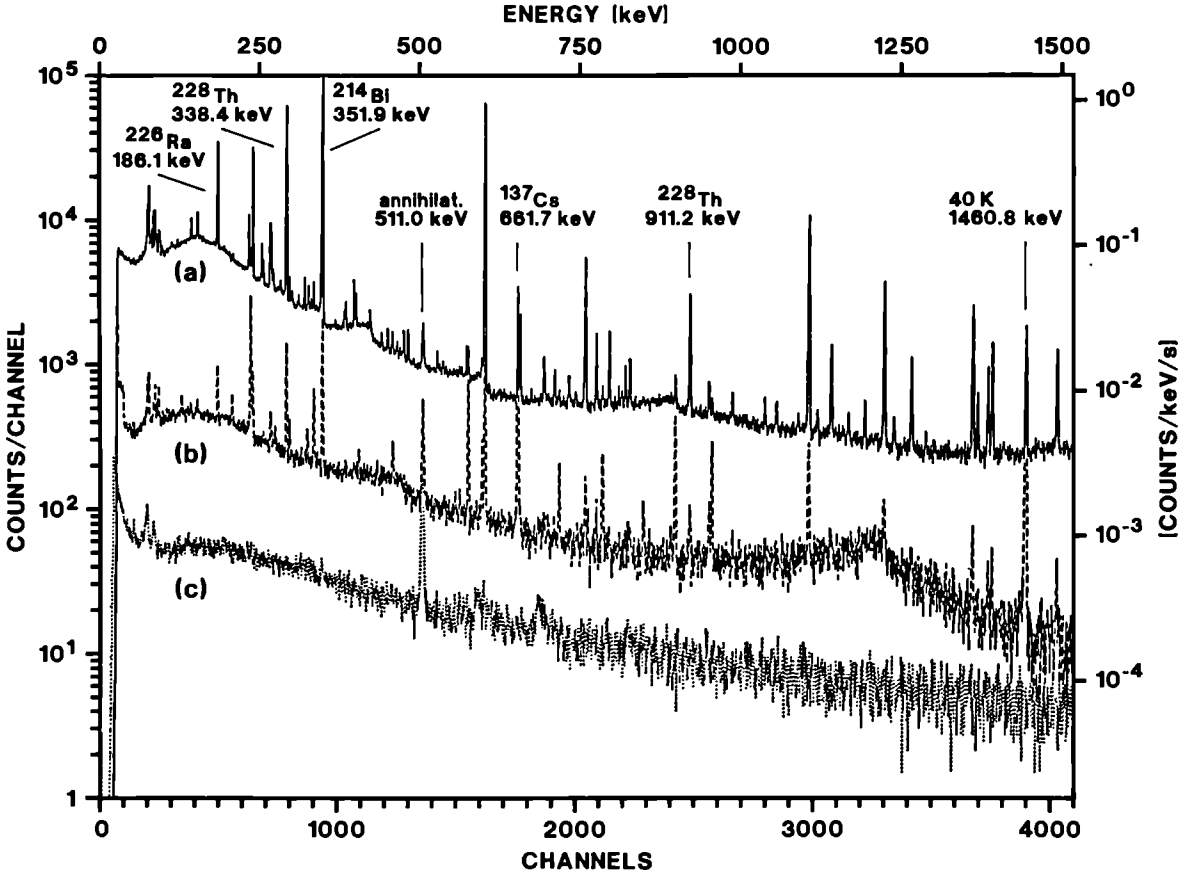

Fig. 30. ***Spectra recorded during two days with a low-level 100 cm^3 intrinsic Ge detector: (a) river sediment samples close to the industrial facility and (b) similar samples collected far from any industrial site. (c) background***

Further Reduction of Background

R. Wordel, D. Mouchel

In collaboration with SCK/CEN, Mol (B), in the underground laboratory HADES a study is going on to reduce the background of a low-level high-purity

Ge detection system. First results with the shielded system show an integrated count rate within the energy interval (70 - 3000) keV of (0.0156 ± 0.0006) s^{-1}. The reduction with respect to the same detector and shielding situation in the counting room at sea level is larger by a factor of 30, and by about 3200 if one compares with the unshielded system at sea level.
The achieved sensitivity for γ-ray spectroscopy reaches below mBq/kg corresponding to better than 10^{-10} g/g of uranium and thorium.

Modelling of Alpha-Peak Shape

E. Steinbauer*, P. Bauer*, J.P. Biersack**, G. Bortels

The work dealt with the influence of plural and multiple scattering of high energy projectiles in two characteristic applications: Rutherford backscattering spectroscopy (RBS) and the response of particle implanted and passivated silicon detectors (PIPS) to monoenergetic MeV alpha particles.
The detector response to 3183 keV alpha particles is calculated using a detector model, which assumes a dead layer near the front contact followed by a fully sensitive volume. All model parameters are determined either from theory or from measurements. The calculated alpha spectrum perfectly agrees with the measurement both in the resolution (FWHM) and in the asymmetric shape.

Alpha Spectrometry in Relation with Calorimetry

G. Bortels

Most important transuranics are alpha-particle emitters. More than 99 % of their heat output is due to alpha emission and the associated recoil energy. Therefore, alpha spectrometry is a complementary measurement technique to the non-destructive calorimetric measurements. Current achievements with alpha spectrometry at CBNM, in particular with respect to the measurement of $^{239}Pu/^{240}Pu$ and $^{238}Pu/^{241}Am$ mixtures were described in a conference paper.

Installation of a New Liquid Scintillation Counter (LSC)

T. Altzitzoglou

A commercial LSC has been installed for the standardization of β-particle emitters of interest in various fields e.g. metrology, nuclear medicine

* Institut für Experimentelle Physik, Universität Linz, Austria
** Hahn-Meitner Institut Berlin, Germany

diagnostics and environmental studies. It includes the feature of pulse shape discrimination to distinguish pulses produced by alpha or beta particles.
The time resolving circuitry allows, in connection with the new generation of liquid scintillation cocktails, to significantly reduce the background.
The computer programme EFFY4[1] has been implemented in a personal computer. It calculates the theoretical counting efficiency for a given nuclide and links that to the figure of merit and the quench factor given by the instrument. Then, a single quench curve (normally obtained using tritium samples) is sufficient to calculate the quench-corrected efficiency for any β-particle emitting nuclide that is measured.

TDPAD STUDIES AT THE 7 MV VAN DE GRAAFF

The technique of time-differential perturbed angular distributions (TDPAD) of γ-rays has been used with the pulsed beam facility at the Van de Graaff for the study of pure and applied physics issues in some selected cases.

Search for the Quadrupole Moment of the 583 keV State in ^{22}Na

F.-J. Hambsch, P. Martin*, H. Postma**, P. Rietveld, D. Surono***

An experimental determination of the quadrupole moment of the 583 keV ($J^{\pi} = 1^+, T_{1/2} = 243$ ns) level in ^{22}Na provides a basis for differentiating between the deformed or shell model descriptions of the nucleus. On a pure shell model basis, a half-filled shell of $d_{5/2}$ protons and neutrons should produce a zero quadrupole moment for this state. On the other hand, rotational models or shell models with mixed configurations indicate that $Q \sim 0.06$ b. Highly oriented pyrolytic graphite (HOPG) was used as a substrate for recoil implantation of ^{22}Na produced by the $^{19}F(\alpha,n)^{22}Na$ reaction. The large electric field gradient expected in HOPG ($\sim 10^{18} V/cm^2$) can interact with the quadrupole moment of the ^{22}Na state to produce a perturbation of the γ-ray angular distribution, such as that shown in Fig. 31 for the 197 keV state ($J^{\pi} = 5/2^+$, $T_{1/2} = 89$ ns) of ^{19}F. In the case of ^{22}Na, however, no perturbation is observed for the 583 keV level, as evidenced by the flat spectrum shown in Fig. 32. Results indicate that $Q < 0.005$ b for the ^{22}Na state, and are consistent with a pure $d_{5/2}$ shell model description.

---

* Visiting Scientist from the University of British Columbia, Vancouver, Canada
** Visiting Scientist from Technical University of Delft, The Netherlands
*** PhD Student from the University of British Columbia, Vancouver, Canada
(1) Garcia-Toraño, E. and Grau, A. "EFFY, a New Program to Compute The Counting Efficiency of Beta Particles in Liquid Scintillators", Comp. Phys. Comm. 36 (1985) 307

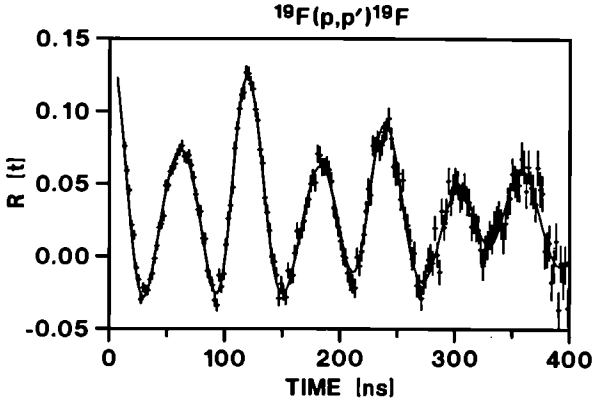

Fig. 31. ***Perturbation spectrum for the 197 keV level of ^{19}F in HOPG***

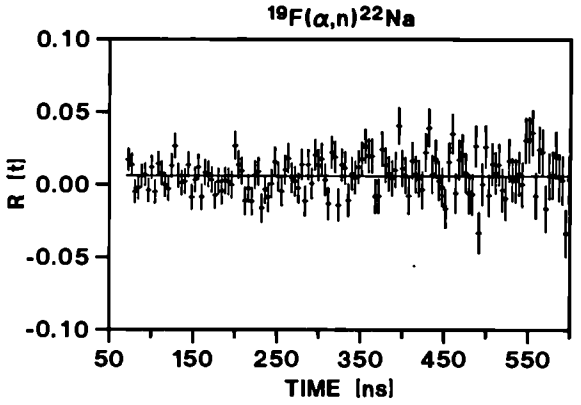

Fig. 32. ***Perturbation spectrum for the 583 keV level of ^{22}Na in HOPG***

Fluorine Residence Sites in Silicon and Germanium

F.-J. Hambsch, P. Martin*, P. Rietveld, D. Surono**

The role of fluorine in the manufacture of semiconductors is extremely important; it can control key parameters such as doping efficiency, improve photovoltaic characteristics, reduce leakage currents in p-n junctions and increase the reliability of metal oxide semiconductor (MOS) capacitors. Using the $^{19}F(p,p')^{19}F$ reaction, fluorine was recoil implanted from thin films of CaF_2 into silicon and germanium substrates. The interaction of the quadrupole moment of the 197 keV state of ^{19}F with the local electric field gradient within the substrate material was used to determine the nature of the residence sites. An example of the results together with theoretical fits are shown in Figs. 33 and 34 for silicon (111) and germanium (111) samples respectively. The industrial heat treatment of fluorine-doped silicon and germanium is a major factor in affecting the role played by fluorine in these materials.

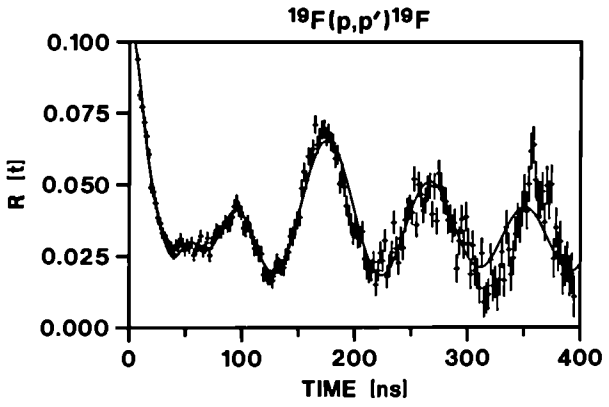

Fig. 33. ***Perturbation spectrum for the 197 keV level of ^{19}F in silicon***

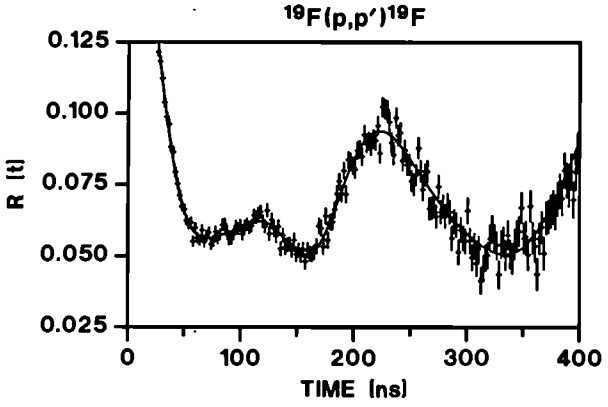

Fig. 34. ***Perturbation spectrum for the 197 keV level of ^{19}F in germanium***

* Visiting Scientist from the University of British Columbia, Vancouver, Canada
** Ph-D Student from the University of British Columbia, Vancouver, Canada

Further studies will be pursued to investigate the residence sites in previously fluorine-implanted samples subjected to different heat treatment protocols. Identification of the fluorine sites should then help to elucidate the role played by the fluorine in altering the physical behaviour of MOS devices.

Radiation Damage Studies in GaAs

F.-J. Hambsch, P. Martin*, D. Surono**

Using the $^{71}Ga(p,n)^{71}Ge$ reaction on a GaAs target, a flat perturbation spectrum was obtained for the 175 keV ($J^{\pi} = 5/2^{+}$, $T_{1/2} = 84$ ns) level of ^{71}Ge. Since GaAs has cubic symmetry and consequently zero electric field gradient, the result implies that the ^{71}Ge also experiences a cubic environment. Consequently TDPAD will be used to investigate the effects of impurities and radiation damage in GaAs.

* Visiting Scientist from the University of British Columbia, Vancouver, Canada
** Ph-D Student from the University of British Columbia, Vancouver, Canada

TECHNICAL APPENDIX

LARGE FACILITIES

ACCELERATORS

Electron Linear Accelerator

J.M. Salomé

The GELINA electron beam was available during 2325 hours for physics experiments. The parameters are shown in Table 14.

Table 14. Beam parameters of the GELINA

Pulse length [ns]	Repetition rate [Hz]	Peak current [A]	Mean current [μA]	Mean energy [MeV]	Time [h]	Time [%]
1-2	800	~100	55-60	100	1571	67.6
12	100	7	8	100	675	29
10-1400	100	<4	<14	40-100	71	3
Other parameters					8	0.4

Neutrons are produced in a rotary uranium target via (γ,n) and (γ,f) reactions. According to the requested neutron energies, various moderators are placed on both sides of the target. Twelve flight paths are equipped for neutron time-of-flight experiments. On the average, 5.7 neutron beams were used simultaneously when GELINA was operated at very short bursts and 3.3 of them when operated in other conditions.

On the main electron beam line of 0°, an optical transition radiation system (10 μ aluminium radiator foil) is used to determine some parameters of the beam as divergence and energy. However, the divergence growth due to the radiator foil perturbs the operation of the compression magnet. Thus, such measurements will be made only to adjust the electron beam and the radiator will be removed in normal operation.

To one side of the main line, a 40 MeV electron beam has been deflected to allow experiments with X-ray transition radiation. This set-up is suitable for measurements at very low currents with various radiators.

For radiation protection reasons the target room may be closed with lead doors when the neutron beams are not in use. In view of improving the staff protection, the control system of these doors was completely renewed.

The refurbishment of the Linac was started by placing the first orders at the end of the year. The work essentially will imply the replacement of the two long sections and the corresponding equipment in view of applications in neutron and radiation physics. The specifications are very stringent concerning the performance of the new parts which will have to be matched for the achievement of the low emittance electron beam needed for the radiation physics experiments. The modernised Linac should be ready by the end of 1994 after a six months period of breaking its operation.
The present experimental possibilities in the neutron target hall are not adequate for the radiation physics programme. Therefore, a new experimental hall is foreseen at the 0° beamline outside the target hall. The drawings for this new experimental hall have been completed and the order placed. Ground works will start in early 1993. A new system to extract the electron beam at 0° by remote control has been designed. It will allow to use the electron beam alternatively for the neutron physics or for the radiation physics programmes.

Measured Fast Neutron and Gamma-Ray Fluence Close to the GELINA Target
W. Schubert, C. Tsabaris*, E. Wattecamps

In preparation to perform radiation damage irradiations by fast neutrons at a fluence level of 10^{15} n/cm^2 and larger within irradiation times of some hours or days, the fast neutron and γ-ray fluence at 46 cm distance from the GELINA target at various spots in a horizontal plane at 23 cm below the target have been measured. The machine was operated at 150 MeV electron energy and 6 kW beam power. The neutron energy spectrum and the neutron fluence were determined by the activation technique with a set of eleven threshold activation reactions.
An estimate of the gamma ray fluence was deduced from γ-ray activation measurements relying on the reaction ^{59}Co(γ,n)^{58}Co.
Details of the experiment and a discussion of the results are given elsewhere[1,2].
The measurements lead to the following conclusions:

- the neutron yield is strongly angular dependent and the largest fluence was observed at a neutron emission angle around 115 degrees;
- at 6 kW beam power the neutron flux at 46 cm distance from the target, amounts to $7.4 \cdot 10^8$ n/s·cm^2, and the γ-ray fluence is at least $2.5 \cdot 10^8$ γ-rays/s·cm^2;
- assuming an isotropic neutron yield distribution a source strength of $1.96 \cdot 10^{13}$ n/s in 4π sr is deduced from the activation measurements.

---

* EC Fellow from University of Athens, Greece
(1) C. Tsabaris, W. Schubert and E. Wattecamps, Internal Report GE/R/VG/73/92
(2) W. Schubert and E. Wattecamps, Internal Report GE/R/VG/72/92

Van de Graaff Accelerators

A. Crametz, P. Falque, J. Leonard, W. Schubert

The total working time of the two accelerators was 4677 hours. A break down of this total is given in Table 15.

Table 15. Exploitation of the Van de Graaff accelerators

	CN - 7 MV	KN - 3.7 MV
	Time [h]	Time [h]
Adjustments	100	98
Experiments	2421	1410
Conditioning	100	-
Maintenance	382	166

All the experiments at the 3.7 MV accelerator are related to non-neutron activities (RBS, PIXE and microbeam); the experiments at the 7 MV are divided in 1107 hours for non-neutron activities (NRA and TDPAD) and 1314 hours for neutron activities (data for standards and for fission and fusion technologies). In total, the ratio non-neutron to neutron activities is nearly equal to 2 : 1.

The CN-7MV accelerator has been opened for the replacement of the RF ion source and for the installation of a fourth gas bottle (^{3}He) in the high voltage terminal. For the first time a $^3He^+$-ions beam has been achieved.

Both accelerators were operated simultaneously during 980 hours.

Due to the new development of the accelerator-based materials analysis technique, namely hydrogen profiling, a 90° analyzing magnet with a mass·energy product of 140 amu·MeV has been bought to bend a $^{15}N^+$-ions beam. In order to have a permanent access to that materials analysis experimental facility even when neutron experiments are running, the possibility to install it in an existing separate room is under investigation. This minor modification may be completed in 1993.

After 23 000 hours of operation, the belt of the KN 3.7 MV has been renewed.

Accelerator-based Materials Analysis Techniques at the 7 MV Van de Graaff Accelerator

G. Giorginis, P. Misaelides*, A. Crametz, M. Conti

Surface modification is used for the production of advanced materials with properties tailored to a particular application. In this field of surface engineering light elements play an important role and there is an increasing demand for the determination of their concentration and depth distribution. Nuclear methods offer for this purpose tools for a highly sensitive, quantitative and nondestructive microanalysis.

At the 7 MV Van de Graaff accelerator a programme for the installation and development of accelerator-based analytical techniques[1] is in progress. The Nuclear Reaction Analysis (NRA) technique is in operation since the beginning of 1992 and is used currently in two applications. The one is the determination of the boron/nitrogen stoichiometry in boron-nitride thin films (superhard coatings) in collaboration with VITO and the other is the study of the oxygen diffusion in aluminium implanted stainless steel samples (oxidation protective layers) in collaboration with the University of Thessaloniki.

Light elements (boron, carbon, nitrogen, oxygen) are detected using (d,p) and (α,p) nuclear reactions. Analysis of the energy spectrum of the reaction products provides the concentration and the depth profile of the element under study. The energy-depth relation can be derived using well established energy loss tables. The concentration determination is based on cross sections which in many cases have to be measured. In this context a cross section evaluation programme for the (d,p) and (α,p) reactions on the above mentioned elements has been started at the 7 MV Van de Graaff accelerator.

Fig. 35(a) shows the excitation function of the $^{14}N(\alpha,p_0)^{17}O$ reaction, while Fig. 35(b) and Fig. 36 show preliminary results for the $^{10}B(\alpha,p_0)^{13}C$ and $^{11}B(\alpha,p_0)^{14}C$ reactions, respectively.

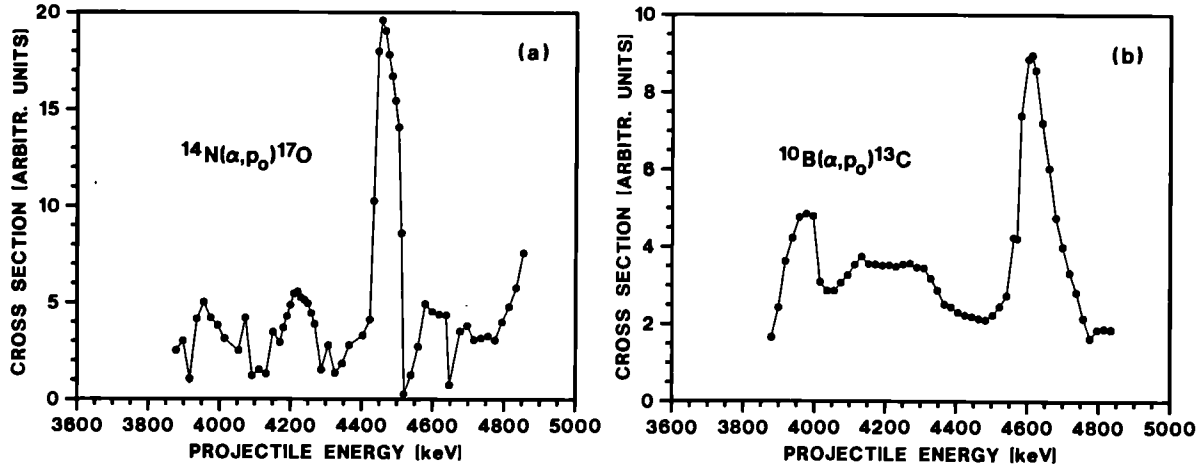

Fig. 35. Excitation functions of (a) the $^{14}N(\alpha,p_0)^{17}O$ and (b) the $^{10}B(\alpha,p_0)^{13}C$ reactions, measured at a laboratory scattering angle $\theta_L = 135°$

* Visiting Scientist from Aristotle University Thessaloniki, Greece

(1) CBNM Annual Report 91, EUR 14374 EN

The lower curve in Fig. 36 is the contribution of the $^{10}B(\alpha,p_1)^{13}C$ to the $^{11}B(\alpha,p_0)^{14}C$ peak. For its separation two boron targets with different $^{11}B/^{10}B$ contents have been used. The cross section errors are dominated by the statistical accuracy with σ-values at the points of low statistics of 4 % in Fig. 35(a) and Fig. 35(b) and 10 % in Fig. 36. All targets used, 25 µg/cm^2 polyimide foils and 9 - 10 µg/cm^2 boron deposits, had a polished tantalum backing.
In the second study oxygen determination by means of the $^{16}O(d,p)^{17}O$ reaction has been performed on Al-implanted AISI 321 steel samples before and after thermal treatment in air. The analysis of the results as well as a critical evaluation of the corresponding reaction cross sections is in progress.
The (α,p) reaction on boron and nitrogen enables a simultaneous and clean identification of these elements as can be seen from Fig. 37 showing an energy spectrum of this reaction using a BN coating on a silicon substrate as target. Due to the negative Q value (Q = – 1.193 MeV) of the $^{14}N(\alpha,p_0)^{17}O$ reaction a beam energy of $E_\alpha \geq 4$ MeV was required in the experiment to clearly separate the nitrogen line from background.

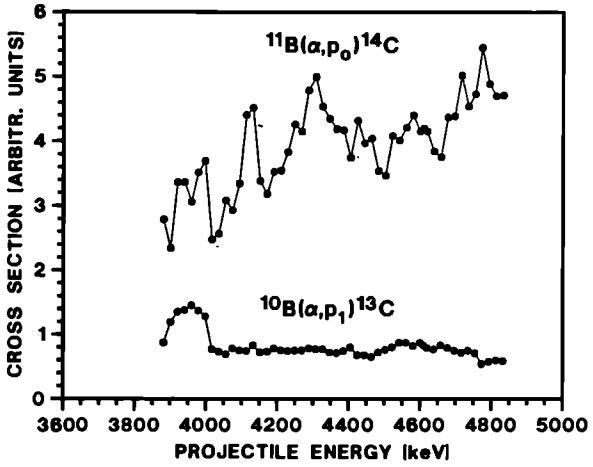

Fig. 36. Excitation functions of the $^{11}B(\alpha,p_0)^{14}C$ and $^{10}B(\alpha,p_1)^{13}C$, reactions measured at a laboratory scattering angle $\theta_L = 135°$

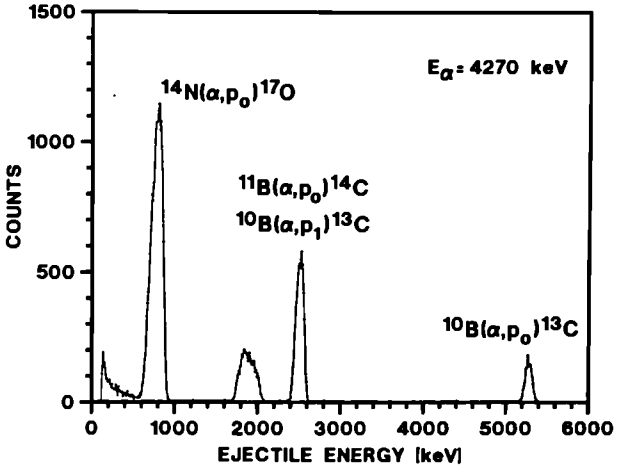

Fig. 37. Energy spectrum from the α-bombardment of a BN-coating on a silicon substrate

SPECIAL LABORATORIES

Clean Chemical Laboratory (CCL)

P. De Bièvre, A. Lamberty, J. Broothaerts

The construction of the Clean Chemical Laboratory has been finished. The inner plastic walls, the HEPA filters in the ceiling as well as the special

laboratory furniture (acid distillation modules, clean benches, clean down-flow fume hoods, conventional fume hoods, storage modules), made of PVC and polypropylene, have been installed. The technical supplies (vacuum, compressed air, water, gas, electrical outlets) have been connected to the equipment. Also the Millipore Water Purification System which provides de-ionized water at each working place, has been installed. First tests of the HEPA filters in the ceiling showed good air quality expressed in particles of > 0.5 µm per m^3. (Table 16). The HEPA filters incorporated in the laboratory furniture are now being tested.

Table 16. ***Air quality measured at different places in and around the CCL***

place	particles of > 0.5 µm per m^3
under HEPA filter	$< 4 \cdot 10^1$
laboratory	$3.5 \cdot 10^4$
entrance corridor	$5.3 \cdot 10^4$
adjacent office	$7.1 \cdot 10^5$
outside	$> 1.8 \cdot 10^7$

Metrological Support

B. Dijckmans, F. Hendrickx, J. Verdonck

Metrological support was given to a large number of projects in the specific CBNM programme, in the activities of scientific and technical support to the Commission and in those for third parties work. In 1992 about 50 orders for precision weighings and preparation of solutions were executed, comprising gravimetric work on far more than 1000 samples of liquids, bulk materials and powders. In addition, 10 demands for precise length determinations (diameters of evaporation masks and deposited layers, lengths of time-of-flight distances, beam line adjustment) were handled.

DATA PROCESSING AND ELECTRONICS

CBNM Computer Network

C. Bernard, C. Cervini, H. Horstmann, C. Nazareth, C. Van den Broeck*, L. Van Rhee, P. Van Roy

The X.400 message handling system of CBNM has been extended to VAX/VMS computer systems by the installation of the DFN-EAN software. X.400 message handling is now available for the IBM/MVS, VAX/VMS and XEROX/Viewpoint environment.
A 3380 disk storage system has been installed for the main computer (IBM 4381) of the CBNM computer network. Most of the data volumes on the old 3375 disk storage system have been moved to the new units.
SYSTRAN, a fully automatic language translation system in use at CEC Luxembourg, has successfully been tested by means of the X.400 mail system.
A study for a workgroup network based on PCs and the existing Ethernet has been made. The network server will be able to support DOS, Windows, OS2/2, MAC and UNIX workstations.
An IBM RS/6000 computer running under AIX has been installed and customized. Client server tests with a PS/2 have been made. A connection to the public X.25 network has been established. Some APL applications have successfully been downloaded from the IBM 4381 system.
Plans have been made to replace the present CPU of the IBM 4381 computer system by a second-hand unit of double processing power in early 1993.
A set of interactive graphic facilities for the analysis of neutron data measured at GELINA has been developed.

MPA/TP, a Multiparametric Acquisition System with Transputers

C. Bastian, S. de Jonge, J. Gonzalez

Hardware modules containing 16 bit transputers can be used to monitor simultaneously up to 4 detector signals per module. A chain of up to 4 of these modules may produce a stream of multiparametric events involving up to 16 parameters of a nuclear reaction together with their coincidence pattern.
On-line analysis of the event stream is performed with 32 bit transputers on commercial boards hosted by a microVAX II. Complex schemes of on-line event analysis can be described in few lines of a dedicated configuration language and implemented on the transputer network.

---

* COMPAREX, Brussels, Belgium

Standard VMS command files are available to compile any scheme of event analysis to a load module for the 32 bit transputer, to test the load module nominally and to implement it as a full MPA system in combination with listing or histogramming facilities of the host. A user's guide is in preparation.

The AGS File System for Spectrum Analysis

C. Bastian

A new file format AGS (Analysis of Geel Spectra) was designed for the storage and the off-line analysis of multichannel counting spectra. All steps of an analysis can be saved in a single AGS file, starting from raw experimental results (counting histograms) and resulting in a series of cross section values. The results of the analysis are stored as integer or floating point spectra, including experimental constants, channels bounds, observation vector and covariance matrix.
In the AGS system, the analysis is performed in elementary steps (e.g. deadtime or background correction). Every step is a program reading results of the previous steps as spectra from the file and appending new results to the file. A basic set of AGS programs is already available in C. It may be complemented ad libitum by user-written programs, using a dedicated function library for e.g. spectral data access, matrix operations or covariance propagation.

Special Electronic Equipment for Laboratory Use

E. De Roost, H. Nerb, W. Stüber

The picoampere current source for mass spectrometry measurements was improved. A special vacuum capacitor was designed for this unit. - A delay-meter synchronizer, to be used for automatic correction of time delays in coincidence measurements and developed by an outside firm, has been tested for acceptance[1]. - An ADC multiplexer to be used for neutron data measurements was designed.

Handling Large Data Amounts

F. Gunsing*, C. Nazareth, P. Ter Meer, C. Cervini

For the experiment of spin assignment of ^{238}U an amount of 300 Mbyte per measuring day with a total in the order of 10 Gbyte has been collected with a

---

* EC Fellow from the Technical University of Delft, The Netherlands

(1) Internal Report GE/R/DE/01/92

PC-based FAST Data acquisition system.
Originally the data were transferred each day from the PC hard disk via Ethernet to the IBM 4381 mainframe and there backed up onto tape and sorted into spectra.
The transfer rate was on average about 30 kbyte/s resulting in nearly three hours of transfer time a day. During this period, data acquisition on the FAST was halted whilst job running on the mainframe were processed very slowly because of conflicting priorities.
Data are now transferred to the Micro VaxII giving a transfer rate of 80 kbyte/s. Then the data are backed-up onto an Exabyte 8200 unit having a capacity of 2.5 Gbyte per data casette. The transfer does not significantly affect processes running on the Micro Vax.
On a Macintosh Quadra 700 system, a program has been developed to sort the data using the sorting algorithm of the mainframe. The data, which are stored on the Micro Vax, are fully transparent to the Macintosh via Ethernet due to special client/server network software. The spectra are then available for analysis programs used on the Macintosh. At the end of the experiment, accumulated data can be sent to the mainframe by one single file transfer where they are available in the IFSPEC format for use by other analysis programs.

LISA - LIstmode and Spectral Data Analysis

A. Oberstedt*, F.-J. Hambsch

LISA is a programme package which enables both off-line listmode and spectral data evaluation as well as on-line monitoring while multiparameter experiments are running. This program has been developed on and for SUN - workstations, but can be executed in principle on every computer under an UNIX operating system with an X-WINDOW environment and running PV-WAVE from Precision Visuals Inc. This package is basically written in the language PV-WAVE CL which provides a powerful treatment and a fast visualization of large multidimensional datasets. Integration of subroutines written in the C-language and execution of UNIX shell commands leads to an additional increase of performance.
Besides providing maximum speed, optimum comfort for users was aimed. This could be reached by standardizing all routines as far as possible. Going more into details this means that users only have to input a few characteristic parameters either interactively or by the more convenient way using a command file to get an immediate visualization of their raw data. For data evaluation, concerning data modification, calculations or creation of new

* Visiting Scientist from Technische Hochschule Darmstadt, Germany

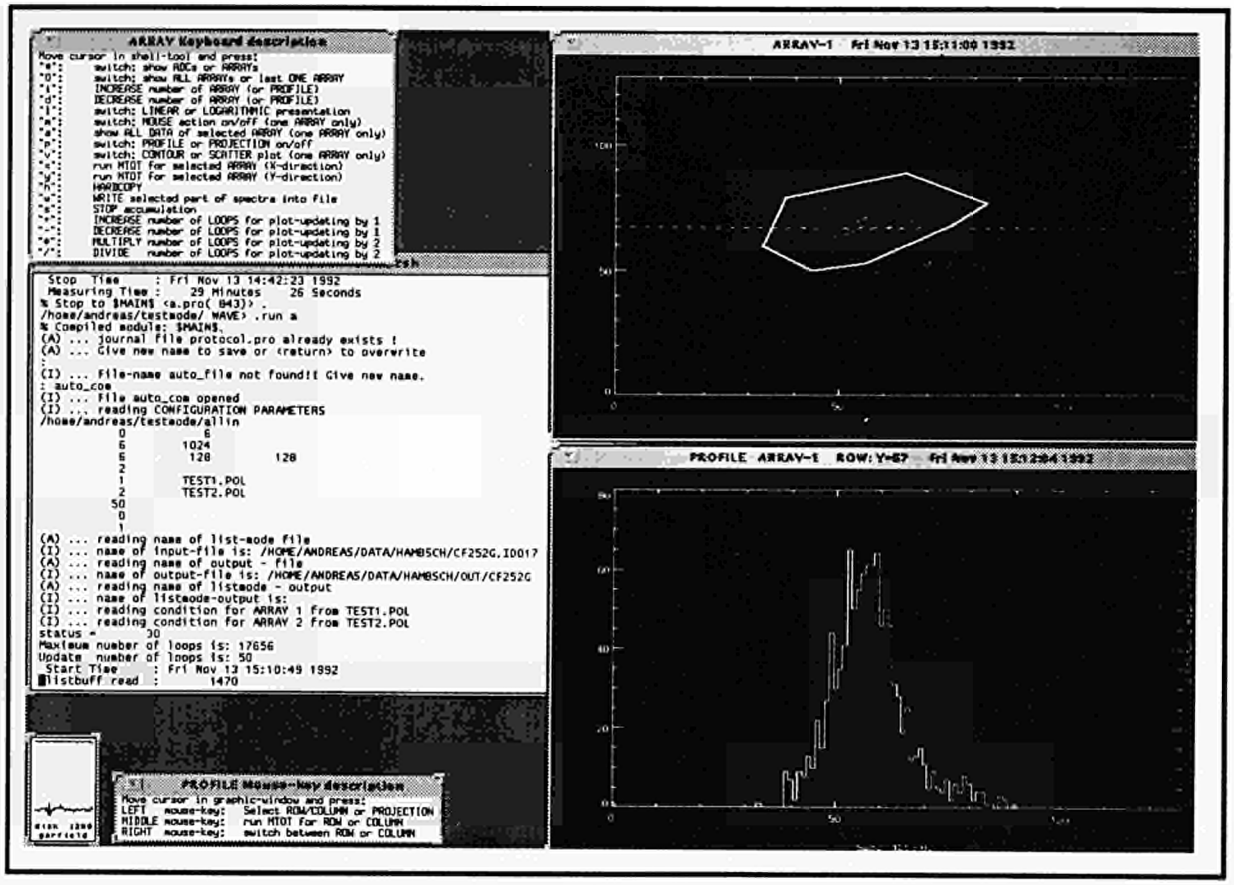

Fig. 38. ***Typical workspace for data evaluation with LISA. A two-dimensional configuration as well as a profile is displayed. Possible mouse and keyboard actions are shown***

datasets, the user is obliged to write a small C-procedure which has to be compiled and linked to the package. For the data analysis of typical experiments these procedures are already available. Thus, only a basic knowledge of the C-language is necessary for the analysis of listmode data independent from which type of experiments they are coming. While performing data treatment the user may apply a series of different options, e.g. he may choose between several display modes, etc. This user interface is provided in a very handy manner by entering single-character keyboard input, moving a mouse and pushing its buttons. A typical workspace is displayed in Fig. 38.

Last but not least it has to be pointed out, that all options for data evaluation are available as well in the case of data acquisition. These features have been tested by using a new data acquisition system which was developed in collaboration with the firm DELTA-t Entwicklungsgesellschaft mbH, Hamburg (D). First experiences have proven that the combination of this data acquisition system with LISA is a well suitable alternative for the old NUCLEAR DATA system still in use at CBNM.

DISCRETIONARY RESEARCH

Radiation Physics

R. Cools, P. Goedtkindt*, O. Haeberlé**, N. Maene***, F. Poortmans***, H. Riemenschneider, P. Rullhusen, J.-M. Salomé, F. Van Reeth

X-ray Transition Radiation.

Transition radiation is a very promising technique for production of intense soft X-ray beams at energies of about 1 keV using electron accelerators[1]. One week of beam time was used to accomplish the final measurements of X-ray energy spectra and angular distributions for the thesis of P. Goedtkindt. The data have been evaluated and the thesis is nearly completed.

At the end of this measuring period also a multilayer, which was provided by the University Pierre et Marie Curie, Paris, has been used as radiator. This experiment was done in order to look for a new radiative effect proposed. No effect was seen, which could, however, be due to the rather bad beam quality.

Optical Transition Radiation.

The new techniques envisaged for the radiation physics programme at GELINA require an excellent beam quality, which will be available after the second step of the proposed refurbishing plan. A system has been installed to perform beam emittance measurements using optical transition radiation. The system is running well and is able to deliver online information about the electron energy, the beam size and the beam divergence. An internal report has been prepared[2].

Smith-Purcell effect.

The Smith-Purcell effect is attracting considerable interest in several laboratories (i.e. Mainz, Darmstadt, Brookhaven, Lawrence Livermore, Oxford). The idea is to use this effect to produce intense X-ray beams using ultrarelativistic electrons travelling close to a metallic grating. Unfortunately, no rigorous theoretical treatment has been published yet and only one experiment has been achieved in the far infrared using a rather moderate electron energy of 3.6 MeV. A new mathematical algorithm has been developed on the basis of the Greens-function method proposed for optical diffraction in order to calculate the Smith-Purcell radiation emitted by ultrarelativistic electron beams. The code works well for rectangular and sinusoidal gratings and is being extended to apply also to more general gratings. An experiment at optical wavelengths using a 100 MeV electron beam at GELINA is envisaged.

---

* EC Fellow. Present address: Université Paris Sud, LSAI, Orsay, France
** EC fellow from Université de Strasbourg, France
*** VITO, Mol, Belgium

(1) CBNM Annual Report 91, EUR 14374 EN
(2) S. Schaeffer, Internal Report GE/R/LI/1

Trace Metal Analyses in Biological and Environmental Media

F. Cordeiro-Raposo, J. McCourt, J. Chivot*, A. Muñoz**, J. Mendieta***, G. Bordin, A. Rodriguez

Various studies - spectrophotometric, electrochemical and chromatographic - have been conducted on cadmium, zinc thioneins, on cysteine and on the peptide Lys-Cys-Thr-Cys-Cys-Ala Metallothionein I fragment 56-61 (FT), both of the aforementioned organic molecules intrinsic to the metallothionein structure, with the aim of establishing analogies between the behaviour of these selected compounds.

Analytical Characterization by Liquid Chromatography

The main characteristics of metallothioneins (MT's) and the samples studied (three MT's from rabbit liver (RL), one from horse kidney (HK)) have been presented earlier[1]. The MT's have been studied on two types of HPLC columns differing in separation principle: size-exclusion and reversed-phase chromatography.

- Size-exclusion chromatography (SEC) (separation based on relative size of molecules)

  Conclusion from recent experiments was that the four MT's were probably partially dimerised: each chromatogram showed two unequal peaks, the first one attributed to the dimeric form (D) (Table 17) and the second one to the monomer (M).

Table 17. Share of dimer for various metallothioneins

MT	Dimer [%]
M 7641 RL	23.2 ± 2.6
M 5267 RL-I	13.9 ± 2.8
M 5392 RL-II	26.5 ± 4.6
M 4766 HK	9.7 ± 2.9

It was possible to calculate the respective monomer (C_M) and dimer (C_D) concentrations for each MT at different total concentrations, and to study the functions $A_D = f(C_D)$ and $A_M = f(C_M)$, where A_D is the first peak area and A_M the second peak area.

---

* Visiting Scientist from CEN Fontenay-aux-Roses, France
** EC Fellow from the University of Madrid, Spain
*** EC Fellow from the University of Alcala de Henares, Spain
(1) CBNM Annual Report 91, EUR 14374 EN

Table 18 includes the slopes of A = f(C) for the four MT dimers and monomers.

Table 18. Properties of various metallothioneins

MT	Slope k of A = f(C) $[10^{-8}]$		k_D/k_M
	Dimer: k_D	Monomer: k_M	
M 7641 RL	2.75 ± 0.18	1.42 ± 0.04	1.94
M 5267 RL-I	2.54 ± 0.15	1.08 ± 0.17	2.35
M 5392 RL-II	2.49 ± 0.21	1.14 ± 0.12	2.18
M 4766 HK	2.92 ± 0.67	1.25 ± 0.09	2.34

As can be seen, the slope ratio is close to 2 for each MT. The partial dimerization of the MTs, at different levels according to the nature of each MT, therefore appears to be well established.

RL being a "mixture" of RL-I and RL-II and knowing the various dimer ratios, the respective proportions of the two isoforms of RL can be calculated. This leads to the identification of a MT RL being composed of (26 ± 5) % RL-I and of (74 ± 12) % RL-II.

- Reversed-phase chromatography (RPC) (separation based on hydrophobic interactions of the solute with the stationary phase). This mode of separation gives more selective information on the chemical structure than the SEC mode. The Figs. 39 and 40 show the RP chromatograms of the MT-RL and of the MT-HK.

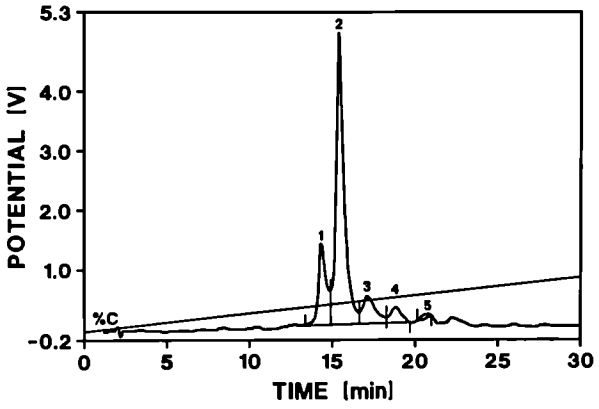

Fig. 39. Reversed-phase chromatogram of RL

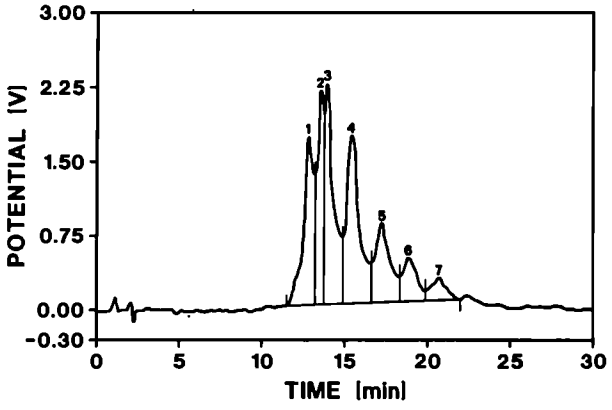

Fig. 40. Reversed-phase chromatogram of HK

Depending on the structure of each MT, the number of "important" peaks varies: 2 for RL-I and for HK, 3 for RL-II and 4 for RL. Their retention times (t_R) are given in Table 19.

Table 19. Various types of metallothioneins and their retention times

MT	t_R [min]				
M 7641 RL	12.85	13.59	13.91		15.36
M 5267 RL-I			13.74		15.28
M 5392 RL-II	12.82	13.47			15.28
M 4766 HK				14.30	15.30

Observations:
- one peak (t_R = 15.3 min) is common to all MT's;
- the first peak of HK (t_R = 14.3 min) is characteristic of this MT;
- qualitatively, the two first peaks of RL can be attributed to RL-II, the third one to RL-I, the fourth one being common.

Studying the linearity of the UV response of the different peaks as a function of concentration, we could calculate the contribution of the common peak to each MT. These data resulted in the estimation of the composition of MT-RL:

$$(20 \pm 5)\ \%\ \text{of RL I} - (80 \pm 14)\ \%\ \text{of RL II}$$

These results are in excellent agreement with the previous ones found by SEC. Hence, liquid chromatography is very efficient for the characterization of the polymorphism of the MT's.

Analytical Characterization by Polarography

Only the most significant conclusion drawn from the overall results obtained by polarography is presented in this report. Fig. 41 shows the oxido-reduction potentials corresponding to each polarographic peak found which could be attributed to the different electrochemical systems. The polarographic response can therefore be used for elucidation of the chemical forms of compounds (speciation) present.

Two different electrochemical systems were distinguished: in the first one, the mercury electrode itself is involved in the charge transfer step; in this case peaks are attributed to the oxidation of the mercury electrode in the presence of a chelating agent (L) according to $Hg(O) + L \rightarrow Hg(II)L + 2e$. The second electrochemical system corresponds to the reduction of metal cations in a dropping mercury electrode either of free ions $M^{2+} + 2e \rightarrow M(Hg)$ or complexed $M(II)L + 2e \rightarrow M(Hg) + L$, M indicating cadmium or zinc.

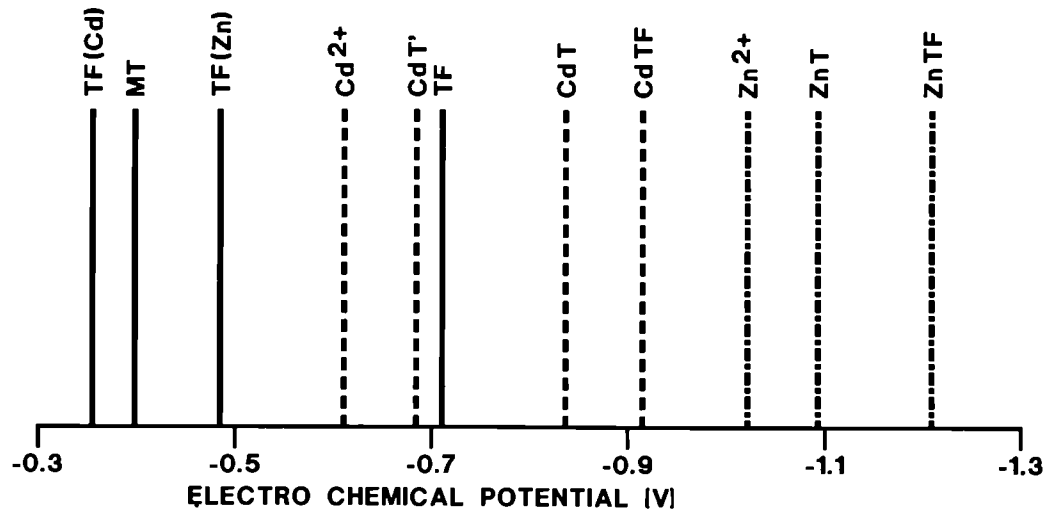

Fig. 41. Peak potentials, vs Ag/AgCl, in TRIS-HCl 2.5 10^{-2} M at pH 7.5 System Hg(II)/Hg(O), - - - System Cd(II)Cd(O), -·-·- System Zn(II)/Zn(O)

In Fig. 41 peaks indicated by MT(I), TF(Cd), TF(Zn) and TF were attributed to the first electrochemical system described above, Hg(II)/Hg(O), and respectively correspond to the oxidation of the mercury electrode in the presence of cadmium, zinc thioneins, to the peptidic fragment bound to the cadmium or to the zinc and to the peptidic fragment alone. Peaks Cd^{2+}, CdT', CdT and CdTF are due to the reduction of the system Cd(II)/Cd(O) and were attributed to the reduction of the free cation, to the cadmium bound to the thionein (forming two complexes of different stability and also probably different stoichiometry) and to the cadmium complexed by the peptidic fragment, respectively. Similarly, peaks Zn^{2+}, ZnT and ZnTF correspond to the reduction of free zinc, zinc complexed by thioneins and fragment, respectively.

Trace Metals in Marine Bivalves

The knowledge of the total metal concentrations in a living organism is necessary but not enough. Therefore, we started to study the intracellular distribution of four elements copper, cadmium, zinc and iron in the marine clam *Macoma balthica* from the Westerschelde estuary. In terms of metal bioavailability, the important cell fraction is the soluble phase, the cytosol. For more than one year metal concentrations in the cytosol (and in the insoluble fractions) of bivalves from two sampling locations, Baalhoek (B) and Paulinapolder (PP) have been measured (Table 20).

Table 20. Metal concentrations in bivalves samples from two locations

Concentration in the cytosol [% of total element]	Copper		Zinc		Cadmium		Iron	
	B	PP	B	PP	B	PP	B	PP
Range	15-33	10-33	15-33	10-33	8-26	<d.l-10	2-5	2-8
Average	26	21	12	10	17	4	3	5

The most striking result is that of cadmium. While cytolic copper, zinc and iron show no significant location difference as a proportion of total metal, cadmium exhibits a behaviour depending on the site. This cadmium particuliarity was already observed for the total element, probably due to its non-essential character. This is reinforced by the recent results obtained with samples artificially contaminated in metals (copper, cadmium, zinc); the uptake distributions of copper and zinc do not differ significantly from the natural ones, while for cadmium, the percentage of cytosolic metal rises at Paulinapolder from 4 to 20 % on average, after uptake.

SCIENTIFIC AND TECHNICAL SUPPORT TO THE COMMISSION

SUPPORT TO DG I: INTERNATIONAL COLLABORATION - NUCLEAR SAFEGUARDS

Preparation and Characterization of Metallic U-Pu spikes

J.M. Orea Rocha*, C. Ingelbrecht, F. Peetermans, P. Robouch, R. Eykens, K. Mayer, A. Alonso, R. Garcia, A. Verbruggen

This work has been carried out to improve the homogeneity and ductility of uranium and plutonium containing metallic spikes required for the IDMS assay of uranium and plutonium in undiluted input samples of reprocessing plants. The work during 1992 was concentrated on the examination of the compositions U-Pu-Ti, U-Pu-Zr-Nb and U-Pu-Nb. Metallography supported by electron microprobe examination, carried out during secondment to the Institute of Transuranium Elements, Karlsruhe, indicated good microhomogeneity of two of the alloys, but with some uranium segregation in the U-Pu-Zr-Nb composition. Homogeneity control by γ-ray spectrometry using both solid and liquid samples showed that a relative standard deviation in the plutonium concentration of 0.1 to 0.2 % was achieved and this was confirmed by IDMS measurements on samples of the U-Pu-Nb alloy, which is the most attractive candidate spike alloy. The preparation of a production batch of spikes will be carried out during 1993.

Preparation, Certification and Sales of U-Pu Dried Spikes

A. Verbruggen, F. Hendrickx, A. Alonso, K. Mayer, P. De Bièvre

In 1992, 238 units of solid (dried) U-Pu spikes, CBNM IRM-1027b, were prepared. A certificate is issued for each individual unit indicating the number of the vial to which it belongs as well as the mass of original solution (in g) from which the solid (dried) spike was made. Certified values are based on the weighing data, on the certified values of the base materials and on the mass spectrometric measurements for the isotope abundances of plutonium.
Molar concentrations of ^{235}U and ^{239}Pu in the mother solution are certified to be:

$$(1.627\,6 \pm 0.001\,6)\cdot 10^{-2}\ \text{mol}\ ^{235}\text{U}\cdot\text{kg}^{-1}\ \text{of solution;}$$
$$(2.438\,0 \pm 0.002\,4)\cdot 10^{-3}\ \text{mol}\ ^{239}\text{Pu}\cdot\text{kg}^{-1}\ \text{of solution.}$$

From the certified values, the following element concentrations are derived:

$$(19.454 \pm 0.019)\cdot 10^{-3}\ \text{kg U}\cdot\text{kg}^{-1}\ \text{of solution;}$$
$$(6.000\,0 \pm 0.006\,0)\cdot 10^{-4}\ \text{kg Pu}\cdot\text{kg}^{-1}\ \text{of solution.}$$

---

* EC Fellow from Universidad Complutense, Madrid, Spain

The material is supplied with uranium and plutonium isotopic composition as follows:

	mole %	mass %	
$^{233}U/U$	< 0.000 1	< 0.000 1	
$^{234}U/U$	0.333 5	0.328 7	± 0.000 3
$^{235}U/U$	19.865 4	19.665 0	± 0.002 2
$^{236}U/U$	0.030 4	0.030 2	± 0.000 1
$^{238}U/U$	79.770 7	79.976 1	± 0.002 2

The atomic weight of uranium is $A_r(U) = 237.439\,479 \pm 0.000\,067$.

	mole %	mass %	
$^{238}Pu/Pu$	0.004 4	0.004 3	± 0.002
$^{239}Pu/Pu$	97.145 8	97.134 0	± 0.005 0
$^{240}Pu/Pu$	2.808 7	2.820 2	± 0.004 9
$^{241}Pu/Pu$	0.035 8	0.036 1	± 0.000 2
$^{242}Pu/Pu$	0.005 3	0.005 4	± 0.000 2
$^{244}Pu/Pu$	< 0.000 1	< 0.000 1,	

with the atomic weight of plutonium being $A_r(Pu) = 239.081\,125 \pm 0.000\,050$.

Test on the dissolution of the solid (dried) spikes have been performed during the verification measurements on the isotope abundances and during the U/Pu content determinations by IDMS of the series CBNM IRM-1027a and 1027b. By applying common chemical preparation procedures, complete dissolution was achieved within 30 minutes.
Verification measurements by IDMS led to a uranium concentration of (19.430 ± 0.034) mg U/g in agreement with the certified value of (19.454 ± 0.019) mg U/g and to a value of (599.28 ± 0.95) µg Pu/g which compares well to the certified value of (600.00 ± 0.60) µg Pu/g.
In 1992 a total number of 162 spikes were delivered on orders from IAEA and EURATOM Safeguards for use in various reprocessing plants.

Special Abundance Measurements in Natural Uranium
K. Mayer, W. De Bolle, R. Ovaskainen*

CBNM's facilities for highly accurate isotope abundance measurements were used on request of the IAEA. Samples were measured by thermal ionization mass spectrometry and, after conversion to UF_6, by gas source mass

* Fellow from Helsinki University, Finland

spectrometry. Small differences in the $^{235}U/^{238}U$ ratio ($< 6 \cdot 10^{-4}$) as well as in the $^{234}U/^{235}U$ ratio ($< 2 \cdot 10^{-4}$) of natural uranium helped to identify different material origins.

SUPPORT TO DG VI: AGRICULTURE

Preparation of Ewe-Curd Reference Material

J. Pauwels, G.N. Kramer, C. Louvrier, P. de Vos

A feasibility study for the preparation of two dry (< 1 % H_2O) ewe-curd reference materials, containing respectively no and 1 % cow milk was carried out. Such RM's are required for the control of adulteration of ewe cheese with cow milk. Fifty 20 g dry powder samples were prepared from cow curd by freeze-drying, stud milling under controlled atmosphere (< 100 vpm H_2O), and final bottling in penicillin vials under argon.
The test samples were analyzed at the University of Freising (D) and found to be fully acceptable for the preparation of the proposed CRM's.

SUPPORT TO DG XIII: TECHNOLOGY TRANSFER

Gas Encapsulation in Zeolites

P. De Bièvre, E. Vansant*

The development of gas mass spectrometric analysis methods was continued. The procedure now has reached the stage of being 'near-absolute' by extensively using the know-how obtained in the Avogadro Constant project. Direct measurement of synthetic CO_2/N_2 mixtures using these procedures, yielded gas mixture composition values which agreed with the gravimetric values to within 0.1 % (for the CO_2/N_2 ratio). In addition, this measurement procedure is directly traceable to the mole. The potential and the consequences of the availability of such a measurement procedure for international comparability of gas measurements can hardly be overstressed.
New patents were granted on adsorption procedures for isotopes on solids: "Process for ultra-drying of a gas" (CAN 1 296 654 (1992-03-03) and JAP 1 678 442 (1992-07-13)).

* University of Antwerpen, Belgium

SUPPORT TO DG XVII: NUCLEAR SAFEGUARDS

ECSAM

K. Mayer, A. Alonso, M. Bickel, W. Leidert, A. Michiels, F. Hendrickx, A. Verbruggen, P. De Bièvre

The European Commission's Safeguards Analytical Measurements (ECSAM) activity is backed by the external quality control programme REIMEP assuring the quality of the results obtained by the Commission's safeguards laboratories. Participation of ECSAM laboratories in the REIMEP programme is compulsory.

In the framework of the continuous technical support to the EC Safeguards verification measurements a number of U/Pu safeguards samples have been analysed at CBNM for element content and isotopic composition.

Consulting for the On-Site Laboratories (OSL) in Sellafield and La Hague was continued. These highly automated laboratories will be extensively equipped with techniques for non-destructive analysis (NDA). One of these techniques is neutron coincidence counting which, in combination with γ-ray spectrometry, can be used for measuring the plutonium inventory in the product stream (PuO_2) of a reprocessing plant. External quality control of the OSL will be compulsory through the REIMEP programme.

80 Grams of EC-NRM 210 (PuO_2) were heat treated, weighed and filled into special containers according to the specifications of DG XVII after being certified for isotopic composition.

A set of 15 PuO_2 reference materials was bottled in 10 special stainless steel containers (containing 1 to 10 g PuO_2, respectively) and five polycarbonate containers (containing 1 to 9 g PuO_2 in 2 g steps, respectively). The material (EC-NRM 210)was certified for both element content and isotopic composition to better than 0.1 %.

The certified values are (by June 30th, 1992):

	mole %	accuracy (2s)
^{238}Pu	0.011 5	± 0.000 2
^{239}Pu	93.492 4	± 0.002 2
^{240}Pu	6.292 2	± 0.001 9
^{241}Pu	0.165 8	± 0.000 6
^{242}Pu	0.038 5	± 0.000 3,

with a plutonium content of (879.82 ± 0.44) $g \cdot kg^{-1}$ and an atomic weight of $A_r(Pu) = 239.119\,540 \pm 0.000\,028$.

However, for the neutron coincidence counting measurements the ^{240}Pu content is important. Therefore, it has been calculated individually for each sample bottle by combining element concentration, ^{240}Pu isotope abundance and mass of PuO_2. The respective uncertainties were calculated from the various uncertainty components.
Furthermore, the long term stability in mass of this Reference Material was checked. The evolution of mass for both containers and the respective relative humidity has been followed during 20 weeks. The mass changes were found to be lower than $8 \cdot 10^{-4}$ for the polycarbonate container and 10^{-3} for the stainless steel container. It can be concluded that, by using the described Reference Material, verification measurements will be achievable to an accuracy of 0.1 %.

SUPPORT TO THE CONSUMER POLICY SERVICE

Chemical Methods of Analysis
J. McCourt, G. Bordin, A. Rodriguez

After many exchanges of views, notes and several meetings with the participation of some members of the Consumer Policy Service (CPS), the Environment Institute (EI) and the Central Bureau for Nuclear Measurements (CBNM), an agreement was reached on the transfer of several activities from EI to CBNM. The execution of the various tasks concerning support to CPS and the time schedule were discussed.
The contribution of CBNM was started with Chemical Methods of Analysis in Cosmetic Products. In this topic, the scientific and technical coordination and the chairmanship of the meetings of the Working Group "Analytical Methods of Cosmetics" were assumed.
Contacts with TNO, Nutrition and Food Research (NL), under contract to CPS and with the Inspectie Gezondheidsbescherming (NL) were taken. In the latter case, a joint direction of a post-doctoral position was proposed and accepted. The subject "Application of Liquid Chromatography (HPLC) to the Study of Oxidative Hair Dyes" was previously suggested by the Working Group in agreement with the CPS.
One of the tasks of the CPS is to harmonise the efforts to establish reliable and simple methods for the analysis of different compounds in cosmetic products. In this context, the determination of lead in several hair lotions and creams was performed using three different methods: Electrothermal Atomic Absorption

Spectrometry (ET-AAS), Inductively Coupled Plasma Atomic Emission Spectrometry (ICP-AES) and Differential Pulse Polarography (DPP). The results obtained for different samples are in good agreement, regardless the method of analysis applied. The lead content has been found to be below the limits recommended in the EC Directives (level of lead less than 0.6 %).
A new activity, the development and updating of a data bank concerning safety of products, will be started in 1993.

WORK FOR THIRD PARTIES

In 1992 again a series of requests from external customers could be satisfied. Works concerned, (1) the supply of a great number of samples and reference materials, (2) the activity determinations of radioactive waste barrels, (3) The standardization of a strong radioactive ^{152,154}Eu source, (4) the elaboration of a particular fitting programme of α-particle spectra and (5) a couple of REIMEP rounds. It was a very successful year with regard to the received payments: the income could again be increased compared to that of the preceding year.
The work to be executed on request from third parties requires, however, sometimes intensive development and testing efforts even before a customer tailored offer can be submitted. In addition, during the execution of an order often some unexpected cumbersome details have to be settled. Moreover, the total sum of incoming money is based on a relative high number of small orders (about 120) which were carried out mostly in the frame of the Project Reference Materials.

Samples and Targets for Nuclear Measurements
J. Pauwels, C. Ingelbrecht, P. Robouch, R. Eykens, C. Louvrier, F. Peetermans, A. Dean, H. Mast, J. Van Gestel

In total 65 samples and targets have been prepared, characterized and supplied in response to 25 orders from six countries. Details are given in Table 21. They concern thin deposits for nuclear physics experiments and bulk samples prepared by various metallurgical methods, including quantitative alloying. Bulk samples comprise reactor melt-wire temperature monitors prepared from low melting point binary and ternary eutectics, encapsulated in quartz, with melting point determination by differential thermal analysis. Some of these compositions were very brittle and were made by direct casting into wire form. ^{6}Li metal samples required special handling and canning under inert atmospheres to avoid reactions with air.

Reactor Neutron Dosimetry Samples
C. Ingelbrecht, F. Peetermans, S. Palmeri

A number of special samples and alloys for neutron dosimetry falling outside the dosimetry reference materials programme have been supplied to external customers during 1992. In total 1132 samples have been delivered in response to 12 orders from five countries. Details are given in Table 22.

Table 21. Supply of thin deposits, films and bulk samples to external customers

Preparation	Customers' countries	Number of Samples	Preparation Methods(1)
Thin deposits			
Hydrogen	D	3	VD
^{nat}LiF	D	2	VD
^{6}LiF	D	2	VD
$^{239}PuF_3$	D	1	VD
$^{240}PuF_3$	D	1	VD
$^{235}UF_4$ or $^{235}U_3O_8$	F	2	VD, SU
$^{238}UF_4$ or $^{238}U_3O_8$	D, F, S, USA	15	VD, SU
Films			
Polyimide	D	2	CE
Bulk samples			
Cd-Pb	B	3	M-MA-CAN
Cd-^{57}Fe	B	1	M
Gadolinium	CS	1	R
Indium	B	4	MA-CAN
^{6}Li	C	1	R-MA-CAN
Lead	B	4	MA-CAN
Pb-Ag	B	4	M-MA-CAN
Pb-Ag-Sn	B	4	M-MA-CAN
Pb-Cd	B	4	M-MA-CAN
Pb-In	B	4	M-MA-CAN
Sb-In	B	3	M-MA-CAN
Sn-Zn	B	4	M-MA-CAN

(1) CAN canning; M melting; MA machining; R rolling; SU suspension spraying; VD vacuum deposition

Table 22. Supply of special dosimetry preparations to external customers

Preparation	Customers' countries	Number of samples	Preparation methods(1)
Al-^{235}U	JAP	800	LM, R, MA, CAN
Al-^{239}Pu	JAP, B	301	LM, R, MA, CAN
Al-Lu	F	1	LM, R
Al-^{232}Th	B	1	LM, R
Niobium, titanium, iron, cobalt monitors	CAN	11	MA, CAN
$^{235}UO_2$	B	10	CAN
Niobium	B	2	R, MA
Vanadium	B	2	R, MA
Zirconium	B	2	R, MA
$^{238}UO_2$	B	1	CAN
Al-Au	NL	1	LM, R

(1) CAN canning; LM levitation melting; M melting; MA machining; R rolling

Many of these preparations were aluminium alloys prepared by levitation melting including Al-Pu discs canned by pressing into aluminium containers without external contamination. In addition, complete flux monitor capsules containing niobium, titanium, iron and Ni-Co monitor samples were prepared by encapsulation in quartz ampoules and electron beam welding into stainless steel tubes.

Reference Samples and Reference Materials

J. Pauwels, G.N. Kramer, K.H. Grobecker, C. Louvrier, P. de Vos, C. Hofmann*, S. Mickel**

Two reference materials were prepared on behalf of the BGA (Bundesgesundheitsamt), Berlin (D): innards powder (CBNM-401) and tomatoes powder (CBNM-404).
Of each material 300 samples of 25 g were supplied. Their homogeneity was verified using solid sampling Zeeman atomic absorption spectrometry. For CBNM-404 indicative values for arsenic, cadmium, chromium, copper, mercury, nickel, lead, selenium, thallium and zinc were determined using various methods both at CBNM and outside.
Moreover, specific analytical support by solid sampling atomic absorption spectrometry was given in the frame of a German environmental study: 450 samples of mg-size of soils and plants were analyzed for mercury on behalf of the University of Giessen.

ALFA: A Programme for Accurate Analysis of Complex Alpha-Particle Spectra on a PC

T. Babeliowsky, G. Bortels

ALFA is an interactive graphical tool for analyzing multiplets in alpha-particle spectra using a convolution-type peak-fitting function. A tailing subtraction reduces interference between peaks. Peak positions and areas are calculated by non-linear least-squares fitting. Uncertainties are computed considering covariances. Relevant parameters in the optimization are saved with the spectrum file. ALFA includes full options for management of a database of analyzed spectra. The programme is available for sale.

---

* EC Fellow from University of Gent, Belgium
** EC Fellow from University of Giessen, Germany

Metrology of Radioactive Waste Barrels

D.F.G. Reher, B. Denecke, A. Solé

The Belgian Organisation responsible for the treatment and storage of radioactive waste (NIRAS/ONDRAF) contracted CBNM to analyse conditioned and non-conditioned radioactive waste containers. For this purpose CBNM is using a γ-ray scanning device, allowing to scan heavy waste drums of up to 2000 kg.

The accuracy of the system was improved by the use of Monte Carlo calculations of the efficiency and the geometry. Penetration of photons through the edges of the collimators and compton scattering were included in the model. Comparison of γ-ray scanning results with those from destructive methods gave excellent agreement for ^{60}Co, whereas for ^{137}Cs γ-ray scanning was systematic lower by about 30 %.

The relative activities of six barrels containing ^{233}U waste and six barrels with natural uranium waste were also measured.

Standardization of a 50 GBq $^{152,154}Eu$ Extended Volume Source

D.F.G. Reher, B. Denecke

The standardization of a 50 GBq $^{152,154}Eu$ extended volume source used to determine the linear power dissipation of irradiated fuel pins in materials testing reactors, was carried out for SCK/CEN, Mol (B). The source consisted of a foil of irradiated europium rolled up to a close cylindrical geometry in an aluminium housing.

The major difficulties in the standardization of this source were its high activity, complex geometry, and inhomogeneity. Destructive methods were excluded. A solution of ^{152}Eu was standardized and a quantitative 50 MBq strip source (of the same dimensions and in an identical housing as the $^{152,154}Eu$ volume source) was prepared. Both sources were compared by measuring spectra with the CBNM γ-ray scanning system at a source to detector distance of about 4 m and a collimator of 4 mm diameter. During the measurements the sources were rotated continuously. For this very low geometry corrections for differences in source construction became simple and small.

From the measurements with the ^{152}Eu strip source an efficiency calibration of the system was obtained which served to determine the ^{154}Eu activity in the $^{152,154}Eu$ volume source. The ^{152}Eu and the ^{154}Eu activities were certified to an accuracy of ± 1.1 % and ± 1.5 %, respectively.

Regular European Interlaboratory Measurement Evaluation Programme (REIMEP)

K. Mayer, A. Alonso, P. De Bièvre, M. Bickel, A. Rodriguez, A. Michiels, W. Leidert, F. Hendrickx, W. Nagel, W. De Bolle, A. Verbruggen,

Measurement Round on UF_6 (REIMEP 10): Material for a new round on UF_6 was prepared by mixing two batches of UF_6 and homogeneising it by repeated distillation. Homogeneity was checked by UF_6 gas mass spectrometry (to $2 \cdot 10^{-4}$). The material was characterized and then bottled into UF_6 sample vials (for mass spectrometry) and special containers (for γ-ray spectrometry). These containers were manufactured at CBNM, thickness of measurement window was verified, containers were pressure tested to withstand 15 bar and leak tested. All the containers were verified for isotopic homogeneity versus the bulk material to $2 \cdot 10^{-4}$. The material in the containers for γ-ray spectrometry was conditioned in order to obtain a homogeneous layer of 99.9 % infinite thickness. Samples will be distributed to the participants early 1993.

Measurement Rounds on MOX Pellets, Spent Fuel Solution, Synthetic Input Solution and Plutonium Nitrate Solution (REIMEP 6, 7, 8 and 9): Results are coming in for evaluation. A REIMEP participants meeting was organised at CBNM in November 1992 at the occasion of a joint meeting of the ESARDA working groups on destructive and non destructive analysis. Conclusions of the meeting will be elaborated for incorporation in the programme.

Measurement Round on PuO_2 (REIMEP 11): A new round was announced, the material to be used has been ordered after having discussed details with representatives from industry, DCS and IAEA.

Measurement Rounds on Environmental Samples: In close co-operation with Los Alamos National Laboratory REIMEP rounds on environmental type samples (contaminated water, groundwater, soil) are being prepared.

International Measurement Evaluation Programme (IMEP)

A. Lamberty, P. De Bièvre

The exercises IMEP-1 (lithium in serum) and IMEP-2 (cadmium at four different levels in polyethylene) have been finished. Results were discussed with the participants and have been published.

IMEP-3 (Trace elements in a synthetic and in a natural water) is ongoing Samples were distributed and measured. Participants' results have been collected and are being evaluated.

IMEP-4 (lithium, copper and zinc at different levels in serum) is starting with the certification of the three elements. Distribution of the samples to the participants is foreseen at the beginning of 1993.

CBNM Certification of Boron in NIST SRM Low Alloy Steel Samples by Isotope Dilution Mass Spectrometry

A. Lamberty, L. Van Nevel*

The certification of boron under NIST contract in their SRM Low Alloy Steel materials was continued. After NIST SRM 1761, 1762 and 1763, four more samples, NIST SRM 1764, 1765, 1766 and 1767 were certified. The boron content of these four samples (10 to 1 µg/g) was significantly lower than in the first 3 samples (55 to 20 µg/g) which necessitated strong efforts in order to reduce the chemical blank to an acceptable level. The results of the uncertainty calculation as well as the final certified values are summarized in Tables 23 and 24 (all uncertainties are 2s).

Table 23. Uncertainty of the boron certification measurements in NIST Low Alloy Steel SRM's

Material	Random uncertainty [%]	Systematic uncertainty [%]	Total uncertainty [%]
NIST SRM 1764	3.8	6.0	9.8
NIST SRM 1765	2.3	6.0	8.3
NIST SRM 1766	13	39	52
NIST SRM 1767	1.5	2.8	4.3

Table 24. Final Results of boron certification measurements in NIST Low Alloy Steel SRM's

Material	Boron content (µmol/g)	Boron content (µg/g)
NIST SRM 1764	0.918 ± 0.090	9.93 ± 0.97
NIST SRM 1765	0.864 ± 0.072	9.34 ± 0.78
NIST SRM 1766	0.112 ± 0.058	1.21 ± 0.63
NIST SRM 1767	0.927 ± 0.040	10.02 ± 0.43

For NIST SRM 1766 with a very low boron content (1.2 µg/g), the chemical blank (2.7 µg) could not be sufficiently reduced in order to allow an accuracy better then 52 %. This material will be re-analysed when the new Clean Chemical Laboratory (CCL) is operational.

New orders were received from PTB (D) to determine traces of boron in ^{28}Si and from the Agricultural University of Wageningen (NL) to certify boron in a biological material.

* University of Antwerpen, Belgium

GENERAL INFORMATION

LIST OF PUBLICATIONS

CONTRIBUTION TO CONFERENCES

BABELIOWSKY, T., BORTELS, G.
Accurate analysis of complex alpha-particle spectra using a PC.
Conf. Industrial Radiation and Radioisot. Meas. Appl., Raleigh, September 8-11, 1992

BASTIAN, C.
Covariance of histograms in parallel weighted counting.
Specialists Meeting Eval. and Proc. of Covar. Data, Oak Ridge, October 7-9, 1992

BASTIAN, C.
General procedures and computational methods for generating covariance matrices.
Symp. Nucl. Data Eval. Methodology, Upton, October 12-16, 1992

BAX, H., WÄTJEN, U.
Automation of a PIXE system for series of biomedical and environmental analyses.
Intern. Symp. Bio-PIXE, Sendai, July 16-18, 1992

BEER, H., CORVI, F., MAURI, A., ATHANASOPOULOS, K.
High resolution ^{138}Ba (n,γ) measurements.
2nd Intern. Symp. Nucl. Astrophysics, Karlsruhe, July 6-10, 1992

BORTELS, G.
What information can alpha spectrometry provide to calorimetric assay of mixed alpha emitters?
Intern. Workshop on Calorimetry, Ispra, March 26, 1992

CORDEIRO-RAPOSO, F., BORDIN, G., RODRIGUEZ, A.
A contribution to the study of characteristics of several metallothioneins by liquid chromatography.
12th Intern. Symp. Microchem. Techn., Cordoba, September 7-12, 1992

CORVI, F., GUNSING, F., POSTMA, H., MAURI, A.
Spin assignment of ^{238}U p-wave resonances.
Intern. Seminar on Interaction of Neutrons with Nuclei, Dubna, April 14-17, 1992

DE BIÈVRE, P.
How do we prepare for environmental measurements after "Europe 1993".
22nd Intern. Roland W. Frei Memorial Symp. Env. Analys. Chem., Dortmund, June 18, 1992

DE BIÈVRE, P., VALKIERS, S., SCHÄFER, F.
The determination of the absolute molar mass of silicon single crystals for a better Avogadro Constant.
9th Intern. Conf. Atomic Weight and Fundam. Constants, Bernkastel July 19-24, 1992

DE GENDT, S., SCHELLES, W., TAYLOR, P.D.P., VAN GRIEKEN, R.
Isotope dilution applied to materials by means of glow discharge mass spectrometry.
5th Intern. Coll. Solid Sampl. Atomic Spectr., Geel, May 18-20, 1992

DRUYTS, S., WAGEMANS, C., POMMÉ, S., GELTENBORT, P., TRAUTVETTER, H.
Measurement of the ^{14}N (n,p) ^{14}C reaction cross section.
2nd Intern. Symp. Nucl. Astrophysics, Karlsruhe, July 6-10, 1992

GOEDTKINDT, P., MAENE, N., POORTMANS, F., RULLHUSEN, P., SALOMÉ, J.M.
Transition radiation measurements in the soft X-ray energy domain.
1st Intern. Workshop on Channeling Radiation, Berlin, October 12-13, 1992

HAMBSCH, F.-J., OBERSTEDT, A., JÄCKEL, B.
Data acquisition, analysis and visualization using PV-WAVE.
PV-WAVE User Meeting, Darmstadt, September 8-9, 1992

HAMBSCH, F.-J., SIEGLER, P., THEOBALD, J.P.
Fission modes in ^{252}Cf (SF) and ^{237}Np (n,f).
Spring Meeting, German Phys. Soc., Salzburg, February 24-28, 1992

INGELBRECHT, C., PAUWELS, J.
CBNM reference materials for reactor neutron dosimetry.
Intern. k_0 Users Conf., Astene, September 29 - October 1st, 1992

INGELBRECHT, C., PEETERMANS, F.
Alloy preparation by levitation melting.
16th World Conf. Intern. Nucl. Target Dev. Soc., Padova, September 21-25, 1992

KRAMER, G.N., PAUWELS, J., BELLIARDO, J.J.
Preparation of biological and environmental reference materials of CBNM.
5th Intern. Symp. Biol. and Env. Ref. Mat., Aachen, May 11-14, 1992

KRAUSE, P., KRIEWS, M., WÄTJEN, U., DANNECKER, W.
Characterization of aerosol samples by laser ablation ICP-MS.
5th Intern. Coll. Solid Sampl. Atomic Spectr., Geel, May 18-20, 1992

KURFÜRST, U., PAUWELS, J.
Spectral interference of lead in Zeeman atomic absorption spectrometry by S2 molecular absorption.
5th Intern. Coll. Solid Sampl. Atomic Spectr., Geel, May 18-20, 1992

LAMBERTY, A., DE BIÈVRE, P.
CBNM determination of Li in BCR candidate reference material RM303 and RM304 lyophilized serum by isotope dilution mass spectrometry.
5th Intern. Coll. Solid Sampl. Atomic Spectr., Geel, May 18-20, 1992

LAMBERTY, A., DE BIÈVRE, P., GÖTZ, A.
International Measurement Evaluation Programme IMEP-2: Cd in Polyethylene.
5th Intern. Symp. Biol. and Env. Ref. Mat., Aachen, May 11-14, 1992

MAYER, K., ALONSO, A., DE BIÈVRE, P.
The state of the practice in the assay of fissile material.
3rd Intern. Conf. Nucl. and Radiochem., Vienna, September 7-11, 1992

NAGEL, W., QUIK, F., BICKEL, M.
A new approach: the determination of uranium in uranium ore by gamma spectrometry.
3rd Intern. Conf. Nucl. and Radiochem., Vienna, September 7-11, 1992

OBERSTEDT, S., WEIGMANN, H., WARTENA, J., BÜRKHOLZ, C.
Search for the shape isomers of ^{238}U and ^{230}Th.
Spring Meeting, German Phys. Soc., Salzburg, February 24-28, 1992

OREA ROCHA, J.M., INGELBRECHT, C., CRIADO PORTAL, A.J.
Uranium-plutonium metallic spikes for IDMS measurements: preparation and characterization.
16th World Conf. Intern. Nucl. Target Dev. Soc., Padova, September 21-25, 1992

PAUWELS, J., HOFMANN, C., GROBECKER, K.H.
Homogeneity determination of Cd in plastic CRM's using solid sampling atomic absorption spectrometry.
5th Intern. Coll. Solid Sampl. Atomic Spectr., Geel, May 18-20, 1992

PAUWELS, J., HOFMANN, C., VANDECASTEELE, C.
Independent calibration of solid sampling Zeeman atomic absorption spectrometry.
5th Intern. Coll. Solid Sampl. Atomic Spectr., Geel, May 18-20, 1992

PAUWELS, J., KURFÜRST, U., GROBECKER, K.H., QUEVAUVILLER, P.
Microhomogeneity study of BCR candidate reference material CRM-422 cod muscle
5th Intern. Coll. Solid Sampl. Atomic Spectr., Geel, May 18-20, 1992

PAUWELS, J., VANDECASTEELE, C.
Determination of the minimum sample mass of a solid CRM to be used in chemical analysis.
5th Intern. Symp. Biol. and Env. Ref. Mat., Aachen, May 11-14, 1992

PAUWELS, J., VANDECASTEELE, C.
On the use of SS-ZAAS for the microhomogeneity control of CRM's.
5th Intern. Coll. Solid Sampl. Atomic Spectr., Geel, May 18-20, 1992

PIETRA, R., WÄTJEN, U., SABBIONI, E., GALLORINI, M., TARTAGLIA, G.P.
On the potential of combining neutron activation analysis and particle induced X-ray emission (PIXE) for micro- and micro-distribution analysis of hard metals in human tissues.
Meet. Cobalt and Hard Metal Diseases, Bergamo, March 12-13, 1992

PINHEIRO, T., FERNANDES, R., MAENHAUT, W., HEBBRECHT, G., WÄTJEN, U., HALPERN, M.J.
Trace element changes in cardiovascular diseases.
6th Intern. Conf. PIXE and Analyt. Appl., Tokyo, July 20-24, 1992

PINHEIRO, T., MAENHAUT, W., WÄTJEN, U., HALPERN, M.J.
Trace elements in human blood: alterations associated with myocardial infarction.
Intern. Symp. Bio-PIXE, Sendai, July 16-18, 1992

ROBOUCH, P., LOUVRIER, C.
A personal computer database on INTDS publications.
16th World Conf. Intern. Nucl. Target Dev. Soc., Padova, September 21-25, 1992

RULLHUSEN, P.
Novel X-ray sources produced by electron beams.
European Particle Accelerator Conf., Berlin, March 24-28, 1992

SIEGLER, P., HAMBSCH, F.-J., THEOBALD, J.P.
Fission channel calculations for the compound nucleus ^{238}Np.
North-West European Nucl. Phys. Conf., Edinburgh, March 31st - April 3rd, 1992

STEINBAUER, E., BAUER, P., BIERSACK, J.P., BORTELS, G.
What can we learn about high energy scattering from computer simulations?
Conf. Computer Simulations of Rad. Eff. in Solids, Berlin, August 23-28, 1992

TAYLOR, P.D.P., MAECK, R., DE BIÈVRE, P.
Determination of the absolute isotopic composition and atomic weight of a reference sample of natural iron.
5th Intern. Coll. Solid Sampl. Atomic Spectr., Geel, May 18-20, 1992

WÄTJEN, U.
The CBNM scanning nuclear microprobe analytical facility.
3rd Intern. Conf. Nucl. Microprobe Techn. and Appl., Uppsala, June 8-12, 1992

WÄTJEN, U., BAX, H., RIETVELD, P.
An investigation into the accuracy of PIXE analysis in a case of strong peak interferences.
6th Intern. Conf. PIXE and Analyt. Appl., Tokyo, July 20-24, 1992

WÄTJEN, U., KRIEWS, M., DANNECKER, W.
Status report: preparing an ambient aerosol filter reference material for elemental analysis.
5th Intern. Symp. Biol. and Env. Ref. Mat., Aachen, May 11-14, 1992

WÄTJEN, U., KRIEWS, M., DANNECKER, W.
The preparation of an ambient aerosol filter candidate reference material for elemental analysis.
6th Intern. Conf. PIXE and Analyt. Appl., Tokyo, July 20-24, 1992

SCIENTIFIC OR TECHNICAL ARTICLES

BICKEL, M.
Compounds of thorium with phosphorus-oxygen acids containing phosphorus in a valence state less then five.
In: Gmelins Handbook of Inorganic Chemistry (to be published)

BICKEL, M.
Compounds of thorium with phosphorus-oxygen acids containing pentavalent phosphorus.
In: Gmelins Handbook of Inorganic Chemistry (to be published)

BICKEL, M., KANELLAKOPULOS, B.
Systematics in the magnetic properties of ternary actinoid oxides.
J. Solid State Chem. (to be published)

BICKEL, M., MAYER, K.
Ist Genauigkeit genug? Wozu brauchen wir Standardreferenzmaterialien?
GIT Fachzeitschr. für das Laboratorium (to be published)

BORDIN, G., CORDEIRO-RAPOSO, F., RODRIGUEZ, A.
Contribution à l'étude du polyphovisme de quelques metallothioneines par chromatographic liquide de haute performance.
Analyt. Chim. Acta. (to be published)

BORDIN, G., McCOURT, J., RODRIGUEZ, A.
Trace metals in the marine bivalve macoma balthica in the Westerschelde estuary. Part I: Analysis of total copper, cadmium, zinc and iron concentration.
Sci. Tot. Environ. 127 (1992) 255

BORTELS, G., MOUCHEL, D., ACEÑA, M.L., GARCIA-TORAÑO, E.
Alpha-particle-emission probabilities in the decay of ^{236}Pu.
Appl. Radiat. Isot., Int. J. Radiat. Appl. Instrum. A43 (1992) 247

BROSA, U., KNITTER, H.-H.
The scission neutron spectrum of ^{252}Cf (SF).
Z. Phys. A343 (1992) 39

BRUSEGAN, A., BARACCA, C., VAN DER VORST, CH., ALBERTS, W.G., MATZKE, M.
High resolution neutron transmission measurements for U and Sc thick composite filters.
In: Nucl. Data for Sci. and Techn., S.M. Qaim (ed.), Springer, Berlin, 1992, p. 74

BRUSEGAN, A., SHELLEY, R., ROHR, G., BARACCA, C., ZHOU ENCHEN, VAN DER VORST, CH., POORTMANS, F., MEWISSEN, L., VANPRAET, G.
Resonance parameters of ^{58}Ni + n and of ^{60}Ni + n from very high resolution transmission measurements.
In: Nucl. Data for Sci. and Techn., S.M. Qaim (ed.), Springer, Berlin, 1992, p. 71

CLIMENT-FONT, A., WÄTJEN, U., BAX, H.
Quantitative RBS analysis using RUMP. On the accuracy of the He stopping in Si.
Nucl. Instrum. Methods, Phys. Res. B71 (1992) 81

COCEVA, C., SPITS, A., FIONI, G., MAURI, A.
Measurements of gamma-ray spectra from neutron capture in single resonances.
In: Nucl. Data for Sci. and Techn., S.M. Qaim (ed.), Springer, Berlin, 1992, p. 430

CORVI, F.
The ^{197}Au (n, γ) cross section.
Nuclear Data Standards for Nuclear Measurements, INDC: NEANDC Nuclear Data Standards File (1992)

CORVI, F., FIONI, G., MAURI, A., ATHANASOPOULOS, K.
Resonance neutron capture in structural materials.
In: Nucl. Data for Sci. and Techn., S.M. Qaim (ed.), Springer, Berlin, 1992, p. 44

DE BIÈVRE, P., LYCKE, W., DAMEN, R., GALLET, M., HENDRICKS, F., PEISER, S., ROSMAN, K.
Certification of a three component isotope reference material of uranium.
EUR 14644 EN (1992)

DE BIÈVRE, P., TAYLOR, P.D.P.
Table of the isotopic composition of the elements.
Intern. J. Mass Spectrom. Ion. Proc. (to be published)

DE BIÈVRE, P., VALKIERS, S.
Isotoopmetingen van silicium: de weg naar een nauwkeurige Avogadro Constante.
Natuur en Techniek 60 (1992) 878

DEKEMPENEER, E., POORTMANS, F., WEIGMANN, H., WARTENA, J., BÜRKHOLZ, C.
Double-differential neutron emission cross section of ^{9}Be.
In: Nucl. Data for Sci. and Techn., S.M. Qaim (ed.), Springer, Berlin, 1992, p. 326

DE LAETER, J.R., DE BIÈVRE, P., PEISER, H.S.
Isotope mass spectrometry in metrology.
Mass Spectrom. Rev. 11 (1992) 193

DERUYTTER, A.
Recent progress in fission cross-section measurements.
In: Fast Neutron Physics, Sun Zuxun et al. (eds), World Scientific, Singapore, 1992, p. 85

FORT, E., DERRIEN, H., KAWAÏ, M., LAGRANGE, C., NAKAGAWA, T., WAGEMANS, C., WESTON, L., YOUNG, P.
International evaluation cooperation progress report of the subgroup on ^{239}Pu fission cross section between 1 and 100 keV.
In: Nucl. Data for Sci. and Techn., S.M. Qaim (ed.), Springer, Berlin, 1992, p. 854

GÖTZ, A., LAMBERTY, A., DE BIÈVRE, P.
CBNM-Certification of Cd in polyethylene by isotope dilution mass spectrometry.
Intern. J. Mass Spectrom. Ion. Proc. (to be published)

HAMBSCH, F.-J.
The ^{235}U fission fragment anisotropies.
IAEA Technical Report Series (to be published)

HAMBSCH, F.-J., KNITTER, H.-H., BUDTZ-JØRGENSEN, C.
Cold fragmentation properties of ^{252}Cf (SF).
In: Nucl. Data for Sci and Techn., S.M. Qaim (ed.), Springer, Berlin, 1992, p. 124

HAMBSCH, F.-J., KNITTER, H.-H., BUDTZ-JØRGENSEN, C.
The positive odd-even effects observed in cold fragmentation - are they real?
Nucl. Phys. A (to be published)

HOFMANN, C., VANDECASTEELE, C., PAUWELS, J.
New calibration method for solid sampling Zeeman atomic absorption spectrometry (SS-ZAAS) for cadmium.
Fresenius' J. Anal. Chem. 342 (1992) 936

INGELBRECHT, C., LIEVENS, F., PAUWELS, J.
Certification of a copper metal reference material for neutron dosimetry.
EUR 14645 EN (1992)

INGELBRECHT, C., LIEVENS, F., PAUWELS, J.
Certification of an iron metal reference material for neutron dosimetry.
EUR 14646 EN (1992)

KNITTER, H.-H., HAMBSCH, F.-J., BUDTZ-JØRGENSEN, C.
Nuclear mass and charge distribution in the cold region of the spontaneous fission of ^{252}Cf.
Nucl. Phys. A536 (1992) 221

KURFÜRST, U., PAUWELS, J., GROBECKER, K.H., STOEPPLER, M., MUNTAU, H.
Microheterogeneity of trace elements in reference materials determination and statistical evaluation.
Fresenius' J. Anal. Chem. (to be published)

LAMBERTY, A., VERBRUGGEN, A., HENDRICKX, F., DE BIÈVRE, P.
A CBNM ^{6}Li spike isotopic reference material CBNM-IRM-615.
Intern. J. Mass Spectrom. Ion. Proc. 113 (1992) 223

LAMBERTY, A., VERBRUGGEN, A., HOLLAND, V., LYCKE, W., HENDRICKX, F., DE BIÈVRE, P.
A CBNM ^{11}B spike isotopic reference material CBNM-IRM-611.
Intern. J. Mass Spectrom. Ion. Proc. 113 (1992) 213

LE DUIGOU, Y., LEIDERT, W., STÜBER, W.
A controlled potential coulometer for high precision uranium and plutonium analysis, part I: description and electrical test.
Fresenius' J. Anal. Chem. (to be published)

LÖVESTAM, N.E.G., SWIETLICKI, E.
Off-line data evaluation of elemental maps obtained from scanning proton microprobe analysis.
Scanning Microscopy, 6 (1992) 607

LÖVESTAM, N.E.G., SWIETLICKI, E., WÄTJEN, U., BREITENBACH, L., RIETVELD, P.
The CBNM scanning nuclear microprobe for materials analysis.
Nucl. Instrum. Methods, Phys. Res. B64 (1992) 371

LÖVESTAM, N.E.G., SWIETLICKI, E., WÄTJEN, U., LOUWERIX, E.
The CBNM scanning nuclear microprobe analytical facility.
Nucl. Instrum. Methods, Phys. Res. B69 (1992) 463

MOUCHEL, D., WORDEL, R.
Measurement of low-level radioactivity in environmental samples by gamma-ray spectrometry.
Appl. Radiat. Isot., Int. J. Radiat. Appl. Instrum., A43 (1992) 49

MÜLLER, W.
Transuranium reference measurements and reference materials.
In: Transuranium Elements, a Half Century, L.R. Morss and J. Fuger (eds.), Amer. Chem. Soc., Washington, 1992, p. 496

MUÑOZ, A., CHIVOT, J., RODRIGUEZ, A.
Spectrophotometric study on molecules intrinsic to the metallothionein structure Lys-Cys-Thr-Cys-Cys-Ala thionein fragment (56-61) MT1 and Cysteins.
Analyt. Biochem. (to be published)

MUÑOZ, A., RODRIGUEZ, A.
Spectrophotometric determination of Cd, Zn Thioneins, of the Lys-Cys-Thr-Cys-Cys-Ala Thionein fragment (56-61) MT1 and of Cysteins.
Analyt. Biochem. (to be published)

MUÑOZ, A., RODRIGUEZ, A.
Spectrophotometric study on Cd, Zn Thioneins.
Analyt. Biochem. (to be published)

NAGEL, W., QUIK, F.
A new approach for the high precision determination of the elemental uranium concentration in uranium ore by gamma-ray spectrometry.
EUR 14659 EN (1992)

NAGEL, W., QUIK, F.
A container for the determination of uranium in ore by gamma spectrometry.
Appl. Radiat. Isot., Int. J. Radiat. Appl. Instrum. A (to be published)

PINHEIRO, T., MESQUITA, F., FERNANDES, R., PINTO RIBEIRO, I., WÄTJEN, U., MAENHAUT, W., HALPERN, M.J.
Trace elements and arteriosclerosis.
In: Molecular Biology of Arteriosclerosis, M.J. Halpern (ed.), John Libbey, London, 1992, p. 531

QAIM, S.M., UHL, M., MOLLA, N.I., LISKIEN, H.
^{4}He emission in the interactions of fast neutrons with ^{48}Ti and ^{50}Ti.
Phys. Rev. C46 (1992) 1398

REHER, D.F.G., CLAES, G., DENECKE, B.
RNDAS, a data acquisition system for a radionuclides laboratory.
Nucl. Instr. Methods, Phys. Res. A312 (1992) 47

REHER, D.F.G., DENECKE, B.
A gamma-ray scanning device for the metrology of heavy radioactive waste containers.
Nucl. Instr. Methods, Phys. Res. A312 (1992) 273

REHER, D., WOODS, M.J., DE ROOST, E., SIBBENS, G., DENECKE, B., ALTZITZOGLOU, T., BALLAUX, C., FUNCK, E.
Standardization of ^{192}Ir.
Nucl. Instr. Methods, Phys. Res. A312 (1992) 263

RENER, M., LAMBERTY, A., DE BIEVRE, P.
IDMS of silicon using thermal ionization mass spectrometry.
Analusis 20 (1992) 229

REYNERS, H., GIANFELICI DE REYNERS, E., POORTMANS, F., CRAMETZ, A., COFFIGNY, H., MAISIN, J.-R.
Brain atrophy after foetal exposure to very low doses of ionizing radiation.
Int. J. Radiat. Biol. 62 (1992) 619

ROHR, G.
Study of a fundamental nearest level spacing distribution of neutron resonances.
In: Nucl. Data for Sci. and Techn., S.M. Qaim (ed.), Springer, Berlin, 1992, p. 884

SCHILLEBEECKX, P., WAGEMANS, C., DERUYTTER, A., BARTHÉLÉMY, R.
Comparative study of the fragments' mass and energy characteristics in the spontaneous fission of ^{238}Pu, ^{240}Pu and ^{242}Pu and in the thermal neutron induced fission of ^{239}Pu.
Nucl. Phys. A545 (1992) 623

SCOTT, R.D., PAUWELS, J., EYKENS, R., BYRNE, J., DAWBER, P.G., GILLIAM, D.M.
The characterization of ^{10}B by the measurement of neutron induced charged particle reactions.
Nucl. Instrum. Methods, Phys. Res. (to be published)

SEYFRIED, P., BECKER, P., KOZDON, A., LÜDICKE, F., SPIEWECK, F., STÜMPEL, J., WAGENBRETH, H., WINDISCH, D., DE BIÈVRE, P., KU, H., LENAERS, C., MURPHY, T., PEISER, H.S., VALKIERS, S.
A determination of the Avogadro constant.
Z. Phys. B87 (1992) 289

SOLÉ JOVER, V.A.
Accurate measurement of $P_K\omega_K$ in the decay of ^{58}Co and the fluorescence yield of iron.
Nucl. Instrum. Methods, Phys. Res. A312 (1992) 303

SOLÉ JOVER, V.A., DENECKE, B., GROSSE, G., BAMBYNEK, W.
Measurement of the K-shell fluorescence yield of Ca and K with a windowless Si(Li) detector.
Nucl. Instrum. Methods, Phys. Res. A (to be published)

TAYLOR, P.D.P., MAECK, R., DE BIÈVRE, P.
Determination of the absolute isotopic composition and atomic weight of a reference sample of natural iron.
Intern. J. Mass Spectrom. Ion Proc. 121 (1992) 111

TAYLOR, P.D.P., MAECK, R., DE BIÈVRE, P.
Absolute isotopic composition of an iron reference sample of natural isotopic composition.
Geochim. Cosmochim. Acta (to be published)

WAGEMANS, C., DRUYTS, S., WEIGMANN, H., BARTHÉLÉMY, R., SCHILLEBEECKX, P., GELTENBORT, P.
(n,p) and (n,alpha) cross-section measurements with astrophysical applications.
In: Nucl. Data for Sci. and Techn., S.M. Qaim (ed.), Springer, Berlin, 1992, p. 638

WAGEMANS, C., SCHILLEBEECKX, P., DERUYTTER, A.J., BARTHÉLÉMY, R.
Measurement of the subthermal neutron induced fission cross-section of ^{241}Pu.
In: Nucl. Data for Sci. and Techn., S.M. Qaim (ed.), Springer, Berlin, 1992, p. 35

WÄTJEN, U., BAX, H., RIETVELD, P.
Evaporated and implanted reference layers for calibration in surface analysis.
Surf. Interf. Anal. 19 (1992) 253

WATTECAMPS, E.
The ^{10}B (n,α) ^{7}Li cross section.
IAEA Technical Report Series (to be published)

WATTECAMPS, E.
Measurement of double differential (n, alpha) cross sections of Ni, ^{58}Ni, ^{60}Ni, Cu, ^{63}Cu and ^{65}Cu in the 5 to 14 MeV neutron energy range.
In: Nucl. Data for Sci. and Techn., S.M. Qaim (ed.), Springer, Berlin, 1992, p. 310

WATTECAMPS, E., ROLLIN, G., KETERS, M.
A 27 cm^2 scintillator for alpha particle detection of some MeV with 28 % energy and 240 ps time-resolution.
In: Nucl. Data for Sci. and Techn., S.M. Qaim (ed.), Springer, Berlin, 1992, p. 466

WEIGMANN, H., WARTENA, A.J., BÜRKHOLZ, C.
On alpha of ^{235}U for sub-thermal neutron energies.
In: Nucl. Data for Sci. and Techn., S.M. Qaim (ed.), Springer, Berlin, 1992, p. 38

WOODS, M.J., LUCAS, S.E.M., REHER, D.F.G., SIBBENS, G.
The half-life of ^{192}Ir.
Nucl. Instrum. Methods, Phys. Res. A312 (1992) 346

WOODS, M.J., ROSSITER, M.J., SEPHTON, J.P., WILLIAMS, T.T., LUCAS, S.E.M., REHER, D.F.G., DENECKE, B., AALBERS, A., THIERENS, H.
^{192}Ir brachytherapy sources: calibration of the NPL secondary standard radionuclide calibrator.
Nucl. Instrum. Methods, Phys. Res. A312 (1992) 257

SPECIAL PUBLICATIONS

HANSEN, H.H. (ed.)
Annual Report 91.
EUR 14374 EN (1992)

HANSEN, H.H. (ed.)
Annual Progress Report on Nuclear Data 1991.
NEANDC (E) 312 "U", Vol. III Euratom; INDC (EUR) 026/G
EUR 14514 EN (1992)

GLOSSARY

AERE	Atomic Energy Research Establishment, Harwell (GB)
ALS	Accélérateur Linéaire de Saclay, Saclay (F)
ANL	Argonne National Laboratory, Argonne (USA)
BAL	Broncho-Alveolar Lavages
BCR	Bureau Communautaire de Référence
BIPM	Bureau International des Poids et Mesures, Sèvres (F)
CBNM	Central Bureau for Nuclear Measurements (JRC-Geel), Geel (B)
CEA	Commissariat à l'Energie Atomique, Paris (F)
CEC	Commission of the European Communities
CERN	Centre Européen pour la Recherche Nucléaire
CIEMAT	Centro de Investigación Energética, Medio Ambiental y Tecnología
CIPM	Comité International des Poids et Mesures
CPS	Consumer Policy Service
CRNS	Centre National de la Recherche Scientifique
CRP	Coordinated Research Programme
DA	Destructive Analysis
DFN	Deutsches Forschungsnetz
DG	Direction Générale
DPhN/ STAS	Département de Physique Nucléaire / Services des Techniques d'Accélération Supraconductrice, Saclay (F)
DPP	Differential Pulse Polarography
DPSV	Differential Pulse Stripping Voltametry
EC	European Community
ECN	Energieonderzoek Centrum Nederland, Petten (NL)
ECSAM	European Commission's Safeguards Analytical Measurements
EFF	European Fusion File
ENDF	Evaluated Nuclear Data File
ENEA	Comitato Nazionale: Energia Nucleare e Energia Alternative
ESARDA	European Safeguards Research and Development Association
ETAAS	Electrothermal Atomic Absorption Spectrometry
ETL	Electrotechnical Laboratory, Ibaraki (Japan)
EWGRD	European Working Group on Reactor Dosimetry
FWHM	Full Width at Half Maximum
GELINA	Geel Electron Linear Accelerator
HEPA	High Efficiency Particulate Air (filter)
HPLC	High Performance Liquid Chromatography
IAEA	International Atomic Energy Agency, Vienna (A)
ICPAES	Inductive Coupled Plasma
ICRM	International Committee for Radionuclide Metrology

IDMS	Isotope Dilution Mass Spectrometry
ILL	Institut Laue-Langevin, Grenoble (F)
IMEP	International Measurement Evaluation Programme
INDC	International Nuclear Data Committee
INTDS	International Nuclear Target Development Society
IPN	Institut de Physique Nucléaire, Lyon (F)
IRK	Institut für Radiumforschung und Kernphysik, Wien (A)
IRM	Isotope Reference Material
JAERI	Japan Atomic Energy Research Institute, Tokai-Mura (Japan)
JEF	Joint European File
JENDL	Japanese Evaluated Data Library
JRC	Joint Research Centre
KFA	Kernforschungsanlage, Jülich (D)
KFK	Kernforschungszentrum Karlsruhe, Karlsruhe (D)
KU	Katholieke Universiteit, Leuven (B)
LEU	Low Enriched Uranium
LSAI	Laboratoire de Spectrométrie Atomique et Ionique
LURE	Laboratoire pour l'Utilisation du Rayonnement Electromagnétique
MOX	Mixed Oxide
NBS	National Bureau of Standards, Gaithersburg (USA)
NCG	Nuclear Certification Group
NDA	Non Destructive Analysis
NEA	Nuclear Energy Agency, Paris (F)
NEANDC	Nuclear Energy Agency's Nuclear Data Committee
NIRAS/ ONDRAF	Nationale Instelling voor Radioactief Afval en Splijtstoffen, /Organisme National des Déchets Radioactifs et des Matières Fissiles, Brussels (B)
NIRH	National Institute of Radiation Hygene, Osteras (N)
NIST	National Institute of Standards and Technology, Gaithersburg (USA)
NMI	Nederlands Meetinstituut, Bilthoven (NL)
NPL	National Physical Laboratory, Teddington (GB)
NRC	National Research Council, Ottawa (CAN)
NRM	Nuclear Reference Material
NTI	Negative Thermal Ionization
PAH	Polycyclic Aromatic Hydrocarbons
PHYSOR	International Conference on the Physics of Reactors, 1990, Marseille (F)
PIXE	Particle Induced X-Ray Emission
PTB	Physikalisch-Technische Bundesanstalt, Braunschweig (D)
PVC	Polyvinyl Chlorides
RBS	Rutherford Backscattering
REIMEP	Regular European Interlaboratory Measurement Evaluation Programme

RIVM	Rijksuniversiteit voor Volksgezondheid en Milieuhygiëne, Bilthoven (NL)
RM	Reference Material
RUG	Rijksuniversiteit Gent, Ghent (B)
SCK/CEN	Studiecentrum voor Kernenergie/ Centre d'Etudes Nucléaires, Mol (B)
SI	Système International d'Unité
SIR	Système International de Référence
SNM	Scanning Nuclear Microprobe
SSI-NIRP	Statens Strålskyddinstitut - National Institute for Radiation Protection, Göteborg (S)
SURRC	Scottish Universities Research and Reactor Centre (UK)
TBT	tributyltin
TH	Technische Hochschule
TNO	Toegepast Natuurwetenschappelijk Onderzoek (NL)
TOF	Time of Flight
TR	Transition Radiation
VDI	Verein Deutsches Ingenieure
VITO	Vlaamse Instelling voor Technologisch Onderzoek (B)
WRENDA	World Request List for Neutron Data Measurements
XRF	X-Ray Fluorescence

European Communities - Commission

EUR 15029 - ANNUAL REPORT 92 of the
Central Bureau for Nuclear Measurements

H.H. Hansen (ed.)

Luxembourg: Office for Official Publications of the European Communities

1993 - pag. 121 - 21.0 x 29.7 cm

EN